MAX-PLANCK-INSTITUT
FÜR METEOROLOGIE

# Internal variability of sea ice and surface air temperature in a warming Arctic climate

Céline Gieße

Hamburg 2023

Berichte zur Erdsystemforschung
*Reports on Earth System Science*

260
2023

## Hinweis

Die Berichte zur Erdsystemforschung werden vom Max-Planck-Institut für Meteorologie in Hamburg in unregelmäßiger Abfolge herausgegeben.

Sie enthalten wissenschaftliche und technische Beiträge, inklusive Dissertationen.

Die Beiträge geben nicht notwendigerweise die Auffassung des Instituts wieder.

Die "Berichte zur Erdsystemforschung" führen die vorherigen Reihen "Reports" und "Examensarbeiten" weiter.

## *Notice*

*The Reports on Earth System Science are published by the Max Planck Institute for Meteorology in Hamburg. They appear in irregular intervals.*

*They contain scientific and technical contributions, including PhD theses.*

*The Reports do not necessarily reflect the opinion of the Institute.*

*The "Reports on Earth System Science" continue the former "Reports" and "Examensarbeiten" of the Max Planck Institute.*

## Anschrift / Address


Max-Planck-Institut für Meteorologie
Bundesstrasse 53
20146 Hamburg
Deutschland

Tel./Phone: +49 (0)40 4 11 73 - 0
Fax: +49 (0)40 4 11 73 - 298

name.surname@mpimet.mpg.de
www.mpimet.mpg.de


## *Layout*


*Bettina Diallo and Norbert P. Noreiks*
*Communication*


## *Copyright*



# Internal variability of sea ice and surface air temperature in a warming Arctic climate

Céline Gieße

Hamburg 2023

Céline Gieße
aus Zierenberg, Deutschland

Max-Planck-Institut für Meteorologie
The International Max Planck Research School on Earth System Modelling
(IMPRS-ESM)
Bundesstrasse 53
20146 Hamburg

Universität Hamburg
Erdsystemwissenschaften
Bundesstr. 55
20146 Hamburg

Tag der Disputation: 18. Januar 2023

Folgende Gutachter empfehlen die Annahme der Dissertation:
Prof. Dr. Johanna Baehr
Prof. Dr. Dirk Notz

Vorsitzender des Promotionsausschusses:
Prof. Dr. Hermann Held

Dekan der MIN-Fakultät:
Prof. Dr.-Ing. Norbert Ritter

Coverfoto von Céline Gieße:
*„Floating sea ice in Isfjorden, Svalbard“* (March 2020)

Berichte zur Erdsystemforschung / Max-Planck-Institut für Meteorologie 260
*Reports on Earth System Science / Max Planck Institute for Meteorology* 2023

ISSN 1614-1199 - doi: 10.17617/2.3489349

*All things are difficult before they are easy.*

— Thomas Fuller

# ABSTRACT

The Arctic is one of the regions most vulnerable to climate change. Its climate is governed by self-reinforcing feedback mechanisms that amplify temperature variability and trends. As a result, Arctic surface temperatures have increased almost four times faster than the global average in recent decades and, alongside, the Arctic sea ice is declining. Not only the trends but also the variability of these two key variables are closely linked. In this dissertation, I examine two aspects of the internal variability of sea ice and surface air temperature in a warming Arctic climate using the powerful tool of large ensemble climate simulations.

The first part of this thesis focuses on the persistence/memory of Arctic sea ice on seasonal to inter-annual timescales. This is relevant for sea-ice predictions, which are of growing socio-economic interest due to the retreat of sea ice in the warming Arctic. Previous studies have identified a substantial gap between the operational forecast skill and model-based estimates of the potential predictability of Arctic sea ice. By analyzing lagged correlations of sea-ice area anomalies in large model ensembles and multiple observational products, I show that climate models significantly overestimate the memory of pan-Arctic sea-ice area from the summer months into the following year, which cannot be explained by internal variability. I further show that the overestimation arises from how the seasonal ice zone "remembers" preceding summer sea-ice area anomalies. My results suggest that there is likely a misrepresentation of processes related to the memory of sea ice in climate models, which could explain part of the gap between potential and operational forecast skill of Arctic sea-ice area.

The second part of this thesis addresses the response of daily Arctic surface air temperature to global warming. While the average temperature is rapidly increasing, previous studies have shown that the variability and the amplitude of the seasonal cycle of Arctic surface air temperature are decreasing, all of which can alter temperature extremes. I provide the first quantitative assessment of the projected changes in the distribution of daily Arctic surface air temperatures as a function of global warming in multiple large ensembles. Thereby, I show that the reduction in daily temperature variations throughout the year is mainly caused by the weakened seasonal temperature cycle and complemented by decreasing sub-seasonal temperature variability in the cold seasons (autumn, winter, spring). I further show that the reduced temperature variations dampen the increase in warm extreme temperatures that would be caused only through mean warming by nearly 50% in the cold seasons and amplify the decrease in cold extreme temperatures at even higher rates. My results show that a warmer Arctic climate will be subject to fewer temperature variations and less extreme relative to its new mean temperature, which may ease adaptation to a new Arctic climate state.

Overall, this dissertation contributes to a better understanding of climate variability in the Arctic, its representation in climate models, and its changes under global warming.

# ZUSAMMENFASSUNG

Die Arktis ist eine der am stärksten vom Klimawandel betroffenen Regionen. Ihr Klima wird von sich selbst verstärkenden Rückkopplungsmechanismen bestimmt, die Schwankungen und Trends in der Temperatur verstärken. Infolgedessen sind die Oberflächentemperaturen in der Arktis in den letzten Jahrzehnten fast viermal schneller angestiegen als im globalen Mittel und gleichzeitig zieht sich das arktische Meereis zurück. Nicht nur die Trends, sondern auch die Schwankungen dieser beiden Schlüsselvariablen sind eng miteinander verknüpft. In dieser Dissertation untersuche ich zwei verschiedene Aspekte der internen Variabilität des Meereises und der Oberflächentemperatur in einem sich erwärmenden arktischen Klima unter Verwendung großer Ensembles von Klimasimulationen.

Der erste Teil dieser Arbeit befasst sich mit der Persistenz bzw. dem Gedächtnis des arktischen Meereises auf saisonalen bis zwischenjährlichen Zeitskalen. Dies ist relevant für Meereisvorhersagen, die aufgrund des Rückzugs des Meereises in der sich erwärmenden Arktis von wachsendem sozioökonomischem Interesse sind. Frühere Studien haben eine beträchtliche Lücke zwischen der operativen Vorhersagefähigkeit und modellbasierten Schätzungen der potenziellen Vorhersagbarkeit des arktischen Meereises festgestellt. Durch die Analyse verzögerter Korrelationen von Anomalien der Meereisfläche in großen Ensembles von Klimasimulationen und mehreren Beobachtungsdatensätzen zeige ich, dass Klimamodelle das Gedächtnis der pan-arktischen Meereisfläche von den Sommermonaten bis ins folgende Jahr deutlich überschätzen, was nicht durch interne Variabilität erklärt werden kann. Außerdem zeige ich, dass die Überschätzung darauf zurückzuführen ist, wie sich die saisonale Eiszone an Anomalien der sommerlichen Meereisfläche „erinnert". Meine Ergebnisse deuten auf eine falsche Darstellung von Prozessen im Zusammenhang mit dem Gedächtnis des Meereises in Klimamodellen hin, was einen Teil der Diskrepanz zwischen der potenziellen und der operationellen Vorhersagefähigkeit der arktischen Meereisfläche erklären könnte.

Der zweite Teil dieser Arbeit befasst sich mit der Reaktion der täglichen arktischen Oberflächenlufttemperatur auf die globale Erwärmung. Während die mittlere Temperatur schnell ansteigt, haben frühere Studien gezeigt, dass die Variabilität und die Amplitude des saisonalen Zyklus der arktischen Oberflächentemperatur abnehmen, was sich auf Temperaturextreme auswirken kann. Ich liefere die erste quantitative Einschätzung der projizierten Veränderungen in der Verteilung der täglichen arktischen Oberflächenlufttemperaturen in Abhängigkeit der globalen Erwärmung in mehreren großen Ensembles von Klimasimulationen. Dabei zeige ich, dass die Verringerung der täglichen Temperaturschwankungen über das ganze Jahr hinweg hauptsächlich durch den abgeschwächten Jahresgang der Temperatur verursacht wird und durch die abnehmende sub-saisonale Temperaturvariabilität in den kalten Jahreszeiten (Herbst, Winter, Frühling) ergänzt wird. Ferner zeige ich, dass die verringerten Temperaturschwankungen den Anstieg der warmen Extremtemperaturen, der nur durch die mittlere Erwärmung verursacht würde, in den kalten Jahreszeiten um fast 50% abschwächen und den Rückgang der kalten Extremtemperaturen sogar noch mehr verstärken. Meine Ergebnisse zeigen, dass ein wärmeres arktisches Klima geringeren Temperaturschwankungen und weniger

extremen Temperaturen im Vergleich zu seiner neuen Durchschnittstemperatur unterworfen sein wird, was die Anpassung an einen neuen arktischen Klimazustand erleichtern könnte.

Insgesamt trägt diese Dissertation zu einem besseren Verständnis der Klimavariabilität in der Arktis, ihrer Darstellung in Klimamodellen und ihrer Änderungen im Zuge der globalen Erwärmung bei.

# PUBLICATIONS RELATED TO THIS DISSERTATION

Appendix A:
Giesse, Céline, Dirk Notz, and Johanna Baehr (2021). “On the origin of discrepancies between observed and simulated memory of Arctic sea ice.” In: *Geophysical Research Letters* 48.11, e2020GL091784. DOI: 10.1029/2020GL091784

Appendix B:
Giesse, Céline, Dirk Notz, and Johanna Baehr. "Reduced temperature variations in a warming Arctic climate substantially dampen extreme temperatures" - *to be submitted.*

# ACKNOWLEDGMENTS

Actually finishing this thesis means a lot to me. Coming this far would not have been possible without support from others and far less enjoyable without the company of some wonderful people.

I am extremely grateful to my supervisors Johanna Baehr and Dirk Notz for guiding me throughout this PhD journey. Johanna - thank you for all your support, patience, and for having more trust in me and my abilities than I had myself at times. You were always there to provide guidance and advice when needed, while at the same time giving me all the freedom I could wish for. Dirk - thank you for all your support, encouragement, and empathy. You often helped me see things from a different perspective, scientifically and personally. Thank you also for being so sensitive and caring on my well-being, for reaching out, and offering help. You truly inspire me, as a scientist, as a science communicator, but even more so as an empathetic leader and human being. Moreover, I would like to thank Jochem Marotzke. I really appreciated our panel meetings and your honest and thoughtful advice. I feel very lucky to have had three such intelligent and inspiring people advising me along my journey.

I further would like to thank Armineh Barkhordarian and Dirk Olonscheck for giving me valuable feedback on the second paper of this thesis as well as Laura Suarez-Gutierrez and the Grand Ensemble group for discussions at different points during my PhD. A big thanks goes to the Climate Modelling group. It has been a pleasure to be among you and I learned a lot from your ideas and feedback. Risking to not give appropriate justice to everyone, I still wish to particularly thank Sebastian, David, Patrick, Julianna, Lara, Daniel, and Goratz for their company and valuable exchanges at different stages throughout the years. Another big thanks goes to the Sea Ice group. Thank you for kindly "adopting" me in your group, for exchanges on cool topics and for warm company, especially in pandemic times. I particularly would like to thank Andreas, Lena, and Markus for sharing some of their paths with me. I further would like to thank the IfM Blog team: Yulia, Manita, and Saskia. It was always a welcomed distraction to work on the blog and I really enjoyed doing this together with you. Thanks also to Francisca for helping us get started and, generally, for always being there to support. On the other side of the building, three women were always there for support: Thank you, Antje, Connie, and Michaela for your work and being the heart of the IMPRS-ESM. I am grateful to have been part of this graduate school and would like to thank my fellow IMPRS students - it has always been uplifting to share this PhD experience with you.

Finally, I would like to thank all the lovely people in my life that accompanied me throughout the last years and that make my life so much more colorful: Sina, Jessi, the entire Rostock Crew (with a special thanks to Ludwig and Jean for joining our workation experiment), Flo and Marie, as well as Jonathan and Jane for making the lunch breaks my highlight during lockdowns. And of course my family as well as Anja, Manni, and the rest of my wonderful, big second family - I am very happy to have you in my life. Last, but more than anyone, I want to thank Marvin. Thank you for your unconditional love and support, your endless patience, for always being by my side and cheering me up when I need it. It means the world to me!

# CONTENTS

# Part I

# UNIFYING ESSAY

# 1 INTERNAL VARIABILITY OF SEA ICE AND SURFACE AIR TEMPERATURE IN A WARMING ARCTIC CLIMATE

This dissertation is about the internal variability of climate in the Arctic - a region where climate change occurs faster than anywhere else. Two key variables that characterize the Arctic climate are its surface temperature and the sea ice covering the Arctic Ocean. As they feed back on each other, the trends and variability of these two variables are closely intertwined. In this dissertation, I investigate two aspects of the internal variability of sea ice and surface air temperature (SAT) in a warming Arctic climate, ultimately aiming to advance our current understanding of present and future Arctic climate variability.

The structure of this dissertation is as follows: First, I introduce the essential background to my work, starting with the Arctic climate system and its changing state under global warming (section 1.1.1), continuing with the concept of internal variability and its role in the Arctic climate (section 1.1.2), and ending with large ensemble simulations as the main tool I use to study the research questions of my dissertation (section 1.1.3). I then present the key findings of the two research contributions contained in this dissertation, the first dealing with the persistence of Arctic sea ice (section 1.2, appendix B) and the second with the changing variability of Arctic SAT under global warming (section 1.3, appendix A). Finally, I discuss my findings and their implications in the broader context of a warming Arctic climate (section 1.4).

### 1.1.1 *The Arctic: a region under massive climatic change*

"The Arctic is a barometer for the health of the world. If you want to know how healthy the world is, come to the Arctic and feel its pulse."

— Sheila Watt-Cloutier

*Definition and geography of the Arctic region*

*Characteristics of the Arctic climate*

The Arctic, that is, the northern circumpolar region, is often perceived as a remote, barren, and unpopulated place covered in ice and snow - a romanticized image that does not reflect the complexity of the Arctic region (Brode-Roger, 2021). Geographically, at the core of the Arctic lies the Arctic Ocean, surrounded by continental land masses and islands (Fig. 1.1). The Arctic Ocean is connected to the North Atlantic via the Fram Strait (passage between Greenland and Svalbard), the Barents Sea, and the Canadian Archipelago, and to the North Pacific via the Bering Strait. Southward, the Arctic has no strict geographical boundaries and therefore is not clearly defined. Various definitions have been proposed over time (e.g., Przybylak, 2003), for example, climatological criteria such as the 10°C summer isotherm or geobotanical criteria such as the tree line. The simplest but still commonly applied definition is the astronomical definition, defining the Arctic as all latitudes north of the Arctic Circle at 66.5°N. Due to the Earth's declination, this latitude marks the boundary north of which continuous summer daylight (polar day) and continuous darkness in winter (polar night) are experienced. Climatically, however, "Arctic conditions" can occur well south of the Arctic Circle (Serreze and Barry, 2014). The Arctic climate is characterized by cold surface temperatures, which exhibit strong regional and seasonal variability (e.g., Johannessen et al., 2016). Precipitation is typically low and mostly falls as snow. A large part of the Arctic Ocean is covered by sea ice, varying in its extent throughout the year. Besides the Greenland ice sheet, most Arctic land areas are underlain by permafrost (perennially frozen ground; Obu et al., 2019). Despite its harsh conditions, the Arctic is home to a variety of plant and animal species as well as to about 4 million people, including indigenous communities (Einarsson et al., 2004).

#### *Arctic amplification*

*Amplified climate change in the Arctic*

As the Earth is warming due to anthropogenic greenhouse gas emissions, the Arctic is facing drastic changes and is shifting to a new climate state (Landrum and Holland, 2020; Jeffries et al., 2013). The Arctic is one of the regions most sensitive to climate change and, therefore, often regarded as an early warning system for the rest of the planet. While global mean surface temperatures have risen by 1.1°C since the pre-industrial period (IPCC, 2021d), the Arctic has warmed more than twice as fast (Fig. 1.2a; Serreze and Barry, 2011) - faster than any other region in the world. Considering the recent decades since the beginning of satellite observations in 1979, the Arctic has even warmed nearly four times faster than the global average (Rantanen et al., 2022). This so-called *Arctic amplification* (Serreze and Francis, 2006) of global warming is a fundamental characteristic of the Earth's climate system, hypothesized already by Arrhenius, 1896 and found in early climate simulations (Manabe and Wetherald, 1975; Manabe and Stouffer, 1980).

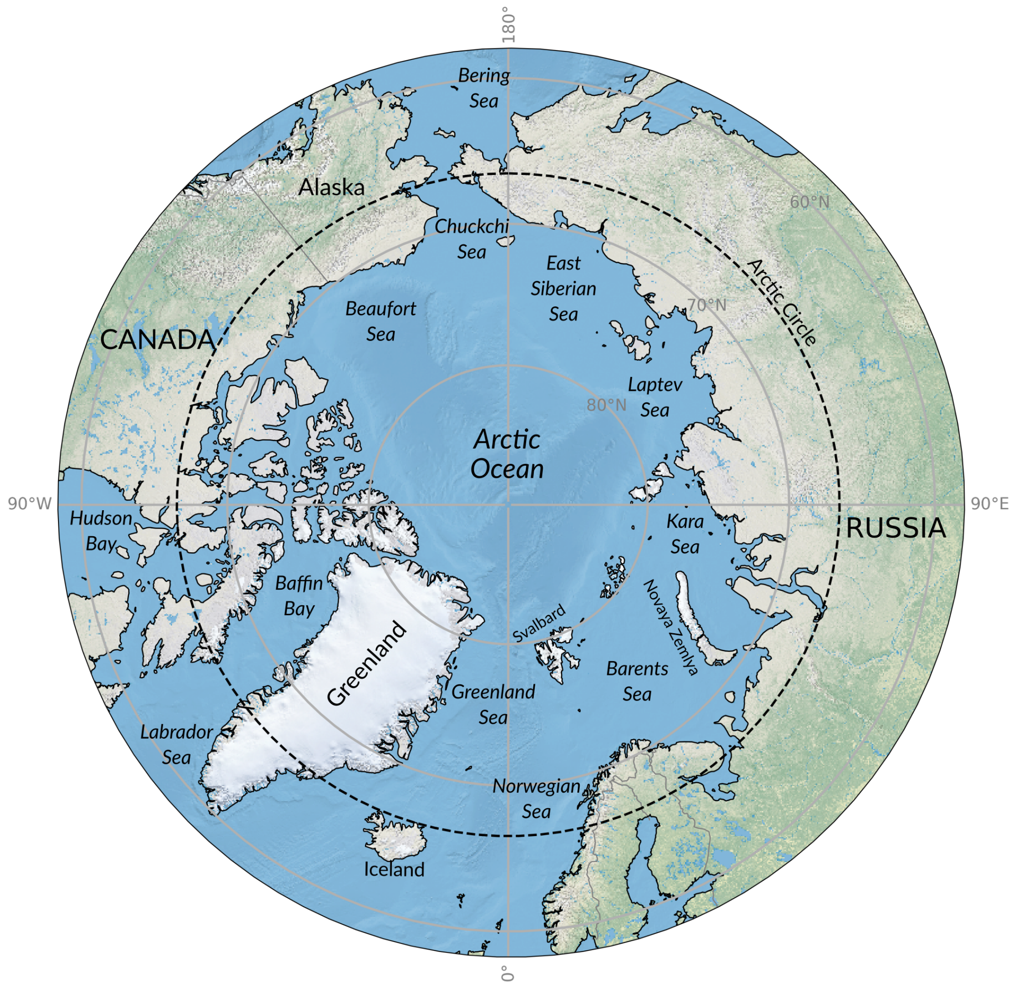


Figure 1.1: Map of the Arctic region with geographic labels. Background image from Natural Earth (naturalearthdata.com).

*Processes causing Arctic amplification*

The Arctic amplification is strongest in late autumn/early winter and weakest in summer (Serreze and Barry, 2011; Rantanen et al., 2022). It is caused by an interplay of different physical processes, most importantly temperature and surface-albedo feedbacks[1] (e.g., Previdi et al., 2021; Pithan and Mauritsen, 2014). The role of the surface-albedo feedback (or ice-albedo feedback) is well-established (e.g., Holland and Bitz, 2003; Serreze and Francis, 2006; Screen and Simmonds, 2010; Crook et al., 2011): As sea ice and snow cover retreat in a warming climate, the surface albedo (or reflectivity) decreases. This means that a larger fraction of the incident solar radiation is absorbed, amplifying surface warming. The surface-albedo feedback can act only when sunlight is present (i.e., in late spring and summer), which is the time of year when the Arctic amplification is weakest. This apparent contradiction is resolved by the heat storage of the Arctic Ocean, taking up heat during summer and releasing it in autumn/winter (Chung et al., 2021; Dai, 2021). The surface-albedo feedback only partly explains Arctic amplification. Another and arguably the most important contribution arises from temperature

1 Climate feedbacks are processes in which a perturbation in one climate quantity causes a change in a second quantity, which ultimately leads to an additional change in the first. In a positive feedback the initial perturbation is enhanced, in a negative feedback the initial perturbation is weakened (IPCC, 2021b).

feedbacks (e.g., Pithan and Mauritsen, 2014; Graversen et al., 2014; Zhang et al., 2018; Previdi et al., 2020). The total temperature feedback can be decomposed into contributions from vertically-uniform warming (Planck feedback) and changes in the vertical temperature gradient in the troposphere (lapse-rate feedback). The Planck feedback results from the Earth's outgoing long-wave radiation being proportional to the 4th power of its surface temperature (Stefan-Boltzmann law). While it acts as a stabilizing feedback mechanism on the global scale, it is weaker in the colder Arctic than at lower latitudes and therefore reinforces Arctic amplification. The lapse-rate feedback is negative in the tropics, where convection leads to a stronger warming of the upper than the lower troposphere, and positive in the Arctic, where surface-based warming is confined to a shallow, stable atmospheric boundary layer. Other processes that play a smaller role in Arctic amplification are cloud and water vapor feedbacks and the poleward energy transport (Previdi et al., 2021).

*Local effects of Arctic warming*

*Sea-ice decline and other climatic changes*

The sharp rise in Arctic temperatures causes further changes in the Arctic climate system. Most prominently, the sea ice is declining. Arctic sea-ice area (SIA) has decreased by about 40% in September (Fig. 1.2b) and by about 10% in March comparing the decadal averages of 1979-1988 and 2010-2019 (IPCC, 2021d). Not only is the area of the sea-ice cover decreasing, but so is its thickness (Kwok and Rothrock, 2009), resulting in an estimated decrease in September sea-ice volume of 72% over the period 1979-2016 (Schweiger et al., 2019). As less sea ice survives the melting season, the fraction of multi-year ice decreases, and the area only seasonally covered by sea ice (seasonal ice zone) is expanding (Bliss et al., 2019). Climate projections suggest that the Arctic will become practically sea-ice-free in September for the first time before 2050 (Notz and SIMIP Community, 2020). A hotspot of warming and sea-ice loss in the Arctic is the Barents Sea (Isaksen et al., 2022; Lind et al., 2018), which is experiencing a so-called *Atlantification* - a transition of Arctic waters to an oceanographic state resembling warmer and saltier Atlantic waters. Moreover, the Arctic warming causes an increase in precipitation and in the fraction of rainfall compared to snowfall (AMAP, 2021). Snow cover on both land and sea ice is decreasing (AMAP, 2021).

*Ecological and socio-economic impacts*

The changing climate in the Arctic has far-reaching impacts on local ecosystems and human communities (Constable et al., 2022). Sea ice is an integral part of marine ecosystems. Its decline leads to a loss of sea-ice algae and sub-ice phytoplankton, which are responsible for more than half of the Arctic Ocean's primary production and underpin the entire marine food web of the Arctic (Post et al., 2013). The loss of sea-ice habitat also threatens Arctic mammals, such as polar bears, walruses, and ringed seals, which rely on the sea ice for foraging, breeding, or resting. This, in turn, affects the food security of indigenous communities. Furthermore, permafrost thaw and enhanced coastal erosion threaten people, villages, and infrastructure and can force relocations (e.g., Jeffries et al., 2013). Despite the high vulnerability of Arctic human communities, they also have a high adaptive capacity (Ford et al., 2015). In addition, the changes in the Arctic create new economic interests in the region, for example, regarding shipping, tourism, and natural resources.

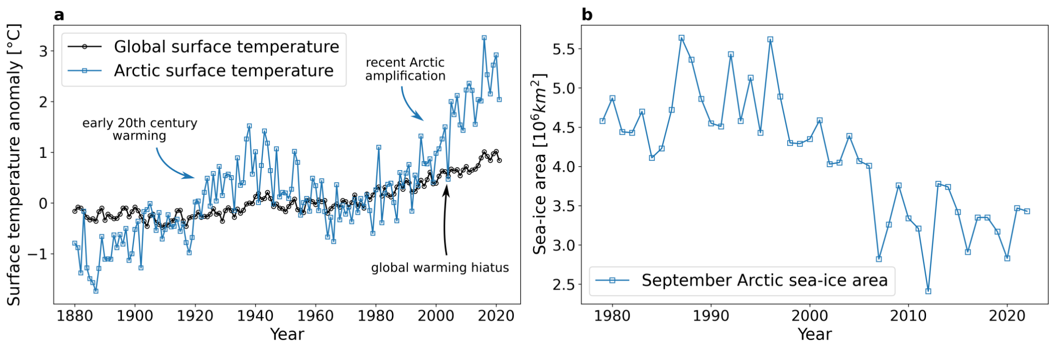


Figure 1.2: a) Time series of global and Arctic (64-90°N) mean annually averaged surface temperature anomaly with respect to the 1951-1980 means. The data are the NASA's Goddard Institute for Space Studies Surface Temperature version 4 (`https://data.giss.nasa.gov/gistemp/`, accessed on 2022-11-04, Lenssen et al., 2019). b) Time series of September Arctic sea-ice area. The data are the National Snow and Ice Data Center's Sea Ice Index version 3 (accessed on 2022-11-04, Fetterer et al., 2017).

*Global and remote effects of Arctic warming*

"You know how they say, 'What happens in Vegas stays in Vegas?' What happens in the Arctic doesn't stay in the Arctic."

— Kumi Naidoo

*Albedo changes*

Arctic climate change has not only local consequences, but also substantial impacts on the global climate. First, the reduced sea ice and snow covers amplify global warming through the previously explained surface-albedo feedback. Estimates of radiative forcing suggest that the amplification of global warming induced by the loss of Arctic sea ice ranges between 14% and 25% (Donohoe et al., 2020; Pistone et al., 2014).

*Release of organic carbon*

Second, vast amounts (~1700 Pg; Miner et al., 2022) of organic carbon are stored in Arctic permafrost soils. With rising temperatures, the permafrost thaws and releases carbon dioxide and methane to the atmosphere, further accelerating climate change (permafrost carbon feedback; Schuur et al., 2015; Miner et al., 2022). The carbon release can either occur gradually through decomposition by soil microbes or abruptly, for example, through coastal erosion (e.g., Nielsen et al., 2022).

*Sea-level rise*

Third, the melting of Arctic land ice significantly contributes to sea-level rise. In the period 1971-2018, the contribution of melting glaciers to global-mean sea-level rise was 22% (with a dominant contribution from Arctic glaciers; Zemp et al., 2019) and that of the Greenland ice sheet 13% with a rising tendency (Fox-Kemper et al., 2021). Regardless of future warming scenarios, the already committed Greenland ice loss will raise sea levels by at least 27 cm (Box et al., 2022). The Greenland ice sheet further is considered a tipping element in the Earth's climate system (Armstrong McKay et al., 2022), meaning that its mass loss may become irreversible after reaching a certain threshold. Its complete meltdown could occur on millennial timescales and raise global sea levels by 7.2 m (Aschwanden et al., 2019).

*Changes in the ocean and atmospheric circulation*

Finally, the Arctic warming could affect ocean and atmospheric circulation. The increased freshwater flux from the melting Greenland ice sheet may reduce convective deep water formation in the Labrador Sea and thereby weaken the Atlantic Meridional Overturning Circulation (Rahmstorf et al., 2015; Böning et al., 2016; Yang et al., 2016), which would strongly impact global and European climate (Jackson et al., 2015). Furthermore, many studies suggest that Arctic warming and sea-ice loss impact Northern Hemisphere mid-latitude weather and climate through changes in atmospheric circulation. Different mechanisms have been proposed, involving changes in storm tracks, the jet stream, and planetary waves and affecting, for example, the occurrence of extremes and the persistence of weather patterns (e.g., Cohen et al., 2020, 2014; Overland et al., 2016). However, these linkages between Arctic and mid-latitudes are highly uncertain, and, as of yet, there is no clear scientific consensus (Doblas-Reyes et al., 2021; Cohen et al., 2020).

### 1.1.2 *Internal variability in the Arctic climate system*

"Predictability: does the flap of a butterfly's wings in Brazil set off a tornado in Texas?"

— Edward N. Lorenz, 1972

*External forcing versus internal variability*

*Chaotic processes in the climate system generate internal variability*

The changes in the Arctic and global climate system described above are forced externally, in this case by anthropogenic greenhouse gas emissions. *External forcing* refers to a forcing agent outside the climate system, which can be natural (e.g., volcanic eruptions and solar activity) or anthropogenic, that is, caused by human activities (e.g., emissions of greenhouse gases or aerosols, and land use). In contrast, the climate also varies due to processes intrinsic to the climate system - the so-called *internal variability*, which is the focus of this dissertation. Because of the chaotic[2] nature of the climate system, slightly differing initial states can evolve into considerably different states (Lorenz, 1963), generating internal variability and limiting predictability. Internal variability occurs on all timescales: Nonlinear dynamical processes in the atmosphere cause short-term fluctuations on weather timescales (i.e., days to weeks) that feed into more slowly responding components of the climate system, such as the ocean, cryosphere, and land vegetation, creating fluctuations on longer climate timescales ranging from years to decades, centuries, and even longer (Hasselmann, 1976). An overview of typical timescales of selected components in the climate system is shown in Figure 1.3.

*The role of external forcing and internal variability in climate predictions*

Externally driven trends in climate variables are overlaid and can be either dampened or enhanced by internal variability (e.g., Chen et al., 2021). A prominent example is the global warming hiatus in the first decade of the 21st century when global-mean surface temperatures warmed considerably slower than expected (see Fig. 1.2a), which can be explained by internal variability (Hedemann et al., 2017; Marotzke and Forster, 2015). When making predictions, knowledge of either external forcing or internal variability can be more important, depending on the variable and timescale of interest. At one end of the scale are numerical weather predictions, in which the state of the atmosphere is predicted several days ahead, which is mainly a question of internal variability. Weather predictions,

2 Chaos theory describes the behaviour of deterministic nonlinear systems. As these systems are deterministic, their trajectory can theoretically be predicted. However, due to a high sensitivity on the initial conditions, slightly different initial states can evolve into considerably different states, making the behaviour appear "chaotic". In practice, such a system is predictable only for a certain time due to uncertainties of the initial state.

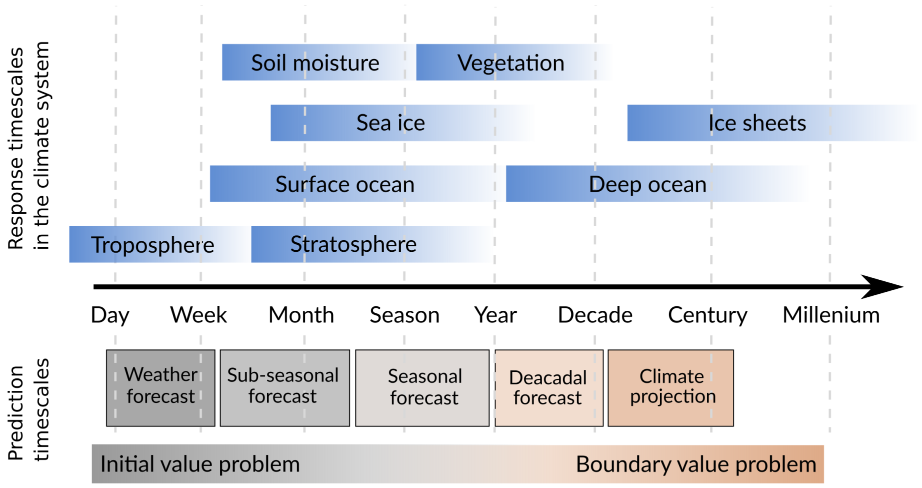


Figure 1.3: Scheme of indicative timescales of selected components in the climate system and climate prediction timescales. Adapted from Meincke and Latif, 1995; Brayshaw, 2018; Meehl et al., 2021.

therefore, require a good knowledge of the initial condition of the atmosphere and are considered an *initial value problem*. At the other end of the scale are climate projections, in which long-term statistical averages of climate variables are predicted multiple decades ahead, which is mainly a question of the external forcing, such as greenhouse gas emissions. Climate projections, therefore, are considered a *boundary value problem*. In between, there is a large range of prediction timescales from sub-seasonal to seasonal, inter-annual, and decadal, which are a combination of initial and boundary value problem (e.g., Brayshaw, 2018; Meehl et al., 2021), as illustrated in Figure 1.3. Generally, the uncertainty from internal climate variability, as opposed to that from external forcing, is increasingly important at shorter timescales and smaller spatial scales, differing for different variables (Hawkins and Sutton, 2009; Deser et al., 2012; Marotzke and Forster, 2015; Maher et al., 2020).

*Magnitude and persistence of variability have major impacts*

Internal variability can be measured in terms of its *magnitude* and its *persistence* (e.g., Lenton et al., 2017). The magnitude of variability, typically measured as the standard deviation of the variable's probability distribution[3], determines the range of experienced climate fluctuations and has substantial socio-economic and ecological impacts (e.g., Stenseth et al., 2002; Thornton et al., 2014). The intensity and frequency of extreme events are very sensitive to changes in the magnitude of variability (Fig. 1.4), which therefore can be considered even more important than changes in the mean (Katz and Brown, 1992). The persistence, measured in terms of auto-correlation/lagged correlation, describes how long climatic fluctuations persist in time. It is a measure of the variable's memory, which differs substantially for different components in the climate system (Fig. 1.3). Persistence is not only important in the context of climate predictions, as detailed above. It also affects the duration of extreme events, which can have strong impacts on society and ecosystems, thinking, for example, of long-lasting heat waves (Gasparrini and Armstrong, 2011) or multi-year droughts (Moravec et al., 2021).

3 The probability distribution is the mathematical function that gives the probabilities of occurrence of the various possible values of a variable.

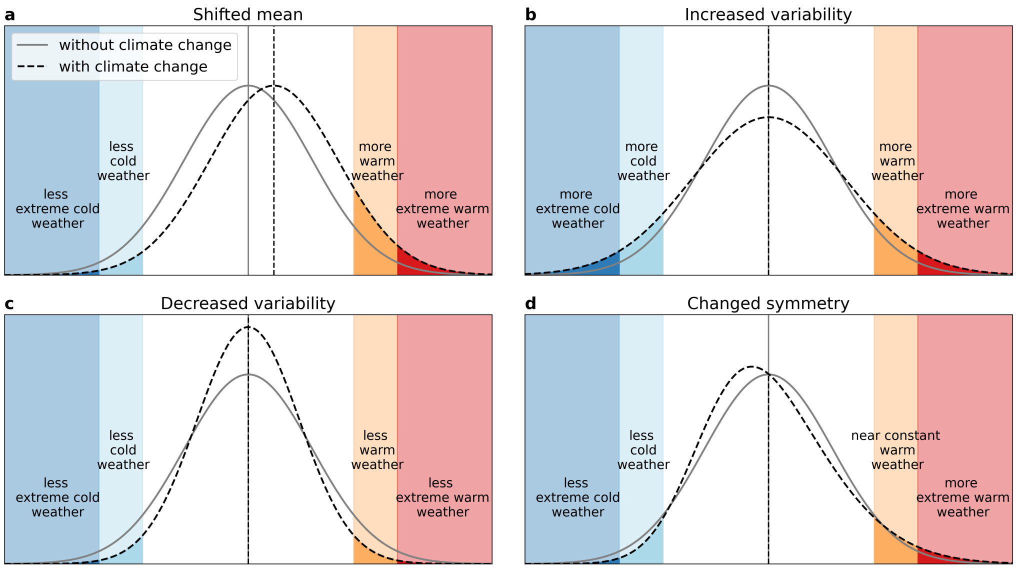


Figure 1.4: The effect of changes in temperature distribution on extremes. Different changes in temperature distributions between present and future climate and their effects on extreme values of the distributions: (a) A simple shift of the entire distribution towards a warmer climate; (b) an increase in temperature variability with no shift in the mean; (c) a decrease in temperature variability with no shift in mean; (d) an altered shape of the distribution, in this example a change in asymmetry toward the hotter part of the distribution. Adapted from IPCC, 2012.

### *Arctic climate variability*

*Variability of Arctic surface temperature*

In the Arctic, internal variability is stronger than at lower latitudes as the prevailing positive climate feedbacks (section 1.1.1) not only amplify externally forced global warming but also internal variability of surface temperatures (see Fig. 1.2a; Serreze and Barry, 2011). Similar to the seasonality of Arctic amplification, the internal temperature variability is highest in winter and lowest in summer (Johannessen et al., 2016). As an atmospheric variable, SAT exhibits variability on short weather timescales but also on longer climate timescales. The tempo-spatial patterns of Arctic temperature variability can be associated with large-scale modes of climate variability[4] (e.g., Johannessen et al., 2016), especially with the Arctic Oscillation[5] (Thompson and Wallace, 1998). On longer timescales, Arctic surface temperatures are influenced by Atlantic and Pacific multi-decadal variability, which jointly drove a warming of the Arctic in the early 20th century at rates comparable to those of recent decades (Fig. 1.2a, Tokinaga et al., 2017).

In a warming climate, the magnitude of internal variability of Arctic SAT on various different timescales decreases (e.g., Chen et al., 2019; Dai and Deng, 2021; Olonscheck et al., 2021). In addition, the amplitude of the seasonal cycle of Arctic SAT also decreases (Dwyer et al., 2012; Chen et al., 2019), further reducing the

4 Modes of climate variability are recurrent space-time structures of variability of the climate system with intrinsic spatial patterns, seasonality and timescales, arising through the dynamical characteristics of atmospheric circulation and/or coupling to other components of the climate system (IPCC, 2021a).

5 The Arctic Oscillation is also known as the Northern Annular Mode and is closely related to the North Atlantic Oscillation (Hurrell et al., 2003). It is characterized by opposite pressure anomalies between Northern Hemisphere high- and mid-latitudes.

temperature variations experienced throughout the year. The resulting narrowing in the Arctic temperature distribution counteracts the intensification of warm extreme events and reinforces the reduction in cold extreme events caused by the mean warming (see Fig. 1.4a,c). In section 1.3, I give more insight into how the interplay of mean warming, seasonality changes, and internal variability changes on different timescales impact the intensity of Arctic temperature extremes, by providing the first quantitative assessment of projected changes in the Arctic SAT distribution as a function of global warming.

*Variability of Arctic sea ice*

The internal variability of SAT and of sea ice are closely linked. In fact, the variability of Arctic SIA is driven primarily by atmospheric temperature fluctuations (Olonscheck et al., 2019). Conversely, the presence or absence of sea ice also impacts the variability of SAT above (e.g., Borodina et al., 2017 and section 1.3), making the interaction bidirectional. It is therefore not surprising that the decline of Arctic sea ice, similar to the trend in surface temperature, has not been uniform over time (e.g., Swart et al., 2015). Internal variability is estimated to contribute up to 50% of the observed sea-ice decline in recent decades (Stroeve et al., 2007; Kay et al., 2011; Zhang, 2015; Ding et al., 2017, 2019), varying seasonally and regionally (England et al., 2019).

However, while SAT as an atmospheric variable has considerable variability on short weather timescales, the sea ice responds more slowly to these perturbations (Fig. 1.3). This is because it is connected and partly driven by the slow ocean underneath and further governed by internal thermodynamic processes (growth and melt of sea ice) with their own characteristic timescales. Anomalies in Arctic SIA persist for about 2-5 months depending on the season, while anomalies in total Arctic sea-ice volume persist for several years (Blanchard-Wrigglesworth et al., 2011b; Day et al., 2014b; Guemas et al., 2016). Moreover, sea ice exhibits memory beyond its persistence timescale through mechanisms that lead to a *reemergence* of SIA anomalies up to a year later. Sea-ice conditions are therefore predictable on timescales of a few months to a few years (depending on the variable, season, and region) and also provide a source of predictability for seasonal forecasts of the atmosphere in high- to mid-latitudes (Chevallier et al., 2018). Predictions of sea ice conditions are of high societal and economic value for various stakeholders (e.g., Jung et al., 2016), in particular with regard to the opening of shipping routes in the Arctic as sea ice is declining (Smith and Stephenson, 2013). In section 1.2, I compare the memory of Arctic sea ice based on observations and model simulations and give new evidence that climate models overestimate the potential predictability of sea ice.

### 1.1.3 *Large ensemble simulations as a tool to study internal variability*

*Challenges in studying internal variability*

Having now a good understanding of internal variability in general and in the Arctic, it is time to talk about methods used to examine internal variability. Indeed, quantifying internal variability in a robust way is a challenging task. Estimating internal variability directly from observations is complicated for several reasons (e.g., Olonscheck, 2018): First, observational records are often too short to infer robust estimates of internal variability, particularly on longer timescales (e.g., Notz, 2015). For example, a consistent time series of SIA (Fig. 1.2b) is available only from 1979 onwards with the beginning of satellite observations. Second, the evolution of an observed variable is a result of both internal variability and external forcing, as seen in the previous section, and disentangling the two is difficult. Additionally, one should note that also observations are subject to uncertainty. In the example of sea ice concentration, the observational uncertainty is particularly large as it cannot be measured directly and the post-processing through satellite-retrieval algorithms adds to the uncertainty (e.g., Bunzel et al., 2016).

*Single-model initial condition large ensembles*

Earth system models are a more flexible tool for studying internal variability. Two different approaches exist, which can also usefully be combined (Olonscheck and Notz, 2017). The first approach is to infer internal variability from a multi-century control simulation with constant external forcing, typically representing pre-industrial conditions. However, with regard to climate change, it is desirable to quantify internal variability also under a changing external forcing. This is possible with the second approach, namely *single-model initial-condition large ensembles* (SMILEs), in which a large number (typically 30-100) of climate simulations with identical external forcing and model configuration but slightly perturbed initial conditions are performed (e.g., Maher et al., 2021; Deser et al., 2020; Milinski et al., 2020). The individual ensemble members then represent different possible realizations of the climate under the same external conditions. This allows for a separation of the externally forced signal (ensemble mean) and internal variability (ensemble spread) (Frankcombe et al., 2015), making it possible to derive robust and continuous estimates of internal variability under a changing external forcing (Olonscheck et al., 2021). With increasing computational power, an increasing number of SMILEs have been produced and made available in the past years (e.g., Deser et al., 2012; Kay et al., 2015; Maher et al., 2019; Deser et al., 2020). The SMILEs are used in various ways, for example, to quantify internal variability (e.g., Suarez-Gutierrez et al., 2018; Dai et al., 2019; Olonscheck et al., 2021), to assess the likelihood of extreme events (e.g., Fischer et al., 2013; Suarez-Gutierrez et al., 2018, 2020; Wiel et al., 2019), to determine the time of emergence of global warming signals from internal variability (e.g., Landrum and Holland, 2020; Holland and Landrum, 2021), and to partition the uncertainty in climate projections (e.g., Lehner et al., 2020; Maher et al., 2020; Bonan et al., 2021; Schwarzwald and Lenssen, 2022). Beyond their scientific value, these applications make SMILEs a valuable tool for assessing climate impacts (Schwarzwald and Lenssen, 2022) and robust adaptation decision-making (Mankin et al., 2020). As every single climate model is subject to model uncertainties, large ensembles become particularly powerful when combining multiple SMILEs into a multi-model large ensemble (Deser et al., 2020), which is increasingly being done in recent studies (e.g., Landrum and Holland, 2020; Olonscheck et al., 2021).

*Scope of this dissertation*

I also take advantage of the growing number of large ensemble climate simulations to answer the research questions outlined in the following two sections. First, I analyze the persistence of Arctic sea ice on seasonal to inter-annual timescales in the recent past and point out discrepancies between observations and model simulations (section 1.2). Second, I study the magnitude of variability in Arctic SAT on daily timescales in projections of the future and quantify the changes in the temperature distribution as a function of global warming (section 1.3). Although the questions raised in the two parts are different in nature and may seem far apart, they both contribute from different angles to the overarching goal of advancing our understanding of the internal variability of sea ice and SAT in a warming Arctic climate.

## 1.2 Persistence of Arctic sea ice: discrepancies between simulations and observations

*A predictability gap in Arctic sea ice predictions*

The first contribution of this dissertation addresses the persistence/memory of Arctic sea ice (Giesse et al., 2021; appendix A). Previous studies have identified a substantial gap between the operational forecast skill and the potential predictability of Arctic sea ice (e.g., Bushuk et al., 2019). The *potential predictability* is a model-based estimate of the upper limit of predictability, in which the skill of a model ensemble in predicting an individual ensemble member is evaluated ("perfect-model" framework). Pan-Arctic SIA has been shown to be potentially predictable at lead times of 1-3 years (depending on the season), whereas operational sea-ice forecasts can make skillful predictions only a few months ahead (3-5 months for summer sea ice and up to a year for winter sea ice; Bushuk et al., 2019; Guemas et al., 2016). While this substantial "predictability gap" indicates great potential for improvements in operational sea-ice forecasts, it could also hint at a systematic overestimation of sea-ice predictability in climate models, as previously suggested by Notz, 2017 and Blanchard-Wrigglesworth and Bushuk, 2019.

*Discrepancies in observed and simulated lagged correlations of sea-ice area*

A way forward to test this hypothesis is to compare the persistence of SIA, a measure of its inherent predictability, in models and observations through lagged correlation analysis. As previous studies (Blanchard-Wrigglesworth et al., 2011b; Day et al., 2014b; Krikken and Hazeleger, 2015; Bushuk et al., 2015; Bushuk and Giannakis, 2015; Bushuk et al., 2017; Ordoñez et al., 2018) show, lagged correlations of monthly pan-Arctic SIA in climate model simulations are characterized by an initial persistence of 2-5 months and two distinct modes of memory reemergence, that is, an increase of correlation after an initial drop (Fig. 1.5a). The first mode, named *melt-to-growth season reemergence*, is related to an imprint of SIA anomalies on sea surface temperature anomalies in the vicinity of the sea-ice edge, which persist over the summer season. The second mode, named *summer-to-summer reemergence* or *growth-to-melt season reemergence*, is caused by a similar exchange of anomalies between SIA and thickness (Blanchard-Wrigglesworth et al., 2011b). In comparison, observations show lower persistence of SIA as well as differences in the pattern of reemergence, in particular, they lack a significant signal of summer-to-summer reemergence (Blanchard-Wrigglesworth et al., 2011b; Day et al., 2014b; Krikken and Hazeleger, 2015).

*Research questions*

The two main factors that could cause the discrepancies between observed and simulated Arctic SIA are model errors (inadequate representation of physical processes or low-frequency variability) and internal variability, as the short observational record starting in 1979 might not be representative of the mean climate (Day et al., 2014b). This motivates my first research question:

1. **Can the discrepancies between observed and simulated persistence of Arctic sea-ice area be explained by internal variability?**

Showing that this is not the case (section 1.2.1) immediately raises the question of what else is causing or contributing to the discrepancies between model simulations and observations. This is not a straightforward question to answer, but I shed some light on this problem by posing the following research question (section 1.2.2):

2. **Where do the discrepancies between observed and simulated persistence of Arctic sea-ice area occur regionally and what can we learn from that about potential causes?**

*Methods*

I answer these questions (Giesse et al., 2021; appendix A) by performing a comprehensive lagged correlation analysis of detrended, monthly pan-Arctic and regional SIA anomalies in the period 1979-2018 based on observational and model data. Using a SMILE, the Max Planck Institute Grand Ensemble (MPI-GE, Maher et al., 2019) with 100 ensemble members, I investigate for the first time whether the observed persistence lies within the range simulated by individual ensemble members. Moreover, I use a multi-model ensemble from the Coupled Model Intercomparison Project phase 6 (CMIP6; Eyring et al., 2016) to ensure that results are robust across different global climate models. To further take into account the uncertainty in observed sea-ice concentration, I use three observational products based on different satellite retrieval algorithms.

### 1.2.1 *Memory of pan-Arctic sea-ice area*

*Discrepancies in observed and simulated summer long-term memory cannot be explained by internal variability*

My analysis of lagged correlations of pan-Arctic SIA (Fig. 1.5a,b and Fig. A.1a-c) confirms the finding of previous studies that observations lack a significant signal of summer-to-summer reemergence and, generally, show a lower persistence of summer SIA anomalies into the following year compared to the ensemble mean of single- or multi-model large ensemble simulations. Beyond that, I show that the observed persistence of SIA anomalies in summer/autumn into the following year, particularly into the spring season, is consistently within or below the 5th percentile of the persistence of individual MPI-GE ensemble members (Fig. A.1d). Defining four different memory regimes (winter persistence, winter long-term memory, summer persistence, and summer long-term memory; see Fig. A.2a), I show that the observed summer long-term memory of all three observational data products is below the model ensemble range of both the MPI-GE and the CMIP6 multi-model ensemble (Fig. 1.5c and Fig. A.2e). This clearly shows that the discrepancies between observed and simulated summer long-term memory of SIA anomalies cannot be explained by internal variability alone.

### 1.2.2 *Regional memory of sea-ice area*

*Observed summer memory can be disentangled regionally into reemergence and negative correlations*

To investigate whether the discrepancies between observed and simulated memory of pan-Arctic SIA have a certain spatial origin, I performed a lagged correlation analysis of regional SIA anomalies. A preliminary analysis of regional SIA anomalies based on geographic location (also provided by Ordoñez et al., 2018) showed that the dominating factor in determining the memory properties of SIA within a certain region is the seasonal cycle of its variability. Therefore, I focus on the auto- and cross-correlations between the seasonal ice zone and the perennial ice zone (see appendix A and Fig. A.3a for definition). I find that the melt-to-growth season reemergence (associated with sea surface temperature anomalies near the sea-ice edge) is primarily a feature of the seasonal ice zone (Fig. A.3f,o), whereas the summer-to-summer reemergence (associated with sea-ice thickness anomalies of multi-year ice) shows up in the perennial ice zone (2nd column of Fig. A.3). More precisely, the summer SIA anomalies of both ice zones, especially those of the seasonal ice zone, reemerge in the perennial ice zone in the following summer. The regional signal of summer-to-summer reemergence is not only a feature of the model simulations but also is present in the observations, implying that it is a

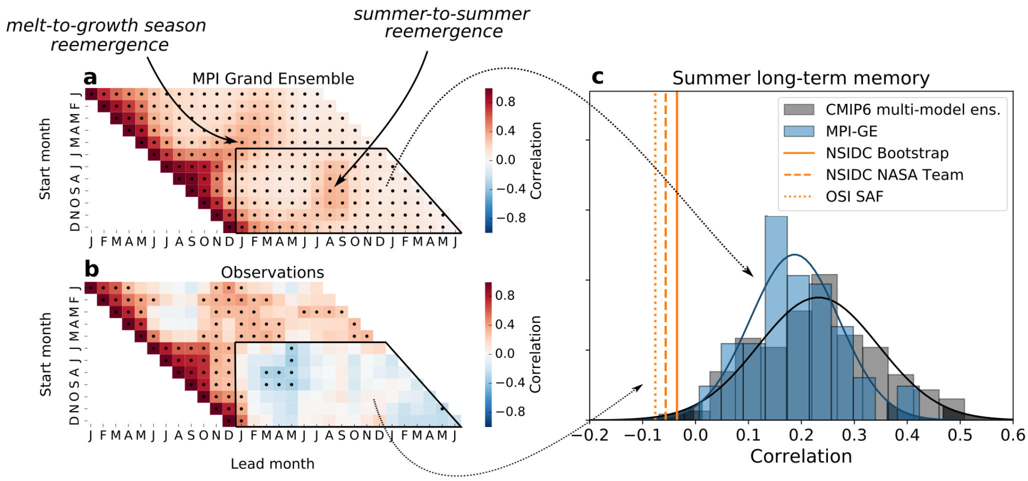


Figure 1.5: **a,b** Lagged correlations of monthly pan-Arctic sea-ice area anomalies in the MPI Grand Ensemble (**a**) and the observational products combined to a "3-member ensemble" (**b**). Correlation coefficients of individual ensemble members or data products are combined using a Fisher's z-transformation. Black dots indicate statistical significance on the 99 % level. **c** Distribution of average correlation coefficients within the summer long-term memory regime shown as histograms for the CMIP6 multi-model ensemble (gray) and the MPI Grand Ensemble (blue), and as lines for observational datasets (orange). The black and blue lines show normal distribution fits to the CMIP6 and MPI-GE data, respectively. Shadings indicate the $2\sigma$-range. Adapted from Giesse et al., 2021.

real-world phenomenon and not just a model artifact. The discrepancies between models and observations rather are caused by an overlaying signal of significant negative correlations between summer SIA anomalies, particularly in the perennial ice zone, and following-year spring and summer SIA anomalies in the seasonal ice zone (Fig. A.3r). With my approach of separating seasonal and perennial ice zones, I could disentangle the observed signals of summer-to-summer reemergence and negative correlations regionally.

*Discussion of potential causes*

My findings hint at a misrepresentation of processes in the climate models. However, it remains unclear what causes the negative correlations in the observations. While stabilizing, negative feedback mechanisms such as the ice growth-thickness feedback (thin ice growing faster than thick ice; e.g., Notz, 2009; Notz and Marotzke, 2012; Goosse et al., 2018; Petty et al., 2018) could be involved, the expected effect would rather be a zero than a negative correlation. There are further factors of uncertainty, such as the observational uncertainty, which is particularly large for summer sea-ice concentration due to the presence of melt ponds (e.g., Kern et al., 2020), or the detrending of the observed SIA time series, which could remove parts of the low-frequency internal variability. It is conceivable that the discrepancies between models and observations stem from a combination of factors, in which also internal variability could play a role, albeit not the only one.

In summary, my findings show that climate models systematically overestimate the observed persistence of summer SIA anomalies, which cannot be explained solely by internal variability. The regional analysis shows that the discrepancies between observations and simulations arise from how the seasonal ice zone "remembers" preceding summer SIA anomalies.

## 1.3 Variability of Arctic surface air temperature: changes under global warming

*Reduced temperature variations in a warming Arctic climate*

The second contribution of this dissertation addresses changes in the distribution of Arctic SAT with global warming (appendix B). Along with its rapid warming (see section 1.1.1), the Arctic has experienced increasingly more heat extremes in the past years (Walsh et al., 2020; Dobricic et al., 2020; Graham et al., 2017; Moore, 2016), while cold extreme events occur less frequently (Matthes et al., 2015; Sui et al., 2017). Moreover, previous studies have shown that in a warming climate, the magnitude of internal variability in Arctic SAT is decreasing, particularly in the cold season and on different timescales ranging from daily (Ylhäisi and Räisänen, 2014; Chen et al., 2019; Dai and Deng, 2021) to monthly (Holmes et al., 2016; Bathiany et al., 2018) to inter-annual (Olonscheck et al., 2021; Borodina et al., 2017). This is primarily a consequence of the sea-ice decline increasing the exposure to the open ocean with a larger heat capacity (e.g., Stouffer and Wetherald, 2007; Huntingford et al., 2013; Olonscheck et al., 2021). Likewise, the amplitude of the seasonal cycle of SAT in the Arctic is decreasing (Dwyer et al., 2012; Chen et al., 2019) due to the seasonality of the Arctic amplification.

*Research questions*

Knowing that global warming is amplified in the Arctic and, at the same time, the variability and seasonality of Arctic surface temperatures decreases, the question arises of how the distribution of Arctic SAT changes with different levels of global warming. In appendix B, I provide a comprehensive, quantitative assessment of the projected response of daily Arctic SAT to global warming, considering changes in the mean temperature, temperature variability on different timescales, and extreme temperatures. Here, I want to focus on two more specific research questions that I answer within the broader context of my analysis and that remained unclear from previous studies focusing only on individual aspects of the temperature response. As previous studies considered internal variability on different timescales and did not consider the combined effect of reductions in internal variability and the seasonal cycle of Arctic SAT in decreasing the range of experienced temperatures, the first research question of this part arises:

3. **What are the relative contributions of changes in seasonality, sub-seasonal variability, and inter-annual variability to changes in the total daily variability of Arctic surface air temperature with global warming?**

The second research question concerns the tails of the temperature distribution. The amplified warming in the Arctic is expected to intensify warm extremes and reduce cold extremes (Fig. 1.4a). However, the decreasing temperature variability counteracts the intensification of warm extremes and reinforces the reduction in cold extremes (Fig. 1.4c), and further changes in higher-order moments of the distribution can asymmetrically affect the intensity and frequency of extreme temperatures (Fig. 1.4d). This motivates my second research question:

4. **What is the relative importance of mean warming and changes in the shape of the temperature distribution in altering seasonal extremes of daily Arctic surface air temperature with global warming?**

*Methods*

I answer these two questions by analyzing the projected changes in daily Arctic SAT, over the entire year and in each season, in five SMILEs of CMIP6 Earth system models. I assess the temperature response as a function of the global warming level (Fig. 1.6), providing results that are independent of timing and warming scenario (Seneviratne et al., 2021). To answer the first question, I decompose the total variability of daily Arctic SAT into its components from inter-annual variability (year-to-year variations), sub-seasonal variability (day-to-day variations), and variability induced by the seasonal cycle, following Fischer and Schär, 2009. For the second question, I analyze the changes in the intensity of warm and cold extreme temperatures (based on seasonal maxima/minima of daily mean SAT) and the respective values if only the mean or only the variability/shape of the distribution were changed. I further study the spatial signals of the projected changes, providing more detail on the heterogeneous Arctic temperature response than previous studies that usually considered the entire globe or the Northern Hemisphere.

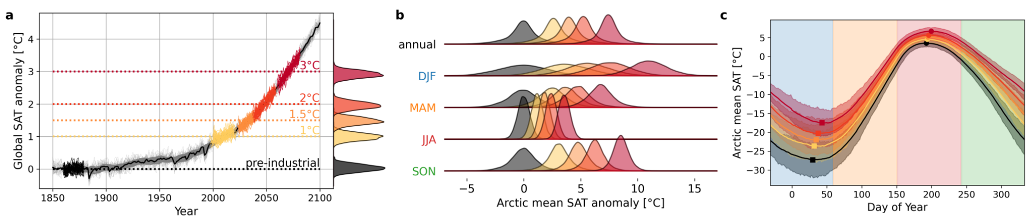


Figure 1.6: Arctic daily temperatures at different global warming levels (GWLs). (a) Time-series of annual global-mean surface air temperature (GSAT) anomaly of each Max Planck Institute Earth System Model (MPI-ESM-LR) ensemble member (thin gray lines), their 20-year rolling averages (gray lines), and their ensemble mean (black line). The colored lines mark the different GWLs (pre-industrial, 1°C, 1.5°C, 2°C, 3°C global warming). Right edge: distributions of detrended GSAT anomalies for each GWL. (b) Distributions of detrended and deseasonalized annual, winter (DJF), spring (MAM), summer (JJA), and autumn (SON) daily Arctic-mean SAT anomalies for each GWL. (c) Seasonal cycle of detrended daily Arctic-mean SAT for each GWL. Lines show the mean seasonal cycle, shadings show the ensemble spread based on the 2.5th and 97.5th percentiles. The circles/squares mark the average day of minimum/maximum daily mean temperature.

### 1.3.1 *Decomposition of changes in daily temperature variability*

*The weakened seasonal cycle is the main contributor to reductions in daily temperature variability throughout the year*

My analysis confirms that the total variability of daily SAT, in the Arctic mean, is decreasing with global warming in all seasons except summer, in which the models project no changes or slight increases of variability (Fig. B.3). The decrease is fastest in autumn but ceases as the seasonal sea ice is lost completely. Over the entire year, the daily temperature variations (measured as the standard deviation of the distribution) decrease by 6 to 10% of their pre-industrial value per degree of global warming in the different models. Most of the reduction in daily temperature variability throughout the year is due to the decreasing amplitude of the seasonal cycle, complemented by reductions in sub-seasonal variability, while the contribution from changing inter-annual variability is negligible. The same holds for the shoulder seasons of autumn and spring. In winter, the daily temperature variability and its reduction are dominated by sub-seasonal variability. Decreasing inter-annual variability adds to the reduction, whereas the temperature variations experienced in winter due to changes in the seasonal cycle increase. This is because the seasonal temperature cycle is delayed in a warming climate and shifts its turning point towards the end of the winter season. Spatially, the temperature variations throughout the year and in the cold seasons decrease practically everywhere in the Arctic region, with the largest local decrease over the ocean areas where sea ice is lost, particularly in the Barents Sea (Fig. B.4). In summer, the Arctic-mean sub-seasonal variability is equally reduced, but increases in the inter-annual variability and the seasonal cycle (again due to a phase delay) lead to a net increase in daily temperature variations. The signal is spatially heterogeneous, with variability increasing over some land areas and over ocean areas of seasonal ice loss.

### 1.3.2 *Effect on temperature extremes*

*Reduced temperature variability substantially dampens cold-season extreme temperatures*

Along with increasing average temperatures, both warm and cold extreme temperatures (Fig. B.5) are projected to increase in a warming climate in all seasons and everywhere in the Arctic. However, only in summer do warm, cold, and average temperatures increase at similar rates. In the cold seasons of autumn, winter, and spring, cold extreme temperatures are projected to increase substantially faster (2 to 3.5 times in the Arctic mean) than the respective warm extremes due to the reduced variability of daily Arctic SAT. For example, in autumn, when the reductions in variability are strongest, cold extremes warm by 4.6°C to 7.2°C per degree of global warming (depending on the model), while warm extreme temperatures increase only by 1.3 to 1.9°C/°C. I find that the increase in warm extreme temperatures that would be caused solely through a shift in mean temperature is dampened by nearly 50% in the cold seasons, while increases in cold extreme temperatures are amplified by 74% in autumn, 60% in spring, and only 13% in winter. In summer, increases in both warm and cold extremes are amplified by about 12% through changes in variability. This shows that seasonal warm and cold extremes are not affected symmetrically by changes in the variability as not only the width but also the skewness of the temperature distribution changes, particularly in summer and winter. I further show that both changes in the seasonal temperature cycle and the sub-seasonal variability contribute to altering the intensity of extreme temperatures, while the inter-annual variability is negligible for the occurrence of extremes. Spatially, the changes in extreme temperatures are largest over the areas of sea-ice loss in the cold seasons, such as the Barents Sea, where mean temperature increases and variability decreases strongest. As a result, local cold extreme temperatures increase substantially (by more than 10°C per degree of global warming), while warm extreme temperatures do not increase more than in other parts of the Arctic (Fig. B.6). Despite the dampening of extremes through reduced variability, it should be noted that Arctic warm extreme temperatures still warm faster than the global average temperature and the strong mean warming will continue to give rise to unprecedentedly hot temperatures in the Arctic.

In summary, my study shows that a warmer Arctic climate will be subject to fewer temperature variations and less intense extremes relative to its new mean temperature. This might ease the adaptation to a warmer Arctic climate.

## 1.4 CONCLUSION

In this dissertation, I investigated two different aspects of internal variability in the Arctic climate system using the powerful tool of large ensemble climate simulations. In the first contribution, I examined the persistence of Arctic sea ice on seasonal to inter-annual timescales, considered the recent past, and evaluated observations against model simulations to gain insights into the inherent predictability of sea ice. In the second contribution, I examined the magnitude of variability in Arctic SAT on daily timescales, considered projections of the future, and gave a quantitative assessment of changes in the temperature distribution with global warming, which can be relevant for political decision-making. Although I analyzed the variability of sea ice and surface temperatures from two different angles, my results implicitly demonstrate the close interconnectedness of these two key variables of Arctic climate. To conclude, I discuss the implications of my findings in the broader context of a warming Arctic climate and give some outlook on potential future research.

### 1.4.1 *Predicting sea ice in a warming Arctic climate*

*Key findings and remaining questions*

In the first part of this dissertation (Giesse et al., 2021, appendix A), I found that the memory of Arctic summer SIA into the following year is significantly overestimated in state-of-the-art climate models and that this cannot be explained solely by internal variability. I further show that the models do show some summer-to-summer reemergence of memory in the perennial ice zone, but the discrepancies between models and observations arise from the relation between SIA anomalies in the seasonal ice zone and preceding summer SIA anomalies. The puzzle of what exactly is causing the discrepancies remains unsolved. My findings suggest that likely model errors in the representation of physical processes and/or the low-frequency variability of sea ice are involved. Identifying the cause(s) of the discrepancies could help the understanding of sea-ice memory and predictability. It is, however, a challenging undertaking and, considering that additional factors such as internal variability, the detrending of the time series, and observational uncertainties may play a role in generating the discrepancies, it is questionable how desirable and achievable a perfect agreement between models and observations actually is (Notz, 2015).

*Implications and prospects for sea-ice prediction*

The results of my study are relevant in the context of sea-ice predictions. As previously suggested by Blanchard-Wrigglesworth and Bushuk, 2019, the overestimation of the memory of Arctic summer SIA could explain a part of the predictability gap between perfect-model experiments and operational forecasts (Bushuk et al., 2019). This would imply that the upper limit of sea-ice predictability is lower than model studies suggest. Nevertheless, the potential to improve operational sea-ice predictions, for instance, through better initialization and exploiting further sources of predictability, is not yet exhausted. In practice, summer pan-Arctic and regional sea-ice conditions, which are of particular interest for marine shipping, can be predicted about four months ahead (e.g., Guemas et al., 2016; Bushuk et al., 2022). Hence, the limiting factor for prolonging the skill horizon of summer sea-ice forecasts currently is not the lack of summer-to-summer memory of SIA but rather a spring predictability barrier that causes forecasts initialized before May to be less skillful (Bonan et al., 2019; Bushuk et al., 2020). Besides the inherent memory of Arctic SIA or extent, additional predictability arises from the upper ocean heat content and the sea-ice thickness (e.g., Chevallier and Salas-Mélia, 2012; Day et al., 2014a). The initialization of sea-ice thickness has been shown to be key in improving sea-ice forecasts (Collow et al., 2015; Dirkson et al., 2017; Blockley and Peterson, 2018). Satellite observations of sea-ice thickness are available since the launch of CryoSat-2 in 2010. However, only recently, a year-round sea-ice thickness record from CryoSat-2, which uses deep learning and numerical simulations to generate sea-ice thickness data also in the crucial melt period from May to September, has been released and offers promising opportunities to improve sea-ice predictions (Landy et al., 2022).

*Changing sea-ice predictability in a warming Arctic climate*

The above statements on sea-ice predictability concern the past and present state of Arctic sea ice. As the sea ice is declining rapidly, its variability (e.g., Goosse et al., 2009) and predictability (Holland et al., 2011; Cheng et al., 2016; Holland et al., 2019) are changing. The variability of Arctic summer sea-ice extent increases as the ice cover becomes thinner and more seasonal, up to a certain point (of about 3 million km$^2$ sea-ice extent), after which the variability decreases as the summer sea ice is lost completely (Goosse et al., 2009). Lagged correlation analyses of SIA anomalies in future climate projections show that the summer-to-summer reemergence, related to long-lived ice-thickness anomalies, is enhanced in the period 2000-2020 compared to earlier periods (Holland et al., 2019) but decreases as climate warming and sea-ice thinning continue, indicating decreasing predictability of summer sea-ice conditions (Cheng et al., 2016; Holland et al., 2019). This implies that the summer-to-summer memory and the associated discrepancies between observations and simulations will be less relevant in a warming Arctic climate. Perfect-model experiments support the existence of a sweet spot for the predictability of summer sea ice in the early 21st century (Holland et al., 2019). Due to its non-stationarity and increasing relevance, the prediction of sea ice in the Arctic will likely remain a topic of high research interest in the coming decades. As sea ice continues to retreat, the focus might shift to predictions of winter sea ice. The melt-to-growth season reemergence, which can facilitate the prediction of winter sea ice and, as I show, is well represented in climate models (Giesse et al., 2021), is expected to intensify as the climate warms (Cheng et al., 2016).

### 1.4.2 *Mitigation versus adaptation to a warming Arctic climate*

*Key findings and remaining questions*

In the second part of this dissertation (appendix B), I analyzed how the distribution of daily Arctic SAT is changing with global warming. I showed that while the Arctic is warming rapidly, particularly in winter and in areas of sea ice loss, temperatures in a warmer Arctic climate will also be less variable and less extreme relative to the new mean temperature. Both a weakening of the seasonal temperature cycle and a decrease in sub-seasonal temperature variability in the cold seasons contribute to a substantial dampening of seasonal extreme temperatures. Moreover, I show that warm and cold extremes are not affected in the same way, indicating changes in the symmetry of the temperature distribution. While I chose to focus on the joint impact of mean warming and variability changes on maximum and minimum temperatures, the sensitivity of Arctic temperature extremes to global warming could be analyzed more extensively in future research. One could, for instance, apply different definitions of extreme events and assess further parameters, such as the frequency, which in contrast to the intensity tends to change non-linearly with global warming (Seneviratne et al., 2021), and the duration. The duration of temperature extremes is less a matter of the magnitude of temperature variability than its persistence, which may increase in the Arctic as sea-ice decline increases the exposure to the open ocean (Bathiany et al., 2018).

*Quantifying the climate response to global warming levels is relevant for political decision-making*

Besides providing new insights into the prevailing timescales of changing Arctic temperature variability and their role in altering extremes, the added value of my study lies in providing a quantitative assessment of the controllability of mean and extreme temperatures with global warming forcing. This is relevant for political decision-making and setting climate targets such as the 1.5°C and 2°C limits on global warming stated in the Paris Agreement of 2015. Since then, studies have increasingly focused on the climate response to specific global warming levels (see, e.g., James et al., 2017) and the Intergovernmental Panel on Climate Change (IPCC) applies this framework throughout its Sixth Assessment Report (IPCC, 2021c). In contrast to many previous studies, I not only look at selected global warming levels but consider the continuous climate response to global warming. Doing so is only possible through the increasing availability of SMILEs with large ensemble sizes. The approach of my study could serve as an example for future research considering different regions, or the entire globe, and different variables. One should, however, keep in mind that the response to global warming can differ between transient and equilibrium climate states (King et al., 2020), especially for more slowly-responding variables.

*Reduced temperature variations may ease adaptation to a warmer Arctic climate*

Regarding the implications of Arctic climate warming, regionally and globally (section 1.1.1), it is crucial to know how surface temperatures in the Arctic are changing with global warming - not only in their mean but also in their variability and extremes. Previous studies have highlighted the severe impacts of increased climate variability on biological and human systems (e.g., Thornton et al., 2014). Conversely, one could expect that a reduction in temperature variability will dampen impacts and ease adaptation to climate change. Arctic human communities and species that do not rely on the presence of sea ice may adapt more easily if they face fewer temperature variations and extreme events. Particularly the reduction in extreme cold temperatures could potentially also facilitate a northward migration of species, ecosystems, and human activities that are not adapted to extreme cold weather. Nevertheless, one should state clearly that for many of the most severe impacts and consequences of Arctic climate change, the mean warming is essential. This includes the loss of sea ice, which directly follows anthropogenic greenhouse gas emissions and temperature rise (Notz and Stroeve, 2016; Stroeve and Notz, 2018), the melting of the Greenland ice sheet, whose tipping point could be reached already at 1.5°C of global warming (Armstrong McKay et al., 2022), as well as gradual permafrost thaw. Thus, regardless of any adaptive capacity and its potential increase due to reduced temperature variations, mitigation of climate change must be the number one priority to minimize negative consequences also in the Arctic.

# Part II

# APPENDICES

# A

# ON THE ORIGIN OF DISCREPANCIES BETWEEN OBSERVED AND SIMULATED MEMORY OF ARCTIC SEA ICE

The work in this appendix has been published as:

Giesse, Céline, Dirk Notz, and Johanna Baehr (2021). “On the origin of discrepancies between observed and simulated memory of Arctic sea ice.” In: *Geophysical Research Letters* 48.11, e2020GL091784. DOI: 10.1029/2020GL091784

CG, DN, and JB conceived and designed the study. CG performed the analysis and wrote the paper. DN and JB contributed through discussions and interpretation of the results and reviewed the manuscript.

# On the origin of discrepancies between observed and simulated memory of Arctic sea ice

**Céline Giesse[1,2], Dirk Notz[1,3], Johanna Baehr[1]**

[1]Institute of Oceanography, Center for Earth System Research and Sustainability (CEN), Universität Hamburg, Hamburg, Germany

[2]International Max Planck Research School on Earth System Modelling, Hamburg, Germany

[3]Max Planck Institute for Meteorology, Hamburg, Germany

Received: 24 November 2020 / Accepted: 15 May 2021 / Published: 07 June 2021

## ABSTRACT

To investigate the inherent predictability of sea ice and its representation in climate models, we compare the seasonal-to-interannual memory of Arctic sea ice as given by lagged correlations of sea-ice area anomalies in large model ensembles (Max Planck Institute Grand Ensemble and Coupled Model Intercomparison Project phase 6) and multiple observational products. We find that state-of-the-art climate models significantly overestimate the memory of pan-Arctic sea-ice area from the summer months into the following year. This cannot be explained by internal variability. We further show that the observed summer memory can be disentangled regionally into a reemergence of positive correlations in the perennial ice zone and negative correlations in the seasonal ice zone; the latter giving rise to the discrepancy between observations and model simulations. These findings could explain some of the predictability gap between potential and operational forecast skill of Arctic sea-ice area identified in previous studies.

## PLAIN LANGUAGE SUMMARY

Sea ice, as a relatively slowly-varying component in the climate system, holds "memory" on seasonal-to-interannual timescales. This means that, based on the current state of the sea ice, meaningful predictions of its state several months into the future can be made, for instance with the use of climate models. Such sea-ice predictions are of growing socioeconomic importance, particularly in the Arctic, where the strong sea-ice loss in the last decades is giving rise to new risks as well as economic opportunities. Here, we provide a comparison of the memory of Arctic sea ice based on model and observational data. We show that current global climate models systematically overestimate the memory of sea ice from one summer into the following year and beyond. We further show that this overestimation arises from how the outer region of the Arctic, which is only seasonally ice-covered, remembers previous summer sea ice. Our findings imply that, first, there is likely a misrepresentation of processes related to the memory of sea ice in climate models and, second, the potential of making skillful sea-ice predictions is less strong than previously assumed based on model simulations.

## A.1 INTRODUCTION

Over the past decade, major advances in the prediction of sea ice have been made. This includes the development of seasonal sea-ice prediction systems based on coupled global climate models (GCMs) utilized for operational predictions (e.g., Wang et al., 2013; Chevallier et al., 2013; Sigmond et al., 2013; Msadek et al., 2014; Peterson et al., 2015) and "perfect-model" studies (e.g., Koenigk and Mikolajewicz, 2009; Holland et al., 2011; Blanchard-Wrigglesworth et al., 2011a; Tietsche et al., 2014; Germe et al., 2014; Day et al., 2014a; Day et al., 2016). The latter provide an upper limit of the predictability of sea ice within a given model framework under the assumption of perfect model physics and knowledge of initial conditions (potential predictability). While perfect-model studies show that pan-Arctic sea-ice area (SIA) or extent (SIE) are predictable at 12-36 month lead times, operational predictions of detrended pan-Arctic SIA/SIE are skillful only for lead times of a few months (1-6 months for summer SIE and 1-11 months for winter SIE depending on the prediction system) (Guemas et al., 2016; Bushuk et al., 2019). This gap between potential predictability and operational forecast skill has been noted in previous studies (e.g., Guemas et al., 2016; Blanchard-Wrigglesworth et al., 2015). Bushuk et al., 2019 provide the first consistent assessment of potential and operational forecast skill within one GCM-based prediction system and find a substantial skill gap in nearly all Arctic regions. This predictability gap could indicate a strong potential for improvements of operational sea-ice predictions, either through improved initialization or improved model physics. However, the skill gap might also hint at a systematic overestimation of sea-ice predictability in state-of-the-art GCMs, as previously suggested by Notz, 2017 and Blanchard-Wrigglesworth and Bushuk, 2019. This brings up the question of which predictability can be expected based on observations, which we address here.

One way to analyze the inherent predictability of sea ice, arising from the memory/persistence of its initial conditions, in models as well as observations are lagged correlation studies (Blanchard-Wrigglesworth et al., 2011b; Chevallier and Salas-Mélia, 2012; Day et al., 2014b; Krikken and Hazeleger, 2015; Bushuk et al., 2015; Bushuk and Giannakis, 2015; Bushuk et al., 2017; Ordoñez et al., 2018; Blanchard-Wrigglesworth and Bushuk, 2019). As found by Blanchard-Wrigglesworth et al., 2011b, the memory of pan-Arctic SIA anomalies is characterized by an initial persistence of 2-5 months and two distinct modes of memory reemergence, in which lagged correlations increase again after an initial drop. The first identified mode of memory reemergence occurs between months of the melt and the freezing season ("melt-to-growth season reemergence") and is related to an imprint of SIA anomalies on sea surface temperature (SST) anomalies in the vicinity of the sea-ice edge, which persist over the summer season. The second mode occurs between the months of one summer and the next ("summer-to-summer reemergence" or in later works also "growth-to-melt season reemergence") and can be explained by a similar exchange of anomalies between SIA and sea-ice thickness. In addition, the ice-albedo feedback adds to the persistence and reemergence during the summer months. Day et al., 2014b showed that, despite some inter-model spread in the magnitude of correlations, the memory patterns are robust across different GCMs.

Comparing the memory of pan-Arctic SIA in model simulations and observations, previous studies noted generally higher lagged correlations in the models than in the observations as well as differences in the occurrence of reemergence (Blanchard-

Wrigglesworth et al., 2011b; Day et al., 2014b; Krikken and Hazeleger, 2015). While the melt-to-growth season reemergence is present in observational data, there is no significant signal of summer-to-summer reemergence. As pointed out by Day et al., 2014b, the attribution of discrepancies to potential causes is complicated by several factors of uncertainty, such as the shortness of the observational record and the detrending of the time series.

With the present study, we aim to systematically analyze differences in the memory of Arctic sea-ice in model simulations and observations: Can they be attributed to internal variability or errors in the model physics? Where do they occur regionally? In contrast to previous studies, we base our lagged correlation analysis of SIA anomalies on a multitude of simulated and observational data: the Max Planck Institute Grand Ensemble (MPI-GE, Maher et al., 2019), a Coupled Model Intercomparison Project phase 6 (CMIP6; Eyring et al., 2016) multi-model ensemble, and several observational data products. By comparing lagged correlations from observational data to the range of model internal variability of large ensemble simulations covering the same period, we systematically identify time lags at which simulated memory is over-/underestimated. By analyzing not only the memory of pan-Arctic SIA but also regional memory of SIA, we gain insights into the spatial origin of discrepancies between models and observations.

## A.2 Data and methods

### A.2.1 *Sea-ice concentration data sets*

For our analysis, we use monthly sea-ice concentration (SIC) data of the period 1979-2018 from various model and observational data products. We analyze model data from the MPI-GE (Maher et al., 2019), combining historical simulations (1979-2005) and representative concentration pathway 4.5 (RCP4.5) simulations (2006-2018) performed with the Max Planck Institute Earth System Model (MPI-ESM, Giorgetta et al., 2013) from 100 model ensemble members. Additionally, we use a CMIP6 (Eyring et al., 2016) multi-model ensemble consisting of 240 members from 37 different models. For this ensemble, we use all available historical simulations (period 1979-2014) except those performed with MPI-ESM. This allows judgment on whether results obtained with the MPI-GE are model-specific or can be generalized for state-of-the-art GCMs. Note that, due to the consideration of all available simulations, the individual models are weighted differently depending on the amount of provided ensemble members, but qualitatively similar results are obtained when analyzing only one member per model. A table listing the contributing CMIP6 models with their number of ensemble members is provided in the supporting information (Table A.1).

Furthermore, we use three observational products of SIC retrieved from satellite records with different retrieval algorithms, namely Bootstrap (Comiso, 2017) and NASA Team (Cavalieri et al., 1996) data from the National Snow and Ice Data Center (NSIDC) and EUMETSAT Ocean and Sea Ice Satellite Application Facility (OSI SAF) data (EUMETSAT Ocean and Sea Ice Satellite Application Facility, 2017, 2019; Lavergne et al., 2019). The usage of different observational products allows us to take into account the uncertainty in observed SIC (e.g., Kern et al., 2019, 2020).

### A.2.2 *Quantification of memory*

We quantify memory of Arctic sea ice in terms of lagged correlations of SIA anomalies. From the SIC data sets, we compute monthly time series of pan-Arctic and regional SIA, differentiating between a seasonal ice zone (SIZ) and a perennial ice zone (PIZ). We define the PIZ to consist of all grid cells with a September SIC of $\geq 0.15$ (corresponding to the annual minimum ice extent) in at least 80% of the years based on the NSIDC Bootstrap data; all other grid cells are considered as SIZ. For the CMIP6 multi-model ensemble, we consider only pan-Arctic SIA, determined as described in Notz and SIMIP Community, 2020. To remove externally driven long-term trends, we detrend the time series of individual months using locally weighted scatterplot smoothing (LOWESS; Cleveland, 1979). This local regression provides a more accurate representation of the sea-ice decline than a linear regression, as the negative trend is increasing with time, particularly in the sea-ice minimum months (e.g., Serreze and Stroeve, 2015). In the supporting information, we provide a visual comparison of the LOWESS and linear detrending (Figure A.4) and show some key results based on linearly detrended time series, allowing for a direct comparison to previous studies. From the resulting monthly SIA anomalies, we calculate lagged correlations with time lags of up to 18 months using Pearson's correlation coefficient $r$. For details on the computation of SIA and the statistical methods applied for the combination of correlation coefficients of ensemble members, the computation of statistical significance, and the detrending, we refer to the supporting information (Text A1).

## A.3 RESULTS

### A.3.1 *Memory of pan-Arctic sea-ice area*

Analyzing the lagged correlations of pan-Arctic SIA, all data sets show an initial decline of memory associated with the persistence of SIA anomalies (Figure A.1a-c and Figure A.5 for the individual observational data sets). Related to the seasonal cycle, two persistence regimes can be differentiated: one centered around the sea-ice maximum (winter persistence, January to May start months) and one centered around the sea-ice minimum (summer persistence, June to December start months). The $e$-folding decorrelation time ranges between 1-6 months depending on the initial month and data set, which is consistent with previous studies (Blanchard-Wrigglesworth et al., 2011b; Day et al., 2014b; Krikken and Hazeleger, 2015). Furthermore, all data sets show a melt-to-growth-season reemergence of memory (high correlations between pairs of months around the sea-ice minimum, i.e., August-September, July-October, etc.; Blanchard-Wrigglesworth et al., 2011b). The correlation between pairs of months around the sea-ice minimum is less clear-cut in the observations than in the models. However, the relation from winter to winter is stronger in the observations than in the MPI-GE, as also noted in previous studies (Blanchard-Wrigglesworth et al., 2011b; Krikken and Hazeleger, 2015). The CMIP6 ensemble reproduces the observed winter-to-winter memory better than the MPI-GE.

For the summer-to-summer memory, differences between observations and model simulations are more apparent than for other time lags. The model ensembles show a clear summer-to-summer reemergence (high correlations between the summer

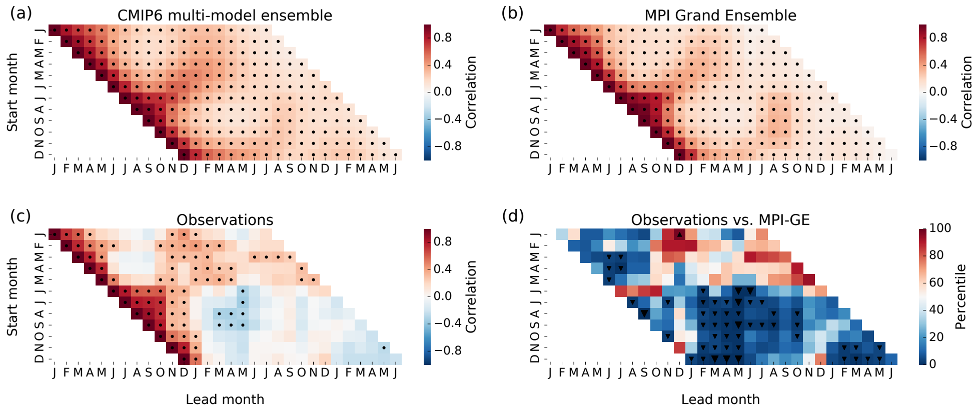


Figure A.1: (a-c) Lagged correlations of monthly pan-Arctic sea-ice area anomalies in (a) the Coupled Model Intercomparison Project phase 6 (CMIP6) multi-model ensemble, (b) the Max Planck Institute Grand Ensemble (MPI-GE), and (c) the observational products (National Snow and Ice Data Center [NSIDC] Bootstrap, NSIDC NASA Team and Ocean and Sea Ice Satellite Application Facility [OSI SAF] Climate Data Records) combined to a "3-member ensemble". Correlation coefficients of individual ensemble members or data products are combined using a Fisher's z-transformation. Black dots indicate statistical significance on the 99 % level. (d) Percentile of MPI-GE members with a lower correlation than observational data for the respective time lag. Downward and upward triangles mark values within the 5th and 95th percentile. Time lags with correlations coefficients outside of the model range (0th and 100th percentile) are marked with a larger triangle.

minimum months, particularly August/September, from one year to the next; Blanchard-Wrigglesworth et al., 2011b). The signal is more pronounced in the MPI-GE than in the CMIP6 ensemble (September 1-year lag correlation of 0.31 and 0.24, respectively). In the observations, the correlations from the summer months beyond the persistence timescale are substantially lower than in the models (e.g. September 1-year lag correlation of -0.06), with even significant negative correlations from summer to spring of the next year. Despite these low correlation coefficients, there is an increase in correlations (from -0.35 at minimum to around zero) in the summer months. This could indicate a reemergence of summer SIA anomalies that is superimposed with negative summer-to-summer correlations caused by a different process. Note that when detrending the time series linearly, the correlation coefficients are higher, rendering the summer-to-summer reemergence in the observations more visible (Figure A.6), but we still find statistically significant negative correlations from summer to spring.

As the model correlation values represent an average of many ensemble members and the observations represent only a single time series, differences could be due to internal variability. Still, one would expect the observations to lie within the range of model variability. There are several patterns or individual time lags for which the correlation coefficients from observations are at the edge of model variability (Figure A.1d). Most evident is the pattern of time lags from the summer months into the following year, in which the observed correlations are consistently within or below the 5th percentile of MPI-GE correlation coefficients. This is a strong indication for a systematic overestimation of memory related to errors in the model physics. Similar patterns of model over-/underestimation are found when ranking the observed correlations within the CMIP6 ensemble (not shown).

For a more detailed view of the internal model variability, we define four different memory regimes (winter persistence, winter long-term memory, summer persistence, and summer long-term memory regime; Figure A.2a) and compare the mean correlation coefficients for each of these memory regimes in the individual data products to their distribution in the MPI-GE and CMIP6 ensemble (Figure A.2b-e). The distributions of correlation coefficients in the MPI-GE and CMIP6 ensemble have a large overlap (75-90% depending on the memory regime), indicating that the MPI-ESM model behaves similarly to other CMIP6 models in terms of memory. The CMIP6 ensemble has a wider spread than the MPI-GE, which is expected due to the larger ensemble size and the variety of contributing models.

Comparing the model ensembles against observations, we find that for the winter persistence, winter long-term memory, and summer persistence regimes (Figure A.2b-d), despite some spread, all observational products show correlation coefficients that lie within the range of correlations simulated in both the CMIP6 ensemble and the MPI-GE. For the summer long-term memory (Figure A.2e), however, the correlations of all three observational data sets are below the model ensemble range (except for two CMIP6 ensemble members having a lower correlation than the NSIDC NASA Team and Bootstrap data). This indicates that the observations are not just an "outlier", but that climate models systematically overestimate the memory in the summer long-term regime. In the case of linearly detrended time series, the observed correlations are within the range of CMIP6 and MPI-GE internal variability, but also in the lower tail of the distribution (Figure A.7).

Note that qualitatively similar results are obtained when analyzing lagged correlations of pan-Arctic SIE (see Figures A.8 and A.9). As noted by Blanchard-Wrigglesworth et al., 2011b, SIE anomalies are slightly less persistent than SIA anomalies as they are more sensitive to dynamic wind forcing. Moreover, the SIE does not account for variations in the interior of the ice cover in summer. As a consequence, there is only a weak signal of simulated summer-to-summer reemergence for SIE. Observed summer-to-spring correlations are negative also for SIE, albeit lower in magnitude than for SIA, suggesting that both variations in the ice pack as well as in the position of the sea-ice edge are involved. Equally as for SIA, all observational data sets show correlations of SIE in the summer long-term memory regime that are below the model ensemble range.

### A.3.2 *Regional memory of sea-ice area*

To investigate whether some of the memory properties and differences between the data sets have a certain spatial origin, we analyze the memory of SIA on a regional level. As shown by Ordoñez et al., 2018, the memory of regional SIA can vary substantially between different Arctic basins: It is impacted on the one hand by the geographic location and associated ocean dynamics, and on the other hand by the seasonal cycle of the regional SIA and its variability. For simplicity, we here choose a variability-based regional separation, differentiating only between the SIZ, which is characterized by thin, seasonal ice in the vicinity of the ice edge, and the PIZ, which contains thick, multi-year ice in the center of the Arctic Ocean (see map in Figure A.3a). While the SIA of the SIZ has a pronounced seasonal cycle and year-round variability (Figure A.3b,d), the SIA of the PIZ is practically constant

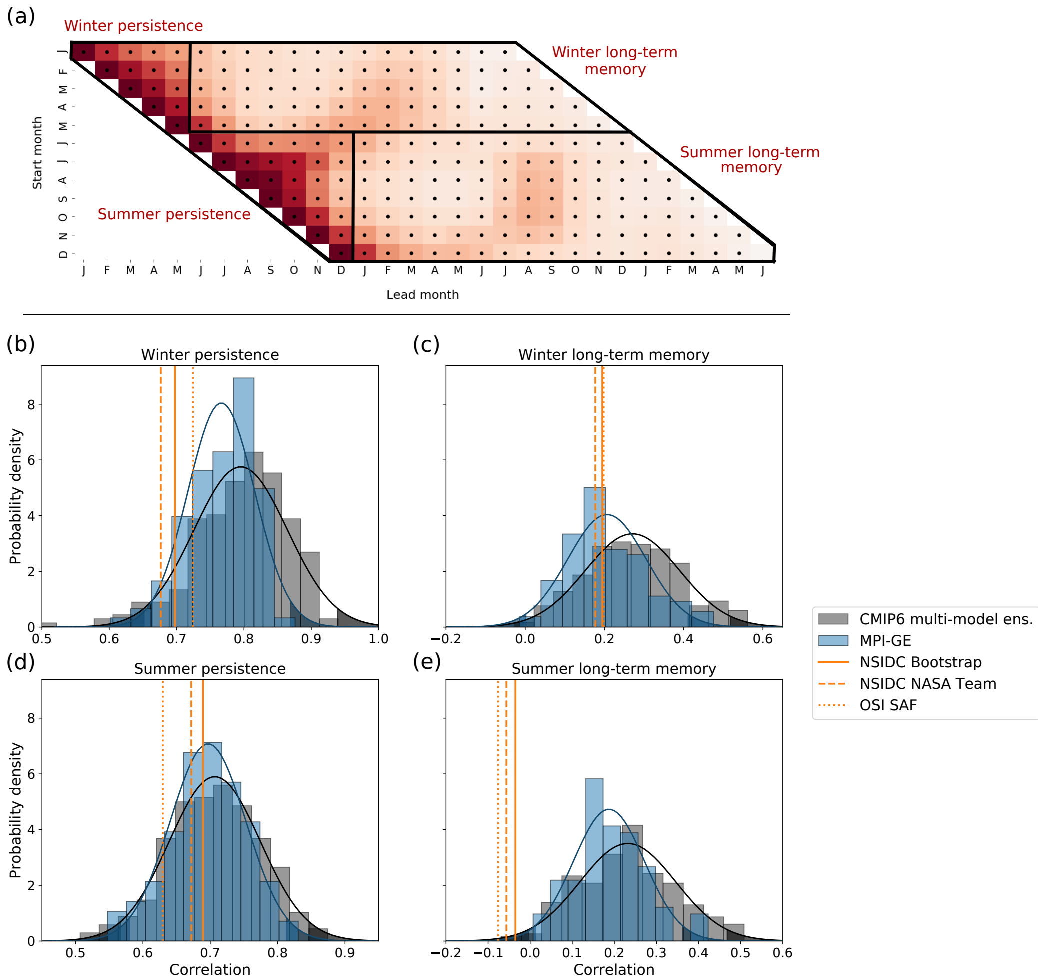


Figure A.2: (a) Definition of different memory regimes. (b-e) Distribution of mean correlation coefficients for the four different memory regimes shown as histograms for the Coupled Model Intercomparison Project phase 6 (CMIP6) multi-model ensemble (gray) and the Max Planck Institute Grand Ensemble (MPI-GE) (blue), and as lines for observational data sets (National Snow and Ice Data Center [NSIDC] Bootstrap, NSIDC NASA Team, and Ocean and Sea Ice Satellite Application Facility [OSI SAF] data). The black and blue lines show normal distribution fits to the CMIP6 and MPI-GE data, respectively. Shadings indicate the $2\sigma$-range.

throughout most of the year with a dip and substantial interannual variability in the months around the sea-ice minimum (Figure A.3c,e). From analyzing the lagged correlations between different combinations of SIZ, PIZ, and pan-Arctic SIA anomalies (Figure 3f-w), we can gain information on the spatial occurrence and origin of memory.

The different memory characteristics, identified on the pan-Arctic scale, show different regional occurrences. The persistence of SIA anomalies is strongly connected to the seasonal cycle. As both ice zones exhibit seasonal variations of ice area in summer, SIA anomalies of both SIZ (Figure A.3f,o) and PIZ (Figure A.3j,s) persist during summer and contribute to the summer persistence on the pan-Arctic scale (Figure A.3h,k,q,t). In winter, the ice area in the SIZ shows strong seasonal variations, while the ice area in the PIZ is practically constant. Thus, only the SIZ (Figure A.3f,o) shows a pronounced signal of winter persistence, reflected also on the pan-Arctic scale (Figure A.3h,q). The observations also show an intra-regional persistence of winter SIA anomalies in the PIZ (Figure A.3s) not present in the model. However, these correlations result from only small fluctuations of the otherwise full ice cover and do not transfer any memory to the pan-Arctic scale (Figure A.3t). Similar to the winter persistence, the melt-to-growth season reemergence is only apparent in the SIZ (Figure A.3, left column) but not in the PIZ (Figure A.3, middle column), as it is related to the imprint of SIA anomalies to the SST in the vicinity of the sea-ice edge. Overall, the regional memory in the persistence and winter long-term memory regimes is consistent between MPI-GE and observations.

The most striking result on the pan-Arctic scale is the overestimation of the summer long-term memory, which is characterized by a summer-to-summer reemergence in the model simulations and negative correlations in the observations. The inter-regional correlations show that summer SIA anomalies from both ice zones (especially from the SIZ) reemerge in the PIZ (Figure A.3, middle column) but barely in the SIZ (Figure A.3, left column). Albeit weaker than in the MPI-GE data, the reemergence signal is also present in the observations, implying that it is a real-world phenomenon and not just a model artifact. As the summer-to-summer reemergence is explained by an imprint of the SIA anomalies to the ice thickness that persists throughout the winter (e.g., Blanchard-Wrigglesworth et al., 2011b), its occurrence in the PIZ but not in the SIZ is plausible. In the SIZ, instead of a reemergence, the MPI-GE shows low, positive correlations in the summer long-term memory regime, whereas the observations show negative correlations in spring and summer of the next year. The observed negative correlations arise primarily from summer SIA anomalies in the PIZ (summer-to-spring, Figure A.3r) and to a smaller extent from summer SIA anomalies in the SIZ (mainly summer-to-summer, Figure A.3o).

Hence, the superposition of reemergence and negative correlations, as seen on the pan-Arctic scale, can be disentangled regionally and the discrepancies between model simulations and observations arise from a different relation between SIA anomalies in the SIZ and preceding summer anomalies. This finding is further reinforced by comparing the inter-regional lagged correlations in the observations to their internal model variability in the MPI-GE (Figures A.10 and A.11). While the memory of pan-Arctic summer SIA anomalies in the PIZ agrees well between the data sets, in the SIZ the correlation coefficients of all observational data sets are be-

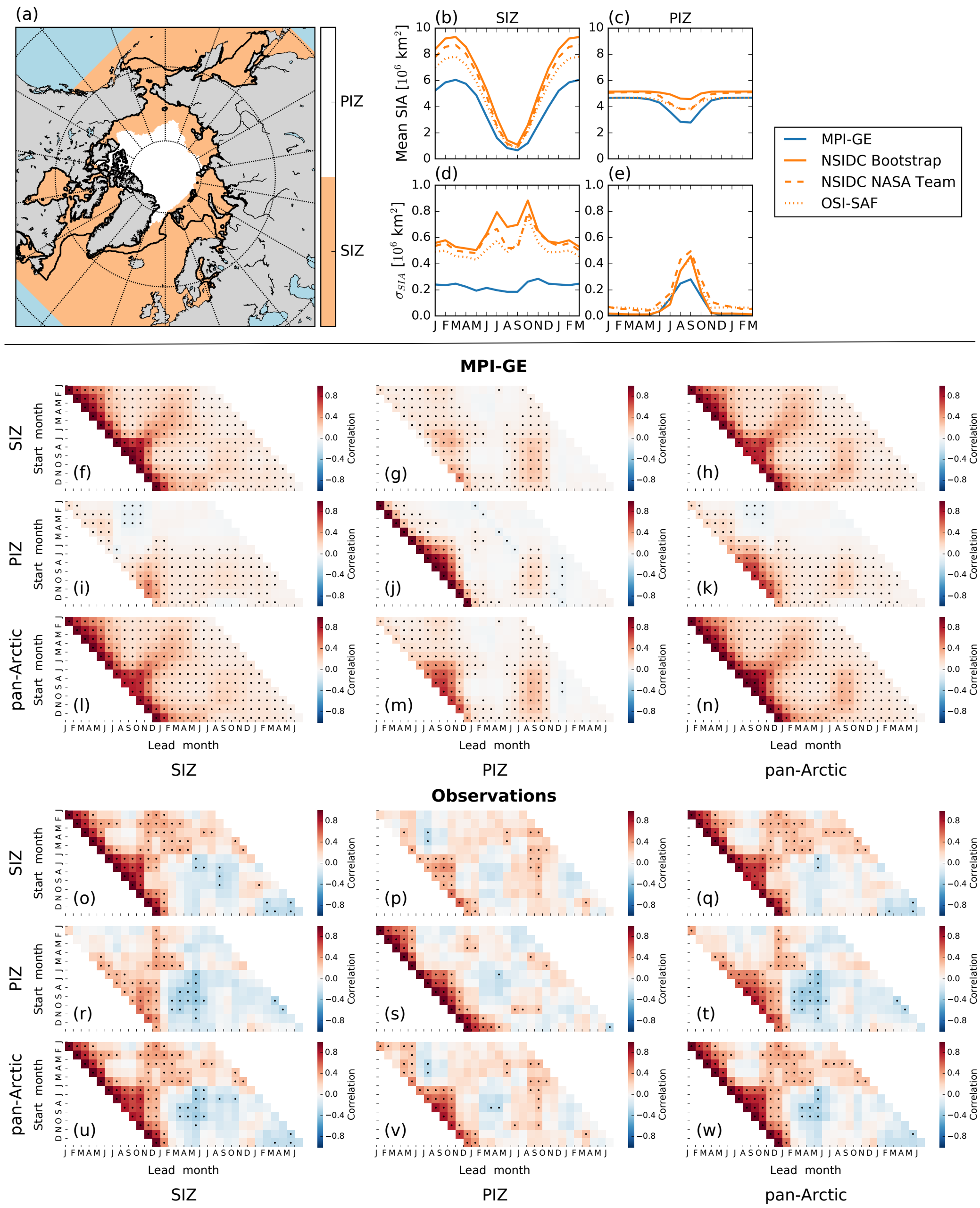


Figure A.3: (a) Map showing the geographical area of the perennial ice zone (PIZ; grid cells with September sea-ice concentration larger than 0.15 in 80% of the years in the National Snow and Ice Data Center [NSIDC] Bootstrap time series) and seasonal ice zone (SIZ; remaining grid cells). The bold black line indicates the average annual maximum sea-ice extent. (b,c) Seasonal cycle of mean sea-ice area in the SIZ and PIZ in Max Planck Institute Grand Ensemble (MPI- GE) and observational data sets. (d,e) Seasonal cycle of the standard deviation of sea-ice area in the SIZ and PIZ in MPI-GE and observational data sets (NSIDC Bootstrap, NSIDC NASA Team, and Ocean and Sea Ice Satellite Application Facility [OSI SAF] data). (d-l) Inter-regional lagged correlations between sea-ice area anomalies in the SIZ (upper row), PIZ (middle row), and entire Arctic (lower row) with succeeding sea-ice area anomalies in the SIZ (left column), PIZ (middle column), and entire Arctic (right column) in the MPI-GE. (m-u) Same as (d-l) but for the observational ensemble.

low the MPI-GE range of correlation values, indicating a significant overestimation of memory, similar to the pan-Arctic scale (Figure A.2e).

## A.4 DISCUSSION

We presented a comprehensive overview and comparison of Arctic sea-ice memory/persistence in a large set of model and observational data based on lagged correlations of SIA anomalies. Our results are consistent with previous studies (e.g., Blanchard-Wrigglesworth et al., 2011b; Day et al., 2014b; Krikken and Hazeleger, 2015) in identifying the same persistence and reemergence characteristics of pan-Arctic SIA and noting an overestimation of the memory from summer into the following year (summer long-term memory) in model simulations compared to observations. While previous studies point out the lack of summer-to-summer reemergence in observations, we additionally note an even larger discrepancy between models and observations in the persistence of summer anomalies into the following spring, where observational data consistently show negative correlations which are not found in model simulations. Comparing our results to Blanchard-Wrigglesworth and Bushuk, 2019, CMIP6 models show better agreement with observations than CMIP5 models, particularly in the winter-to-winter memory (see their Figure 1e). These differences could be related to model improvements or changes in the forcing, but may also be influenced by differences in the methodology (i.e., different time periods, detrending methods, and memory regime definitions).

Beyond that, this study shows the robustness of models overestimating the summer long-term memory in many aspects. By analyzing the distribution of lagged correlations in large model ensembles for the same period as the observational record, we show that the overestimation cannot be explained by internal variability. This reduces the likelihood of the discrepancy being caused by a "sampling error" due to the shortness of the observational time series as suggested by Day et al., 2014b. The overestimation is present not only within a single-model ensemble but also in the CMIP6 multi-model ensemble, showing its robustness across state-of-the-art GCMs. Moreover, the overestimation of summer long-term memory is independent of the considered observational data set. Using three observational data products (NSIDC Bootstrap, NASA Team, OSI SAF) that use different retrieval algorithms to determine SIC from satellite measurements, we reduce the uncertainty associated with observations. However, it should be noted that the discrepancy between model simulations and observations is related to SIC anomalies in the summer months, in which observations have their largest uncertainty due to the presence of melt ponds (e.g., Kern et al., 2020). Another factor of uncertainty is the applied method of detrending, which could either not fully capture the long-term trend or remove parts of the low-frequency internal variability. Applying a linear detrending instead of the LOWESS detrending, as done for instance by Blanchard-Wrigglesworth et al., 2011b and Day et al., 2014b, yields higher correlations and observed summer long-term memory correlations that are no longer outside the range of model internal variability, but still in the lower tail of the distribution (Figures A.6 and A.7). This could be due to the remaining non-linear part of the trend, which may be stronger in observations than model simulations.

While on the pan-Arctic scale the summer-to-summer reemergence is only detectable in model simulations, we could show that, in the PIZ, summer SIA anomalies reemerge also in observational data. The discrepancy between models and observations, however, is found in the relation between SIA anomalies in the SIZ and preceding summer SIA anomalies, where observational data show significant negative correlations not present in the model simulations. The negative correlations arise primarily from SIA anomalies in the PIZ, which suggests a non-local mechanism. However, a part of the negative correlations arises in the SIZ, indicating that also the position of the ice edge is involved. This is reinforced by the finding that the model overestimation of summer long-term memory is significant not only for pan-Arctic SIA but also for SIE (Figures A.8 and A.9). While the variability-based separation between PIZ and SIZ nicely disentangles the summer-to-summer reemergence from the negative correlations, it does not reflect the geographical complexity of the Arctic Ocean and regional sea-ice dynamics. As shown by Ordoñez et al., 2018, the strength of persistence and reemergence features strongly depends on the geographical location. Moreover, it should be noted that the fixed separation between SIZ and PIZ can only be an approximation as it does not reflect the changing mean sea-ice state in the period of interest. Still, our regional analysis provides guidance for future work identifying the causes of the discrepancy between models and observations.

The findings of this study have important implications for the predictability of sea ice. As previously suggested by Notz, 2017 and Blanchard-Wrigglesworth and Bushuk, 2019, the overestimation of memory of pan-Arctic SIA in the summer long-term memory regime could explain a part of the predictability gap between perfect-model experiments and operational forecasts (e.g., Bushuk et al., 2019). This would imply that perfect-model studies overestimate the potential predictability of pan-Arctic SIA arising from knowledge of summer sea-ice conditions and that the potential for improvement of sea-ice predictions is less strong than these studies suggest. Nevertheless, this can only be a partial explanation of the year-round predictability gap and does not diminish the potential for improved operational sea-ice predictions, for instance, through a better initialization. Moreover, there are additional sources of sea-ice predictability that are not considered here, such as ice thickness/volume and oceanic variables. Regarding future research, it should be of high priority to identify the causes of the overestimation of summer long-term memory in state-of-the-art GCMs.

## A.5 Conclusions

In summary, we draw the following conclusions from our analysis and data set-intercomparison of lagged correlations of Arctic SIA anomalies:

- The memory of pan-Arctic SIA from the summer months into the following year and beyond ("summer long-term memory") is significantly overestimated in model simulations compared to observations. Observed lagged correlations in this memory regime are below the range of internal model variability (MPI-GE) and inter-model variability (CMIP6 multi-model ensemble), showing that the result is robust across state-of-the-art climate models.

- The observed summer long-term memory can be disentangled regionally into a summer-to-summer reemergence in the perennial ice zone (PIZ) and negative correlations in the seasonal ice zone (SIZ). The observed negative relation between summer SIA anomalies in both ice zones, particularly in the PIZ, and succeeding spring and summer SIA anomalies in the SIZ is not present in model simulations, giving rise to the model overestimation.

- The results reinforce that a part of the predictability gap between potential and operational forecast skill of Arctic SIA could be caused by over-persistence of summer SIA in models.


### ACKNOWLEDGMENTS

This study is a contribution to the Cluster of Excellence 'CLICCS - Climate, Climatic Change, and Society', contribution to the Center for Earth System Research and Sustainability (CEN) of Universität Hamburg. The data analysis for this study was performed with computing resources from the German Climate Computing Center (Deutsches Klimarechenzentrum, DKRZ). The authors thank Jakob Dörr for providing processed CMIP6 data of sea-ice area. The authors acknowledge the World Climate Research Programme, which, through its Working Group on Coupled Modelling, coordinated and promoted CMIP6. The authors thank the climate modeling groups for producing and making available their model output, the Earth System Grid Federation (ESGF) for archiving the data and providing access, and the multiple funding agencies who support CMIP6 and ESGF. Open access funding enabled and organized by Projekt DEAL.


### DATA AVAILABILITY STATEMENT

All data used for this study are publicly available. The MPI-GE and CMIP6 data can be accessed from the ESGF (MPI-GE: `https://esgf-data.dkrz.de/projects/mpi-ge/`, CMIP6: `https://esgf-node.llnl.gov/projects/cmip6/`). The observational sea-ice concentration data sets are available online (NSIDC Bootstrap: `https://nsidc.org/data/nsidc-0079/`, NSIDC NASA Team: `https://nsidc.org/data/nsidc-0051`, OSI SAF: `www.osi-saf.org`).

This supporting information contains additional information on the methodological details of the lagged correlation computation (Text A1), a table listing all used CMIP6 models and their number of ensemble members (Table A.1), as well as several additional figures. Figure A.4 gives a visual impression of the applied detrending method. Figure A.5 shows the lagged correlations of pan-Arctic sea-ice area (SIA) for the individual observational and reanalysis products. Figures A.6 and A.7 show some of the main results based on linearly detrended time series and Figures A.8 and A.9 show the results for pan-Arctic sea-ice extent. Figure A.10 shows the percentile of MPI-GE members with lower inter-regional correlations than the observations and Figure A.11 shows the distribution of summer long-term memory correlations in the data sets on the regional scale.

**Text A1. Details of lagged correlation computation**

**Computation of sea-ice area.** From the different sea-ice concentration (SIC) data sets, we compute pan-Arctic SIA considering the whole Northern Hemisphere on the original grid and regional SIA after an interpolation on the NSIDC grid (25 km x 25 km resolution) by multiplying the SIC with individual grid-cell area. For the NSIDC data, we fill the observational pole hole with the average SIC around its edge. For OSI SAF data, we use the filled pole hole of the product itself. For the CMIP6 ensemble, we determine the pan-Arctic SIA as described in Notz and SIMIP Community, 2020.

**Detrending.** We detrend the monthly time series of SIA using locally weighted scatterplot smoothing (LOWESS; Cleveland, 1979), that is, a local weighted linear regression. We base the local regression on the nearest two-thirds of data points and perform three residual-based reweightings. For that, we use the Python module `smoothers_lowess` from the `statsmodels` package (`https://github.com/statsmodels/statsmodels/blob/master/statsmodels/nonparametric/smoothers_lowess.py`).

**Combined correlations.** To compute mean correlations for the ensembles, we combine the individual Pearson correlation coefficients $r$ of the ensemble members by applying a Fisher's $z$-transformation, averaging in $z$-space, and transforming back to $r$-space.

**Statistical significance.** We determine the statistical significance of the correlation coefficients based on two-tailed $p$-values tested against a null hypothesis of zero correlation. In the case of ensemble mean correlations, we need to take into account that individual ensemble members can have oppositely directed correlations, in which case the $p$-values should cancel out. To achieve that, we follow the following procedure: We compute the left- and right-tailed $p$-values for each member, combine them by applying Stouffer's method, re-convert the result to a two-tailed $p$-value (as no prior knowledge on the direction of the correlation is available), and determine statistical significance based on the smaller one of the two combined $p$-values.

Table A.1: Models and number of ensemble members contributing to the CMIP6 multi-model ensemble analyzed in this study.

| Model | # ens. members |
|---|---|
| ACCESS-CM2 | 2 |
| ACCESS-ESM1-5 | 3 |
| AWI-CM-1-1-MR | 5 |
| BCC-CSM2-MR | 3 |
| BCC-ESM1 | 3 |
| CAMS-CSM1-0 | 3 |
| CANESM5 | 25 |
| CESM2 | 11 |
| CESM2-WACCM | 3 |
| CESM2-WACCM-FV2 | 1 |
| CNRM-CM6-1 | 10 |
| CNRM-CM6-1-HR | 1 |
| CNRM-ESM2-1 | 5 |
| E3SM-1-0 | 5 |
| EC-EARTH3 | 5 |
| EC-EARTH3-VEG | 7 |
| FGOALS-F3-L | 1 |
| FIO-ESM-2-0 | 3 |
| GFDL-CM4 | 1 |
| GFDL-ESM4 | 1 |
| GISS-E2-1-G | 10 |
| GISS-E2-1-G-CC | 1 |
| GISS-E2-1-H | 10 |
| HADGEM3-GC31-LL | 4 |
| HADGEM3-GC31-MM | 4 |
| INM-CM4-8 | 1 |
| INM-CM5-0 | 10 |
| IPSL-CM6A-LR | 32 |
| MIROC-ES2L | 3 |
| MIROC6 | 10 |
| MRI-ESM2-0 | 5 |
| NESM3 | 5 |
| NORCPM1 | 30 |
| NORESM2-LM | 3 |
| NORESM2-MM | 1 |
| SAM0-UNICON | 1 |
| UKESM1-0-LL | 12 |
| all models | 240 |

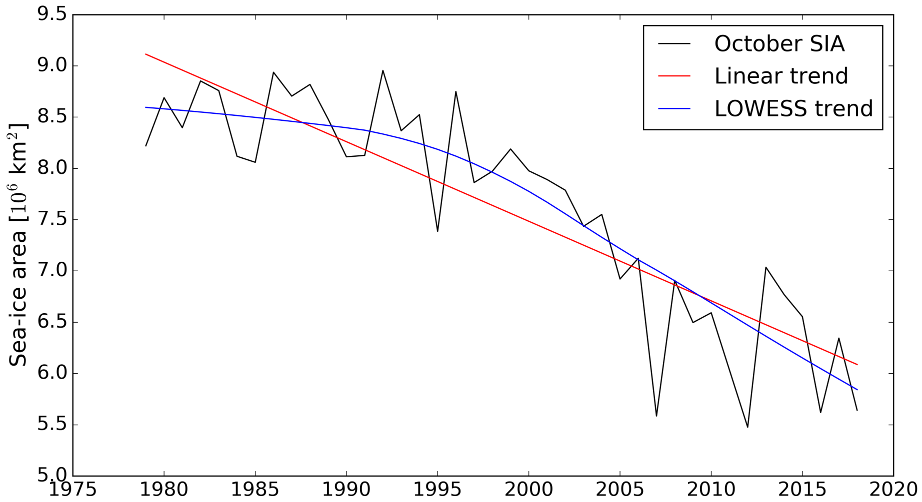


Figure A.4: NSIDC Bootstrap October pan-Arctic sea-ice area with trend determined via linear regression (red) and locally weighted scatterplot smoothing (LOWESS, blue).

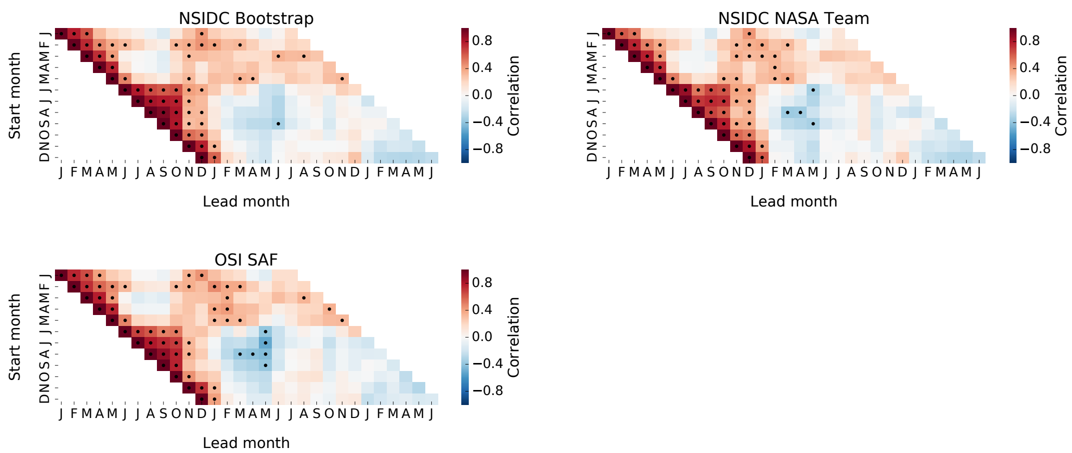


Figure A.5: Lagged correlations of monthly pan-Arctic sea-ice area anomalies in the individual observational products (NSIDC Bootstrap, NSIDC NASA Team and OSI SAF Climate Data Records). Black dots indicate statistical significance on the 99 % level.

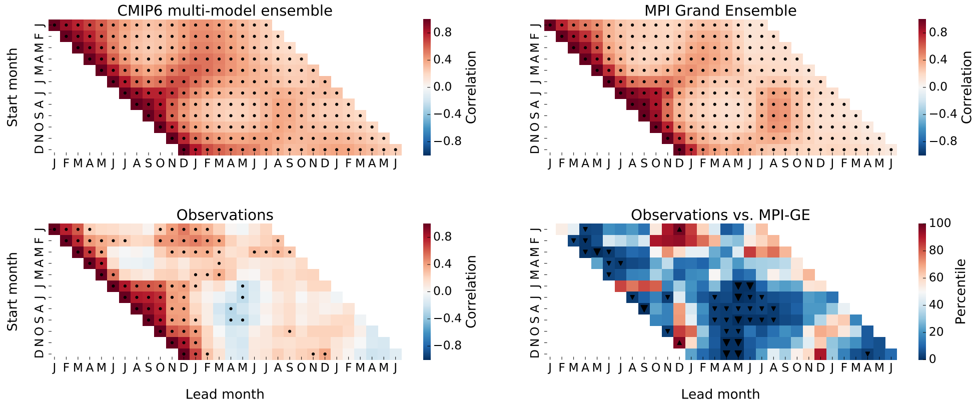


Figure A.6: Lagged correlations and percentile ranks as in Figure A.1a-d but based on linearly detrended time series of monthly pan-Arctic sea-ice area.

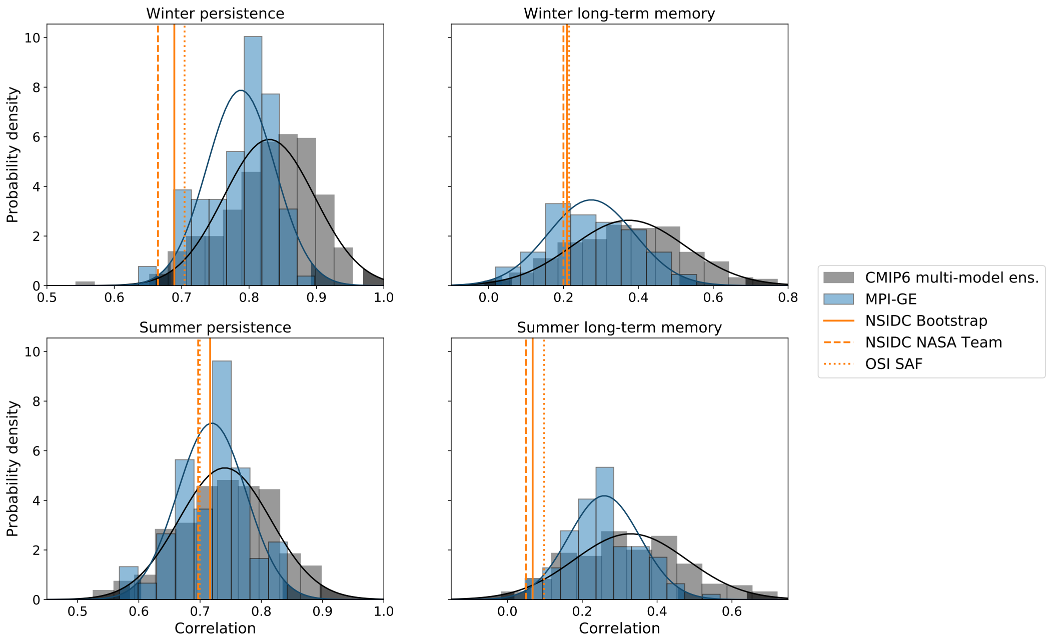


Figure A.7: Distribution of mean correlation values for the four different memory regimes as in Figure A.2b-e but based on linearly detrended time series of monthly pan-Arctic sea-ice area.

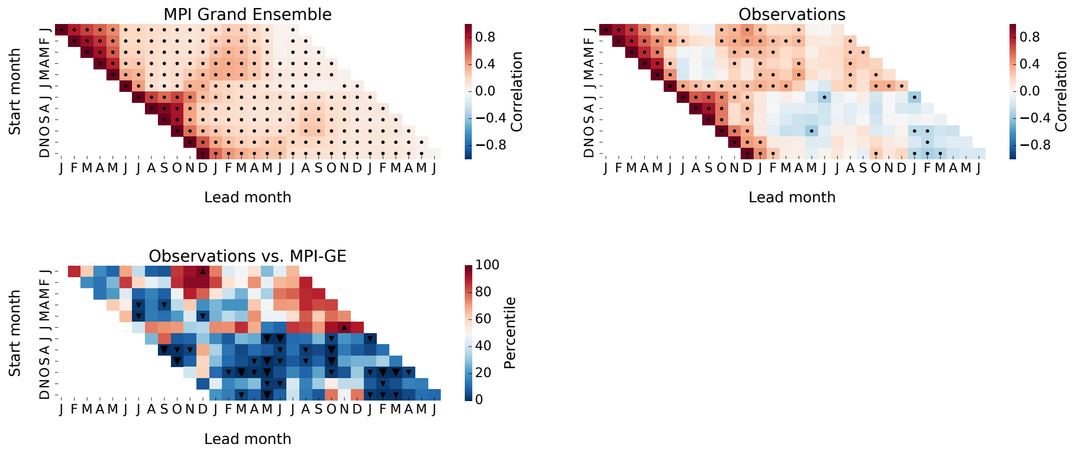


Figure A.8: Lagged correlations and percentile ranks as in Figure A.1b-d but for Arctic sea-ice extent.

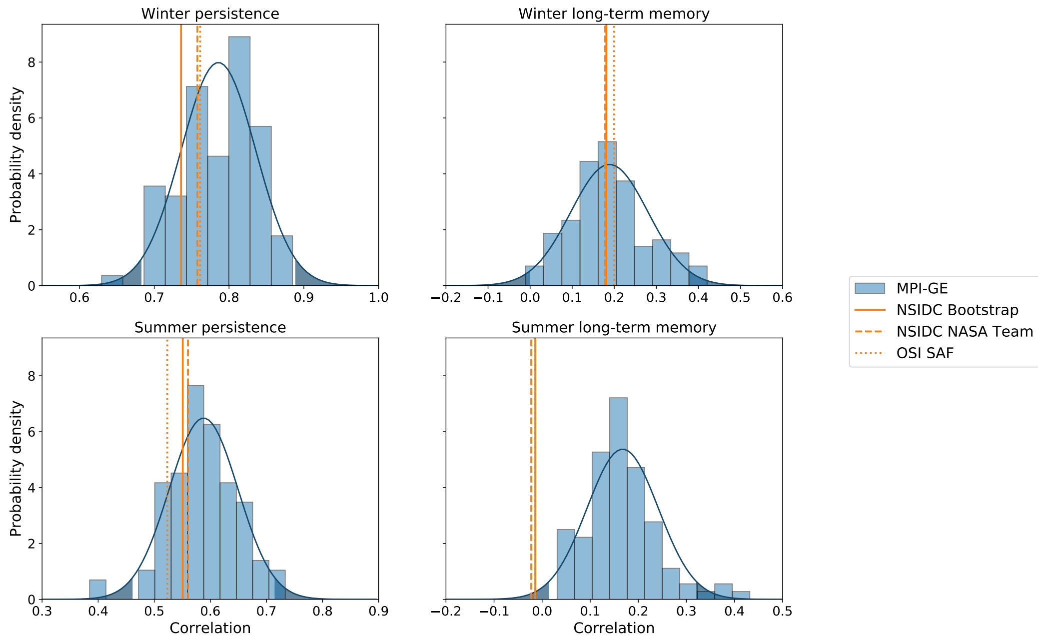


Figure A.9: Distribution of mean correlation values for the four different memory regimes as in Figure A.2b-e but for Arctic sea-ice extent.

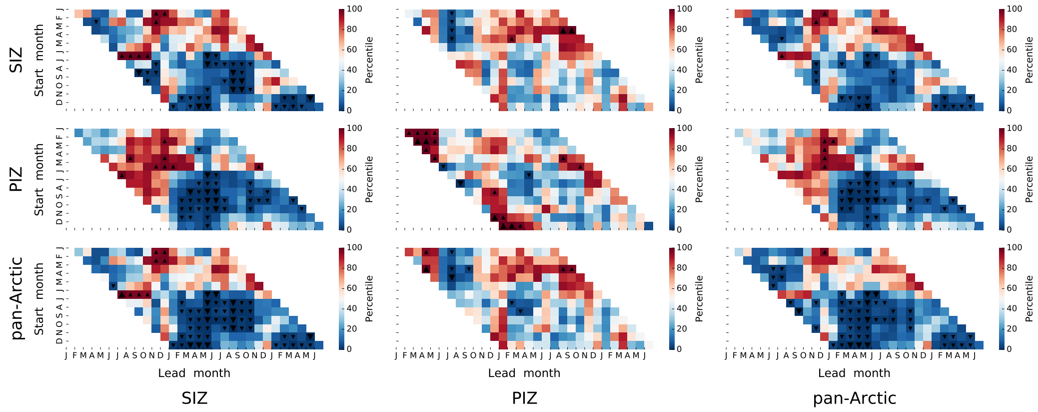


Figure A.10: Percentile of MPI-GE members with a lower correlation than observational data for inter-regional lagged correlations of SIZ, PIZ, and pan-Arctic sea-ice area anomalies as in Figure A.3. Downward and upward triangles mark values within the 5th and 95th percentile. Time lags with correlations coefficients outside of the model range (0th and 100th percentile) are marked with a larger triangle.

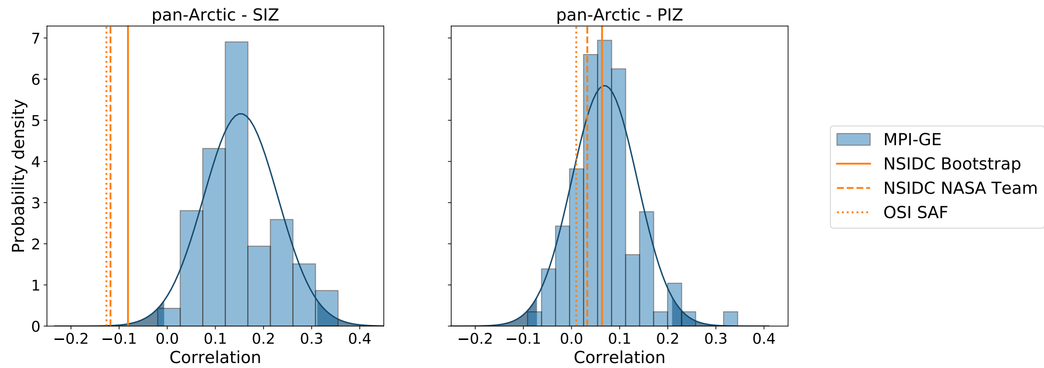


Figure A.11: Distribution of mean correlation in the summer long-term memory regime between pan-Arctic sea-ice area anomalies and succeeding (a) SIZ sea-ice area anomalies and (b) PIZ sea-ice area anomalies shown as a histogram for the MPI-GE (blue) and as lines for the observational data sets (orange). The blue line shows a normal distribution fit to the MPI-GE data; shadings indicate the $2\sigma$-range.

# B

# REDUCED TEMPERATURE VARIATIONS IN A WARMING ARCTIC CLIMATE SUBSTANTIALLY DAMPEN EXTREME TEMPERATURES

The work in this appendix will be submitted as:

Giesse, Céline, Dirk Notz, and Johanna Baehr. "Reduced temperature variations in a warming Arctic climate substantially dampen extreme temperatures" - *to be submitted.*

CG conceived and designed the study, performed the analysis, and wrote the paper. JB and DN contributed to the study design, discussed the results, and reviewed the manuscript. This work might be subject to further changes before it is submitted.

# Reduced temperature variations in a warming Arctic climate substantially dampen extreme temperatures

**Céline Giesse[1,2], Dirk Notz[1,3], Johanna Baehr[1]**

[1]Institute of Oceanography, Center for Earth System Research and Sustainability (CEN), Universität Hamburg, Hamburg, Germany

[2]International Max Planck Research School on Earth System Modelling, Hamburg, Germany

[3]Max Planck Institute for Meteorology, Hamburg, Germany

to be submitted

ABSTRACT

The Arctic is warming faster than any other region in the world. Not only the mean warming but also changes in temperature variability can translate into substantially altered climate extremes. Using state-of-the-art Earth system model large ensemble simulations, we show that the projected reduction of daily variations in Arctic surface air temperature with global warming substantially dampens the intensity of cold-season temperature extremes. The decreasing variability dampens the increase of warm extreme temperatures that would be caused only through mean warming by about 50% and amplifies the decrease in cold extreme temperatures at even higher rates. We further show that the reduction in daily temperature variations is mainly caused by a weakened seasonal temperature cycle, complemented by decreasing sub-seasonal temperature variability. The sharpest decrease in temperature variability occurs seasonally in autumn and regionally in the northern Barents Sea, driven by extensive sea-ice loss. Our results suggest that a warmer Arctic climate will be subject to fewer temperature variations and less extreme relative to its new mean temperature, which may ease adaptation to a new Arctic climate state.

## B.1 INTRODUCTION

The climate in the Arctic is changing faster than in any other region of the world and a new Arctic climate state is already emerging (Landrum and Holland, 2020). In recent decades, surface temperatures in the Arctic have warmed nearly four times faster than in the global average (Rantanen et al., 2022). This prominent feature of climate change is known as Arctic amplification (Serreze and Francis, 2006; Serreze and Barry, 2011; Previdi et al., 2021). Along with its mean warming, the Arctic is experiencing increasingly more extreme temperature events (Walsh et al., 2020), including summer heat waves in the terrestrial Arctic (Dobricic et al., 2020) and winter warming events over the Arctic Ocean (Graham et al., 2017; Moore, 2016). At the same time, cold extreme temperatures occur less frequently (Matthes et al., 2015; Sui et al., 2017). These trends are projected to continue in the future, with cold extremes generally warming faster than warm extremes (Seneviratne et al., 2021; Kharin et al., 2013; Sillmann et al., 2013; Donat and Alexander, 2012).

While extreme temperatures change along with the mean warming, they are even more sensitive to changes in temperature variability (Katz and Brown, 1992). In the global average as well as in many regions around the globe, the direction and magnitude of changes in temperature variability remain uncertain (Huntingford et al., 2013; Olonscheck et al., 2021). In the Arctic, however, the temperature variability has been robustly shown to decrease with global warming, particularly in the cold season and for variations on different timescales ranging from daily (Ylhäisi and Räisänen, 2014; Chen et al., 2019; Dai and Deng, 2021) over monthly (Holmes et al., 2016; Bathiany et al., 2018) to annual (Borodina et al., 2017; Olonscheck et al., 2021). This is primarily caused by the loss of sea ice, reducing the insulation between ocean and atmosphere and increasing the ocean's effective heat capacity (Stouffer and Wetherald, 2007; Huntingford et al., 2013; Borodina et al., 2017; Olonscheck et al., 2021). The decrease in temperature variability also extends to the northern mid-latitudes due to reduced thermal advection as the Arctic amplification weakens the meridional temperature gradient (Screen, 2014; Schneider et al., 2015; Holmes et al., 2016; Collow et al., 2019; Tamarin-Brodsky et al., 2020; Blackport et al., 2021; Dai and Deng, 2021). Moreover, the Arctic is also the region that experiences the strongest changes in the seasonal temperature cycle (Dwyer et al., 2012; Chen et al., 2019). Due to the seasonality of the Arctic amplification, which is strongest in late autumn and weakest in summer (Serreze and Barry, 2011; Rantanen et al., 2022), the amplitude of the Arctic's seasonal temperature cycle decreases with global warming (Dwyer et al., 2012; Chen et al., 2019; Bintanja and Van Der Linden, 2013). Although often neglected in studies of variability, changes in the seasonal cycle can contribute substantially to the experienced range of temperature variations (Thomson, 1995) and thereby impact the intensity of temperature extremes.

In this study, we show what temperatures can be expected in a warmer Arctic climate by providing a comprehensive analysis of projected changes in Arctic surface air temperature (SAT) under global warming. By jointly analyzing mean warming and changes in daily temperature variations, decomposed into contributions from inter-annual variability, sub-seasonal variability, and variability induced by the seasonal cycle (Fischer and Schär, 2009), we quantify their relative importance in altering warm and cold temperatures extremes in the different seasons. We base our analysis on five single-model initial-condition large ensembles (SMILEs; Deser et al., 2020) from the sixth phase of the Coupled Model Intercomparison Project

(CMIP6; Eyring et al., 2016). The SMILEs come with 30-50 ensemble members that simulate the climate under identical external forcing and model configurations but with slightly perturbed initial conditions, allowing us to derive robust estimates of internal temperature variability and extremes (Deser et al., 2020; Olonscheck et al., 2021). Unlike many previous studies, we quantify the response of Arctic SAT to global warming levels (GWLs), providing results that are independent of timing and warming scenario and therefore more useful to stakeholders and policymakers (IPCC, 2021d). The sampling of pre-industrial conditions and discrete GWLs of 1°C, 1.5°C, 2°C, and 3°C is illustrated in Fig. B.1a based on the MPI-ESM-LR model (see "Methods" for details). The response of Arctic mean (north of 66°N) daily SAT to increasing GWLs is characterized by an amplified warming and reduced variability subject to strong seasonality (Fig. B.1b) and a weakened and delayed seasonal cycle (Fig. B.1c). In the following, we demonstrate the changes in the distribution of daily Arctic SAT as a function of global warming for the five SMILEs. First, we show the mean warming; second, we show changes in temperature variability, decomposed into their different timescales; and third, we show changes in cold and warm extreme temperatures and quantify the contribution from mean warming and variability changes.

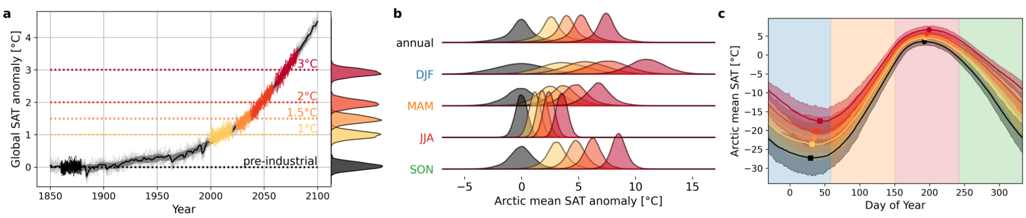


Figure B.1: **Arctic daily temperatures at different global warming levels (GWLs). a** Time-series of annual global-mean surface air temperature (GSAT) anomaly of each MPI-ESM-LR ensemble member (thin gray lines), their 20-year rolling averages (gray lines), and their ensemble mean (black line). The colored lines mark the different GWLs (pre-industrial, 1°C, 1.5°C, 2°C, 3°C global warming). Right edge: distributions of detrended GSAT anomalies for each GWL. **b** Distributions of detrended and deseasonalized annual, winter (DJF), spring (MAM), summer (JJA), and autumn (SON) daily Arctic-mean SAT anomalies for each GWL. **c** Seasonal cycle of detrended daily Arctic-mean SAT for each GWL. Lines show the mean seasonal cycle, shadings show the ensemble spread based on the 2.5th and 97.5th percentiles. The circles/squares mark the average day of minimum/maximum daily mean temperature.

## B.2 MEAN WARMING

The mean warming of the Arctic with global warming in the considered SMILEs is shown in Fig. B.2. The Arctic-mean SAT increases approximately linearly with global warming, as seen in Fig. B.2a based on the MPI-ESM-LR ensemble, and we compute the annual and seasonal Arctic amplification for all considered SMILEs as the linear trends of Arctic versus global SAT anomalies within the global-warming range of 0.5 - 4°C (Fig. B.2b). The ensemble-mean Arctic amplification ranges between 2.3 and 3.2 annually in the considered models and is subject to strong seasonality with the highest seasonal mean warming in winter (3.6 - 4.8),

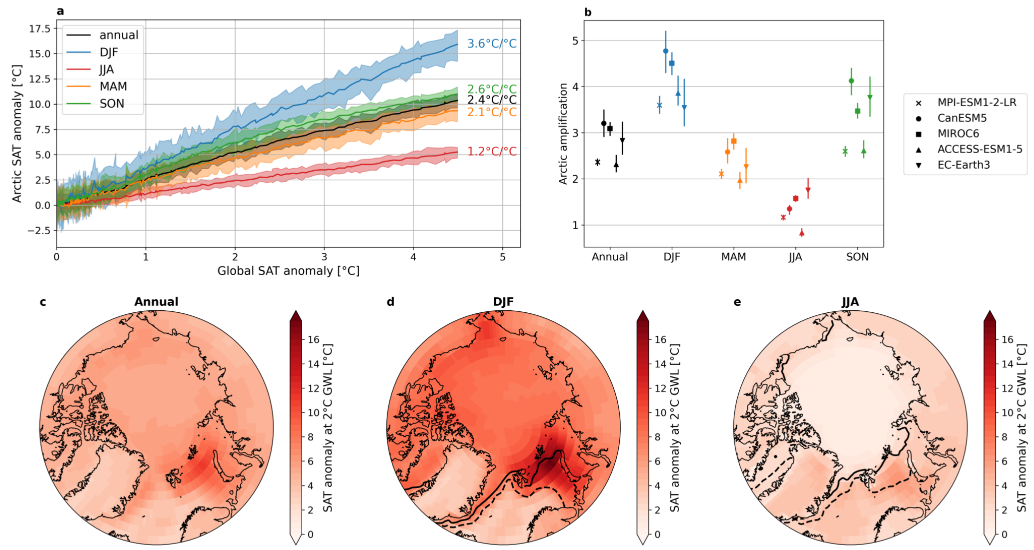


Figure B.2: **Mean warming of the Arctic. a** MPI-ESM-LR annual, winter (DJF), spring (MAM), summer (JJA), and autumn (SON) mean Arctic-mean SAT anomaly as a function of GSAT anomaly. Lines show the ensemble mean and shadings the ensemble spread based on the 2.5th and 97.5th percentiles. The annual/seasonal Arctic amplification factors, computed based on a linear regression within the 0.5 - 4°C global-warming range, are indicated. **b** Annual and seasonal Arctic amplification in the different climate models. Symbols show the ensemble mean, bars indicate the ensemble spread (2.5th - 97.5th percentile range). **c,d,e** Spatial signals of MPI-ESM-LR annual (c), winter (d), and summer (e) mean SAT anomalies in the Arctic domain at the 2°C GWL. For winter and summer, the average sea ice edge at pre-industrial conditions (dashed lines) and 2°C global warming (solid lines) are indicated.

followed by autumn (2.6 - 4.1), spring (2.0 - 2.8), and summer (0.8 - 1.8). These estimates of Arctic amplification are in good agreement with other model-based estimates reported in the literature (Holland and Landrum, 2021; Rantanen et al., 2022). However, climate models as a group have been shown to underestimate the observed Arctic amplification, at least in recent decades (Rantanen et al., 2022). Note further that the assumed linearity is only an approximation and that the rate of Arctic warming decreases for higher GWLs, particularly in autumn. This flattening is caused by a weakened ice-albedo feedback due to the loss of sea ice (Holland and Landrum, 2021; Ono et al., 2022), which is fastest around the sea-ice minimum in September. The Arctic becomes practically sea-ice free (i.e., sea-ice area $< 1$ million km$^2$) in September at about 2.1°C global warming in the MPI-ESM-LR ensemble average (Extended Data Fig. B.7).

Spatially, the warming of the Arctic is non-uniform (Fig. B.2c-e and Extended Data Fig. B.8). The strongest warming occurs in the northern Barents Sea with local winter warming of up to 17.5°C at the 2°C GWL, corresponding to a local Arctic amplification of almost nine times global warming. This hotspot of warming is also evident from observations (Isaksen et al., 2022) and is mainly caused by the loss of cold-season sea ice in that area and the resulting "Atlantification" of the northern Barents Sea (Lind et al., 2018; Polyakov et al., 2017). The weakest annual warming occurs over the northern North Atlantic and Greenland. In summer, there is practically no warming over the central Arctic Ocean as the sea-ice cover keeps the SAT at freezing temperature and all excess heat goes into melting the sea ice.

## B.3 Changes in variability of daily temperatures

The changes in daily SAT variability, measured as the standard deviation of the distribution, with global warming and the contributions from the seasonal cycle, day-to-day variations (sub-seasonal variability), and year-to-year variations (interannual variability) are shown in Figs. B.3 and B.4. Additionally, the composition of the total variability for each season based on the variance of the individual components can be seen in Extended Data Fig. B.9.

In the Arctic mean, the total variability of daily SAT (Fig. B.3a,e) is decreasing in all seasons except summer, in which the models project no changes or slight increases of variability (0 to +5% of pre-industrial variability per degree of global warming). The decrease in total daily variability is sharpest in autumn (-12 to -16%/°C), followed by spring (-5 to -9%/°C) and winter (-3 to -8%/°C). Over the entire year, the daily temperature variations decrease by -6 to -10% per degree of global warming. While annually, in winter, and in spring the variability decreases approximately linearly in the considered global-warming range, in autumn the decrease flattens with increasing GWL and ceases as the seasonal sea ice is lost completely (Extended Data Fig. B.7).

The seasonal cycle accounts for most of the temperature variations annually (about 83%) and in the shoulder seasons of spring and autumn (about 65%; Extended Data Fig. B.9). In these seasons, the seasonal cycle variability decreases with global warming (Fig. B.3b,f). Annually and in spring, it decreases by -5 to -9%/°C; in autumn it decreases even faster by -11 to -15%/°C, again related to the strong sea-ice loss in that season. In winter and summer, the seasons in which the seasonal temperature cycle turns directions, the variability induced by the seasonal cycle contributes considerably less to the total variability (about 15% in winter and 30% in summer, Extended Data Fig. B.9) and is projected to increase. The increase is particularly high in winter with relative changes ranging between +17 and +34%/°C, while it is more moderate in summer (0 to +5%/°C). The reason for the increase in the seasonal cycle variability in winter and summer is that not only the amplitude of the seasonal temperature cycle is reduced with global warming but also its phase is delayed, as can be seen from Extended Data Fig. B.11. As the turning points of the seasonal cycle are shifted away from the mid-points of the summer and, particularly, the winter season, the seasonal cycle-induced temperature variability gets more asymmetric and, therefore, increases, as can also be seen from Fig. B.1c. The phase delay of the seasonal cycle of surface temperatures in a warming climate is robustly simulated in climate models (Mann and Park, 1996; Dwyer et al., 2012; Chen et al., 2019) and has been attributed to the loss of sea ice and the accompanying increase in effective surface heat capacity slowing the temperature response (Dwyer et al., 2012; Hahn et al., 2022). Of course, the phase shift does not physically add any temperature variations over the course of a year but rather changes the timing of the seasons if they were defined based on temperature instead of their meteorological definition.

In winter and summer, the sub-seasonal variability dominates the total daily SAT variability with approximately 75% and 60%, respectively. Annually, in spring, and in autumn, the sub-seasonal variability is the second most contributor ($\approx$ 15%

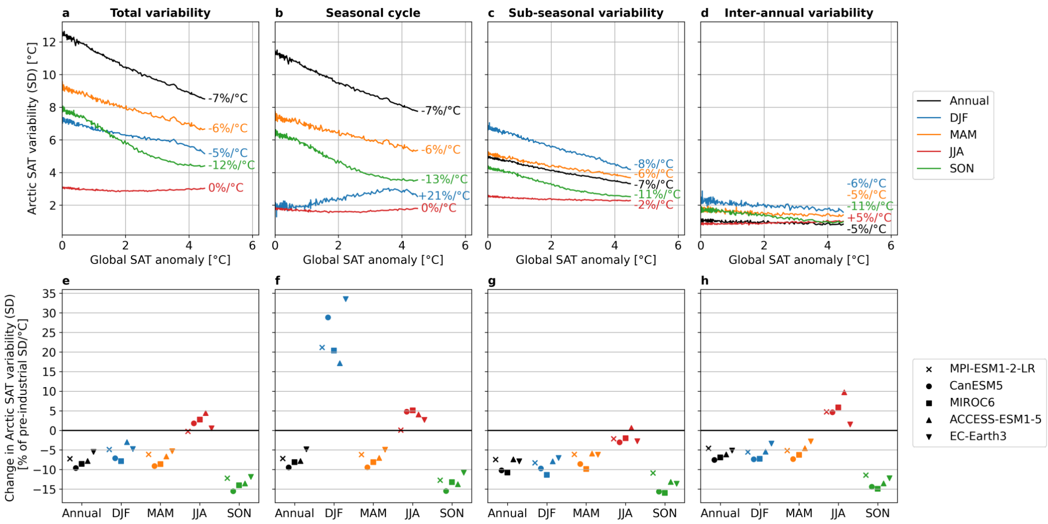


Figure B.3: **Arctic-mean changes in temperature variability and its components. a-d** MPI-ESM-LR annual and seasonal total variability (**a**), seasonal cycle variability (**b**), sub-seasonal variability (**c**), and inter-annual variability (**d**) computed as the standard deviation (SD) of grid-cell SAT averaged over the Arctic domain as a function of GSAT anomaly. The rates of change based on linear regression within the 0.5 - 4°C global-warming range are given as percentage changes relative to the pre-industrial value. **e-h** Multi-model comparison of the percentage change in annual and seasonal temperature variability components with global warming relative to their pre-industrial values.

annually; ≈ 30% for spring and autumn). It is projected to decrease in all seasons (Fig. B.3c,g). The strongest decrease in sub-seasonal variability occurs in autumn (-11 to -16%/°C), followed by winter and spring with a similar rate than annually (-6 to -11%/°C), and summer (-3 to +1%/°C).

The inter-annual variability contributes the least to the total daily SAT variability with about 2% annually, 5% in spring and autumn, and 10% in winter and summer. It decreases in all seasons (-11 to -15%/°C in autumn, -3 to -7%/°C in winter and spring, and -5 to -8%/°C annually) except for summer, in which it increases by +2 to +10%/°C (Fig. B.3d,h).

Spatially, the strongest reduction in total daily variability on annual timescales (Fig. B.4a) and in the cold seasons (winter, autumn, and spring; Fig. B.4b and Extended Data Fig. B.10a,b) occurs in the Barents Sea. Similar to the warming of this area, the decrease in variability is caused by the loss of cold-season sea ice. As the sea ice retreats permanently, shown by the sea-ice edges at pre-industrial conditions and 2°C global warming in Fig. B.4, it leaves behind open ocean. Due to its larger heat capacity, the ocean dampens the variability of near-surface temperatures (Borodina et al., 2017) on all considered timescales, that is, between seasons (seasonal cycle variability, 2nd row of Fig. B.4), within a season (sub-seasonal variability, 3rd row of Fig. B.4) and between years (inter-annual variability, 4th row of Fig. B.4). In autumn (Extended Data Fig. B.10b), this strong reduction in variability is not restricted to the Atlantic sector but occurs around the entire edge of the Arctic Ocean where sea ice is lost, particularly also in the Chukchi Sea, located at the connection to the Pacific.

Apart from the strong effect of sea-ice loss on local temperature variability, it affects the entire region, leading to a decrease in annual and cold-season total daily temperature variability nearly everywhere in the Arctic. The seasonal-cycle induced variability (2nd row of Fig. B.4) in spring, autumn, and annually decreases everywhere except for the North Atlantic and Greenland, similar to the pattern of winter mean warming that causes the reduction in the amplitude of the seasonal cycle. The increase in winter seasonal-cycle variability (Fig. B.4e) is less a result of changes in the amplitude than in the phase of the seasonal temperature cycle, as discussed previously. There is a clear spatial agreement between the increase of seasonal cycle variability in winter and the phase shift of the day of minimum SAT (Extended Data Fig. B.11d). While the sub-seasonal variability (3rd row of Fig. B.4) decreases in the entire Arctic, the inter-annual variability (4th row of Fig. B.4) increases in areas near the new sea-ice edge as they transition from being ice-covered every year to being ice-covered only in some years (Borodina et al., 2017). Since the ice extent is subject to year-to-year variations rather than day-to-day variations, this is also reflected in the variability of local SAT. It also explains the larger relative decrease in Arctic-mean sub-seasonal variability than in Arctic-mean inter-annual variability (Fig. B.3).

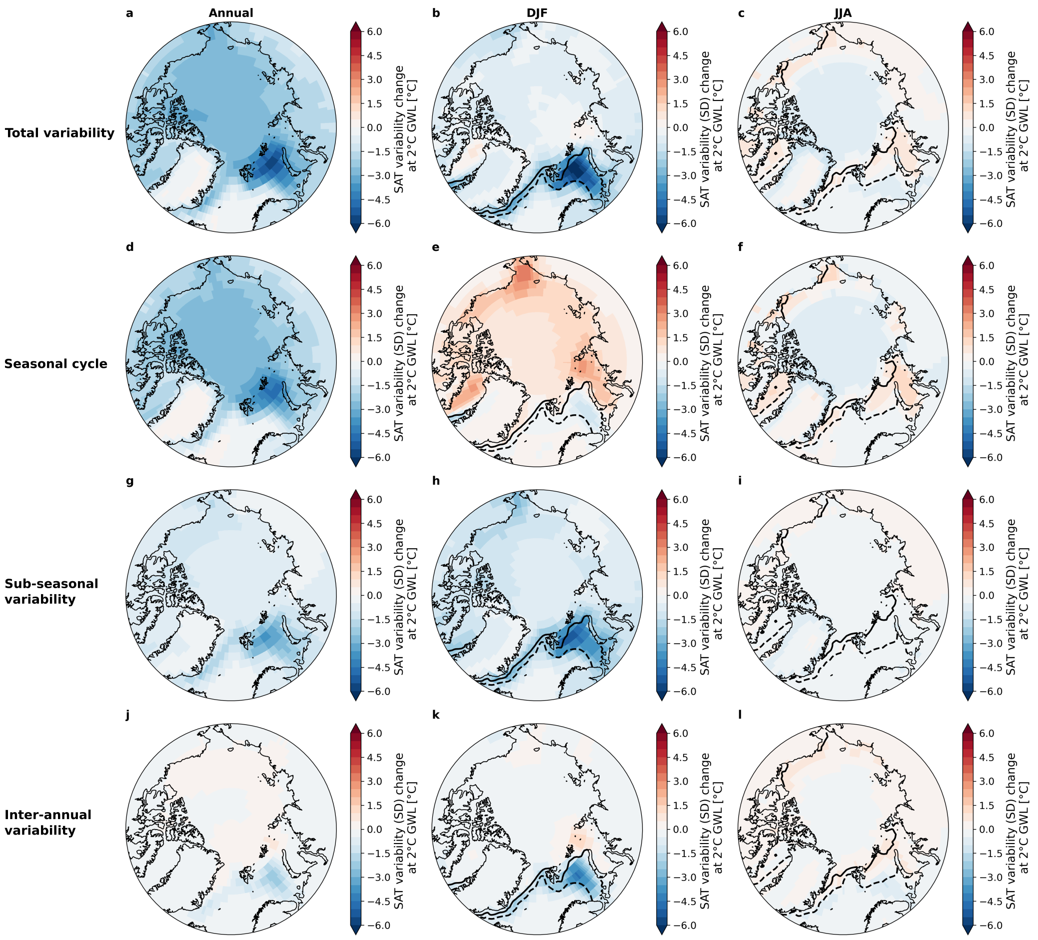


Figure B.4: **Spatial changes in Arctic temperature variability and its components.** Spatial signals of the changes in MPI-ESM-LR annual, winter, and summer (left to right) total variability, seasonal cycle, sub-seasonal variability, and inter-annual variability (top to bottom) of daily SAT at 2°C GWL compared to pre-industrial conditions. For winter and summer, the average sea-ice edge at pre-industrial conditions (dashed lines) and 2°C global warming (solid lines) are indicated.

In summer, the situation is different from the other seasons. The SAT variability over ice-covered areas is practically zero as the temperature stays more or less constant at the freezing point. When the ice-covered areas transition to open ocean, the temperature variability increases. On the one hand, this is due to increasing seasonal-cycle induced variability (Fig. B.4f) resulting from a phase shift in the day of maximum SAT. The phase shift in the day of maximum SAT is much more localized than in the day of minimum SAT (Extended Data Fig. B.11e). It shifts substantially in the regions where the summer sea ice is lost (locally up to 60 days at 2°C GWL), as the open ocean beneath can heat up during summer, thereby increasing the local temperature range of the seasonal cycle during summer. On the other hand, the inter-annual variability of SAT (Fig. B.4l) increases around the new sea-ice edge due to year-to-year variations in summer ice extent. Moreover, in summer, the inter-annual and sub-seasonal SAT variability in the terrestrial Arctic also increase slightly.

Generally, the projected changes in variability are consistent between the different models, differing by approximately ±5%/°C. Only for the positive changes in seasonal cycle variability in winter and inter-annual variability in summer, the ranges of projected relative changes are larger but still consistent in their direction. Spatially (not shown for other models than MPI-ESM-LR), the models consistently show the strongest variability changes in the areas where sea ice is lost, which is physically plausible (Huntingford et al., 2013; Olonscheck et al., 2021; Borodina et al., 2017; Stouffer and Wetherald, 2007). The findings are also consistent with previous studies showing decreasing annual and cold-season Arctic SAT variability (Olonscheck et al., 2021; Ylhäisi and Räisänen, 2014; Chen et al., 2019; Dai and Deng, 2021; Holmes et al., 2016; Borodina et al., 2017; Stouffer and Wetherald, 2007; Screen, 2014; Schneider et al., 2015; Collow et al., 2019; Tamarin-Brodsky et al., 2020; Blackport et al., 2021) as well as a decreasing and shifting seasonality of Arctic SAT (Dwyer et al., 2012; Chen et al., 2019). However, many of these studies do not focus on the Arctic, and they consider different timescales of variability, which we bridge by decomposing the total daily SAT variability. The consistent negative trend in Arctic daily SAT variability in climate models is less evident from atmospheric reanalyses (Davy and Outten, 2020; Chen et al., 2019), which show positive trends over the Arctic sea ice in March (Davy and Outten, 2020). The reason is, however, not clear and could be due to natural variability, poorly represented surface coupling processes in the climate models, or inaccuracies of the reanalysis (Davy and Outten, 2020).

## B.4 Changes in extreme temperatures - contributions from mean warming and variability

Knowing how the mean and variability of Arctic SAT are projected to change under global warming, we now look at how this translates into changes in extreme temperatures, that is, the tails of the temperature distribution. Note that, so far, we have analyzed variability changes only in terms of the distribution width, measured by its standard deviation. However, for non-Gaussian distributions, there can also be changes in the skewness, leading to asymmetric changes in the tails of the distribution. Here, we consider changes in both the warm and cold extremes (Fig. B.5) as a result of the mean warming (shift of the distribution) and variability changes (all changes in the shape of the distribution). We define the warm and cold extreme temperatures as the annual/seasonal maximum and minimum daily SAT in each year of each model simulation (see "Methods").

Considering the average seasonal extreme temperatures, we find that in the cold seasons of autumn (Fig. B.5d,e), winter (Fig. B.5a,e), and spring (Fig. B.5b,e), Arctic-mean cold extreme temperatures increase 2 - 3.5 times faster with global warming than Arctic-mean warm extreme temperatures (in the multi-model average). This is in line with the observed trend of cold extremes warming faster than warm extremes, globally and even more pronounced in the Arctic (Seneviratne et al., 2021). In summer (Fig. B.5c,e), warm and cold extreme temperatures warm at a similar rate. In numbers, the cold extreme temperatures warm strongest in autumn by 4.6°C to 7.2°C per degree of global warming in the different models, followed by winter (4.0 - 5.5°C/°C), spring (3.2 - 4.4°C/°C), and summer (0.9 - 2.0°C/°C). The warm extremes warm strongest in winter (2.1 - 2.6°C/°C), followed by autumn (1.3 - 1.9°C/°C), summer (1.1 - 1.8°C/°C), and spring (0.8 - 1.5°C/°C) with comparable rates. The increase of the extreme temperatures is approximately linear with global warming except for autumn cold extremes, for which the curve flattens substantially with increasing GWL as the September sea ice is lost (Extended Data Fig. B.7).

The cold extremes in autumn, winter, and spring warm not only faster than the respective warm extremes but also faster than the seasonal mean temperature. At the same time, the warm extremes warm slower than the mean. This is also true for the annual absolute extreme temperatures compared to the annual mean temperature. This finding is consistent with the projected decrease in variability and has also been shown to occur for large parts of the Northern Hemisphere extratropical land areas (Gross et al., 2019, 2020). As a result, the annual and cold-season extreme temperature ranges decrease with global warming and both warm and cold extremes become less intense relative to the new mean temperature in a warmer Arctic climate (Fig. B.5f).

The changes in the difference between extreme and mean temperatures (Fig. B.5g), also referred to as "excess changes" (Gross et al., 2019, 2020), are only due to changes in the variability (including all contributions from the seasonal cycle, sub-seasonal variability, and inter-annual variability) and are not necessarily symmetric for warm and cold extremes. The excess changes are largest in autumn (-1.3 to -2.5°C/°C for warm extremes and +2.0 to +3.1 °C/°C for cold extremes), followed by spring (-0.9 to -1.6°C/°C for warm extremes and +1.0 to +1.9°C/°C for cold extremes) and the annual timescale (-1.0 to -1.7°C/°C for warm extremes and +1.2 to +2.2°C/°C for cold extremes). In these seasons, the positive excess changes in cold extremes are somewhat larger than the negative excess changes in warm extremes, that is, the intensity of cold extremes relative to the new mean decreases more than that of warm extremes. Conversely, in winter, the intensity of warm extremes relative to the new winter mean temperature decreases substantially more (excess changes of -1.3 to -2.3°C/°C) than the intensity of cold extremes (excess changes of +0.2 to +0.7°C/°C), indicating a change in skewness towards the left/cold side of the temperature distribution. In summer, warm and cold extremes warm at a similar but slightly faster rate than the seasonal mean temperature, which expresses in positive excess changes of 0 to +0.3°C/°C for warm extremes and +0.1 to +0.2°C/°C for cold extremes in the Arctic-mean. It is remarkable that the cold extremes warm at the same or higher rate than the mean temperature despite slightly increasing variability, indicating a highly asymmetric change in the summer temperature distribution towards a positive skew favoring warm extreme temperatures. The

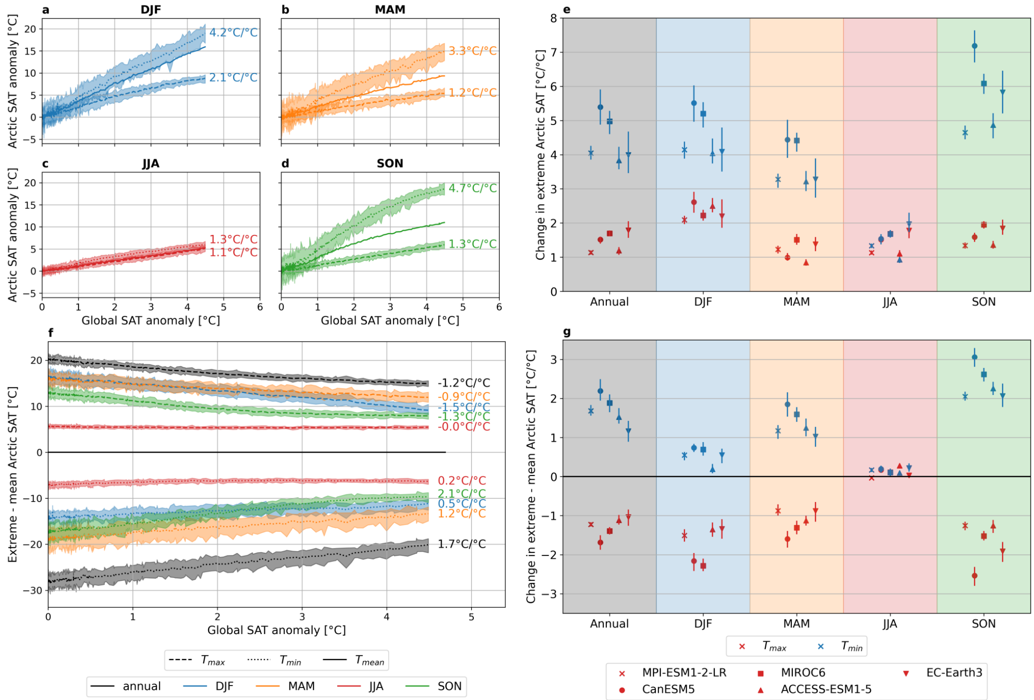

Figure B.5: **Changes in Arctic-mean extreme temperature intensity. a-d** MPI-ESM-LR Arctic-mean (**a**) winter, (**b**) spring, (**c**) summer, and (**d**) autumn mean SAT anomaly ($T_{mean}$, solid lines, as in Fig. B.2a), average warm extreme SAT anomaly ($T_{max}$, dashed lines), and average cold extreme SAT anomaly ($T_{min}$, dotted lines) as a function of GSAT anomaly. **e** Multi-model comparison of the rates of change of annual and seasonal extreme temperatures with global warming for warm extremes (red) and cold extremes (blue) based on linear regression within the 0.5 - 4°C global-warming range. **f** Difference between annual and seasonal extreme temperatures $T_{max}/T_{min}$ and mean temperatures $T_{mean}$ as a function of global warming. **g** Multi-model comparison of the rates of change of annual and seasonal extreme and mean temperature differences ("excess changes") with global warming for warm extremes (red) and cold extremes (blue) based on linear regression within the 0.5 - 4°C global-warming range. The shadings in **a-d,f** and the bars in **e,g** show the ensemble spread based on the 2.5th and 97.5th percentiles.

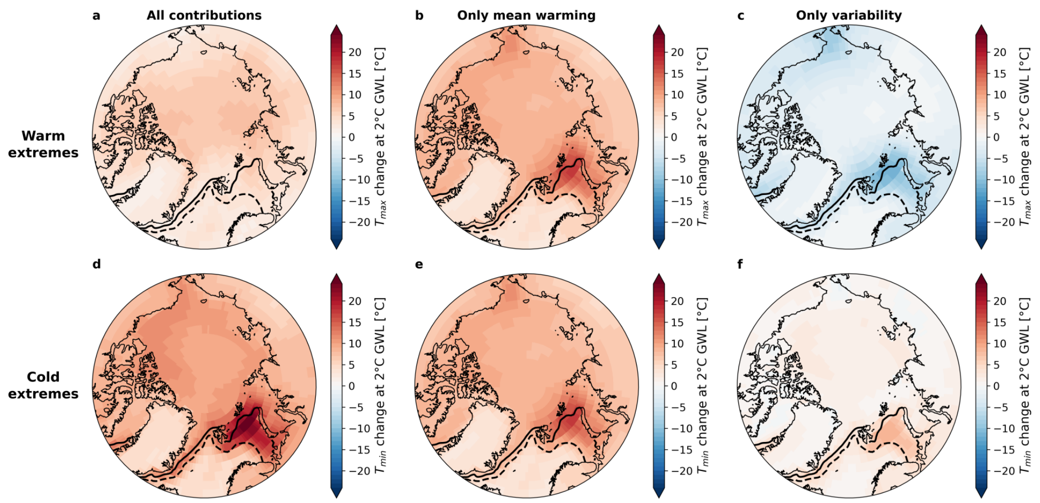


Figure B.6: **Spatial changes in winter extreme temperature intensity.** Spatial signals of changes in MPI-ESM-LR winter average warm extreme temperatures (**a**) and cold extreme temperatures (**d**) at 2°C GWL compared to pre-industrial conditions and their contributions from mean warming (**b/e**) and variability (**c/f**). The dashed and solid lines indicate the average winter sea-ice edge at pre-industrial conditions and 2° GWL, respectively.

asymmetric changes in extreme temperatures emphasize the importance of taking into account changes in skewness in addition to variance changes (Tamarin-Brodsky et al., 2020).

Comparing the magnitude of excess changes (Fig. B.5g) and mean warming (Fig. B.2b), we find that the largest part of the extreme temperature changes (Fig. B.5e) can be explained by the mean warming but a substantial part is also caused by the changes in variability. Considering the multi-model average, the increases in warm extreme temperatures that would be caused solely through a shift in mean temperature are dampened by about 50% annually, in winter, spring, and autumn through the reduced variability, while increases in cold extreme temperatures are amplified by 74% in autumn, about 60% annually and in spring, and only 13% in winter. Increases in summer warm and cold extreme temperatures through mean warming are both amplified by about 12% through changes in variability.

For winter, we exemplarily show the spatial signals of changes in warm and cold extremes and the contribution from the mean warming and variability (excess changes) at 2°C GWL in Fig. B.6. The interplay of mean warming (Fig. B.6b,e) and decrease in variability (Fig. B.6c,f), both particularly strong in the northern Barents Sea, intensifies an increase in cold extreme temperatures, which locally increase by more than 20°C in the Barents Sea at the 2° GWL in the MPI-ESM-LR model (Fig. B.6d). For the warm extremes, however, the decrease in variability counteracts the strong mean warming, and while overall the warm extreme temperatures increase, they do not increase stronger in the Barents Sea than in other parts of the Arctic (Fig. B.6a). The changes in variability affect the warm extremes more than the cold extremes in winter (Fig. B.6c,f), particularly near the new sea-ice edge. This is primarily due to asymmetric changes in the sub-seasonal variability (Extended Data Fig. B.12). The spatial signals of warm and cold extreme temperature changes and the respective contributions from mean warming and the variability components for spring, summer, and autumn can be seen from Extended Data Figs. B.13-B.15. Changes in the seasonal cycle and the sub-seasonal variability impact the intensity of extreme temperature to different extents in different seasons, whereas the inter-annual variability (not shown) is negligible for the occurrence of extreme temperatures.

## B.5 CONCLUSIONS

We use state-of-the-art CMIP6 large ensemble simulations to assess the projected response of Arctic daily SAT to global warming. While isolated aspects such as the Arctic amplification, changes in temperature variability, seasonality, or extremes have been studied before, here we consider the bigger picture: By jointly analyzing changes in mean temperature and variability, decomposed into sub-seasonal, seasonal, and inter-annual contributions, we quantify their relative importance in altering extreme temperatures at different levels of global warming.

We find that the largest part of the changes in annual and seasonal extreme temperatures is due to mean warming, but variability changes substantially dampen the intensity of extreme temperatures. The decreasing variability of daily SAT, annually and in the cold seasons of autumn, winter, and spring, dampens the increase of warm extreme temperatures by about 50% and amplifies the increase of cold extreme temperatures even more (except in winter). As a result, cold extreme temperatures warm 2 to 3.5 times faster than warm extreme temperatures, and relative to the new mean temperature, the extremes become less intense in a warmer Arctic climate. An exception is the summer season, in which there are only small, positive changes in SAT variability, and warm, cold, and mean temperatures increase at similar rates. We further find that the variability induced by the seasonal cycle and the sub-seasonal variability are the dominant contributors to the total daily SAT variability, depending on the season, while the contribution from inter-annual variability is small and negligible for the occurrence of extreme temperatures. Locally, the largest changes in both the mean SAT and its variability occur over the ocean areas that transition from ice-covered to open ocean, affecting particularly the northern Barents Sea. The strong local mean warming and changes in variability act together to greatly reduce the local intensity of cold extremes without increasing the local intensity of warm extremes more than in the rest of the Arctic. As the sea ice declines most rapidly in September, the autumn season experiences the fastest reductions in Arctic-mean SAT variability.

The drastic changes in Arctic temperatures due to amplified global warming, illustrated in this study, have severe consequences for Arctic communities and ecosystems (Constable et al., 2022). At the same time, we show that a warmer Arctic climate will be less extreme and subject to fewer temperature variations. As increased temperature variations pose a greater risk to species than mean climate warming (Vasseur et al., 2014), the reduced temperature variability may ease the adaptation to a warmer Arctic climate.

*Data*

We analyze data from five single-model initial condition large ensembles (SMILEs) from the latest CMIP6 (Eyring et al., 2016) generation of climate models that provide at least 30 ensemble members, namely: MPI-ESM1.2-LR (30 members), CanESM5 (Swart et al., 2019) (50 members), MIROC6 (Tatebe et al., 2019) (50 members), ACCESS-ESM1.5 (Ziehn et al., 2020) (40 members), and EC-Earth3 (Döscher et al., 2022) (50 members). We combine historical simulations (years 1850-2014; for EC-Earth3 data is available only starting from year 1970) and future projections (years 2015-2100) from the high-emission SSP5-8.5 scenario.

Our primary variable of interest is surface air temperature (SAT). We compute annual-mean global-mean surface air temperature (GSAT) and analyze the response of daily mean SAT in the Arctic domain, defined here as latitudes of 66°N-90°N. Temperature anomalies are computed with respect to the pre-industrial period from 1850-1900 (consistent with the Intergovernmental Panel on Climate Change (IPCC) conventions (IPCC, 2021d)). The later initial year in the EC-Earth3 model is corrected for by computing anomalies with respect to the period 1970-2000 and adding the difference between the periods 1970-2000 and 1850-1900 from the MPI-ESM-LR model. We further use monthly sea-ice concentration data to show seasonal average sea-ice edges (Figs. B.2d,e, B.4), defined as the 15%-contour line of sea-ice concentration, and the September northern-hemisphere sea-ice area (Extended Data Fig. B.7).

As the analysis is based on climate model simulations, it is not per se given that they provide an accurate representation of the real world. Comparisons with atmospheric reanalyses show that CMIP6 models commonly have a cold bias in Arctic winter SAT related to overestimated sea-ice extents and simulate overly high inter-annual variability of winter SAT (Davy and Outten, 2020; Cai et al., 2021). There is some considerable inter-model spread in how well CMIP6 models capture Arctic SAT and its tempo-spatial variability, with the MPI-ESM-LR model being among the top ranking models (Cai et al., 2021).

*Global warming levels*

Instead of looking at specific time periods in the climate model simulations, we evaluate the response to different levels of global warming. We do this in two ways:

On the one hand, we look at the continuous global-warming dependence by evaluating Arctic SAT against the respective ensemble-mean GSAT anomaly (black line in Fig. B.1a) in each simulation year. For plotting purposes (Figs. B.2a, B.3a-e), the time series are reordered by GSAT in ascending order. As global warming is accelerating over time, there are more data points at low than at high global warming.

On the other hand, we analyze Arctic SAT at discrete global warming levels (GWLs) by selecting representative data samples for the climate at pre-industrial conditions, 1°C, 1.5°C, 2°C, and 3°C of global warming using a time sampling approach (James et al., 2017) (colored lines in Fig. B.1a). We follow the methodology used by the IPCC (IPCC, 2021d; Seneviratne et al., 2021): For each individual ensemble member, we identify the year in which the 20-year rolling average GSAT anomaly first reaches the given GWL and include the 20-year period around this year into the data sample. Due to internal variability, the timing of the considered 20-year periods can differ between ensemble members but their average GSAT anomaly always corresponds to the target GWL. For the pre-industrial conditions, we simply take the 20-year period 1860-1879 for all ensemble members. To remove the warming trend from the GWL samples, we subtract the linear trend of the ensemble mean 20-year SAT time series at each day of year and grid cell from each ensemble member.

Due to the large ensemble sizes of the considered model simulation, the GWL-sampling approach provides large data samples of 600 to 1000 (depending on the ensemble size of the model) simulation years per GWL. This allows for a more detailed and robust analysis of variability and extremes than the continuous GWL approach where every simulation year is considered individually, that is, the sample size equals the ensemble size.

Note that we perform the analysis based on projections under the high-emission scenario SSP5-8.5, that is, for a rapidly warming climate. The climate response to global warming can differ between transient and equilibrium climate states (King et al., 2020). However, for quickly-responding variables, such as the SAT, the scenario dependence is relatively small (Seneviratne et al., 2021). Performing the same analysis based on SSP1-2.6 scenario simulations (not shown) indicates that there are differences in the spatial signal of the Arctic SAT response, but in the Arctic-mean the results are largely independent of the emission scenario.

*Variability decomposition and computation*

The variability of daily temperatures can be decomposed into different components. We follow the approach of Fischer and Schär, 2009 and decompose the total variability $\sigma_{\text{tot}}$, defined as the standard deviation (SD) of all daily mean temperatures in a year or season at a certain GWL, into contributions from inter-annual variability ($\sigma'$), sub-seasonal variability ($\sigma''$), and variability induced by the seasonal cycle ($\hat{\sigma}$). The daily mean temperature anomaly $T_{y,d}$ on day $d$ and in year $y$ with respect to the annual/seasonal mean temperature $\bar{T}$ within a GWL-sample can be expressed as

$$T_{y,d} = \hat{T}_d + T'_y + T''_{y,d}, \tag{B.1}$$

where $\hat{T}_d$ is the mean seasonal cycle relative to $\bar{T}$, $T'_y$ is the annual/seasonal mean temperature anomaly to $\bar{T}$ in year $y$, and $T''_{y,d}$ is the residual daily temperature anomaly. The decomposition implies $\sum_d \hat{T}_d = 0$, $\sum_y T'_y = 0$, and $\sum_y T''_{y,d} = \sum_d T''_{y,d} = 0$ and therefore independence of the individual temperature contributions. The total variance can hence be written as

$$\begin{aligned} \sigma^2_{\text{tot}} &= \frac{1}{YD} \sum_{y=1}^{y} \sum_{d=1}^{D} T^2_{y,d} && \text{(B.2)} \\ &= \frac{1}{YD} \sum_{y=1}^{y} \sum_{d=1}^{D} (\hat{T}_d + T'_y + T''_{y,d})^2 && \text{(B.3)} \\ &= \hat{\sigma}^2 + \sigma'^2 + \sigma''^2, && \text{(B.4)} \end{aligned}$$

where $\hat{\sigma}^2 = \frac{1}{D}\sum_{d=1}^{D}\hat{T}_d^2$ is the variance induced by the seasonal cycle, $\sigma'^2 = \frac{1}{Y}\sum_{y=1}^{Y}T_y'^2$ is the inter-annual variance, and $\sigma''^2 = \frac{1}{YD}\sum_{y=1}^{Y}\frac{1}{D}\sum_{d=1}^{D}T_{y,d}''^2$ is the sub-seasonal variance.

As the variances of the individual temperature components add up to the total variance, their relative variability contributions can be quantified based on the variance (Extended Data Fig. B.9). Note that variance and standard deviation are only robust measures of scale for normal or at least symmetric distributions. While inter-annual and sub-seasonal temperature variations are approximately symmetric, the temperature variations of the seasonal cycle are asymmetric/skewed, particularly at the turning points of the seasonal cycle, i.e. in summer and winter. This introduces a deviation between total temperature variance and the sum of the variances of the individual temperature components, which in the Arctic mean is about 10% in summer, 6% in winter, 2% in spring and autumn, and negligible on the annual timescale.

We apply the variability decomposition to both the continuous and discrete GWL approach. In the continuous approach, each year is considered individually and the ensemble members form the data sample for the corresponding GWL. Instead of computing the variability across years in time, we compute the inter-annual and sub-seasonal variability across ensemble members, i.e. $\sum_y$ is replaced by $\sum_n$, where $n$ denotes the number of the ensemble member. These two approaches of estimating internal variability are consistent following the quasi-ergodic assumption (Hingray and Saïd, 2014; Olonscheck and Notz, 2017). In the discrete approach, where the GWL samples consist of 20 simulation years per ensemble member, we compute the variability across both years in time and ensemble members, i.e. $\sum_y$ is replaced by $\sum_{y,n}$.

Where we show Arctic-mean SAT variability (Fig. B.3), we compute the variability as the spatial average of the local temperature variability computed at grid-cell level. Note that this is different from the variability of spatially averaged temperature, which is considerably smaller as local variability is suppressed by averaging over the spatially correlated temperature field.

### *Extreme temperatures*

Various approaches exist to define temperature extremes. While often peak-over-threshold approaches are applied, we here use the simpler approach of block maxima/minima to determine warm/cold temperature extremes. We compute warm/cold extreme temperatures $T_{\max}/T_{\min}$ as the maximum/minimum daily mean SAT of a season or the full year in each simulation year and ensemble member for every grid-cell. When showing the Arctic mean (Fig. B.5), the spatial average is performed after computing the extremes at grid-cell level. The results in Figs. B.5, B.6 are based on the average extreme temperature at the respective GWL. The GWL-samples of $T_{\max}/T_{\min}$, which follow a generalized extreme value (GEV) distribution, also allow the computation of their return levels (not shown here).

To determine the contributions from mean warming, total variability and the different variability components to the extreme temperatures (Fig. B.6, Extended Data Figs. B.12-B.15), we re-compute the extremes based on adjusted data samples, in which only the temperature component ($\bar{T}$, $\hat{T}_d$, $T_y'$, $T_{y,d}''$) of interest corresponds to the target GWL-sample, while the other temperature components correspond to pre-industrial conditions.

Note that extreme temperatures are often defined based on daily maximum and minimum temperatures (TXx, TNn). Here, we consider the extremes of daily mean temperatures ($T_{\mathrm{max}}$, $T_{\mathrm{min}}$) to be consistent with the previous parts of the analysis, but an analysis of TXx and TNn gives qualitatively similar results (not shown).

*Linear regression coefficients*

Based on the continuous GWL approach, we compute rates of change (e.g. of Arctic-mean temperature, temperature variability, and extreme temperatures; Figs. B.2a,b, B.3, B.5) with global warming as the regression coefficient of an ordinary least squares (OLS) linear regression. For mean and extreme temperatures, we compute the regression coefficients for each individual ensemble member and show the ensemble mean and ensemble spread as the 2.5th - 97.5th percentile range. In order to not over-represent the historical period with low global warming and to assure comparison of identical global-warming ranges between the climate models, we limit the linear regression to data points within the range of 0.5°C to 4°C of global warming. For temperature variability, we give the rates of change in percent of the temperature variability at zero global warming in the respective climate model based on the regression constant (Fig. B.3f-j).


## ACKNOWLEDGMENTS

This study is a contribution to the Cluster of Excellence 'CLICCS - Climate, Climatic Change, and Society', contribution to the Center for Earth System Research and Sustainability (CEN) of Universität Hamburg. The data analysis for this study was performed with computing resources from the German Climate Computing Center (Deutsches Klimarechenzentrum, DKRZ). We acknowledge the World Climate Research Programme, which, through its Working Group on Coupled Modelling, coordinated and promoted CMIP6. We thank the climate modeling groups for producing and making available their model output, the Earth System Grid Federation (ESGF) for archiving the data and providing access, and the multiple funding agencies who support CMIP6 and ESGF. We thank Armineh Barkhordarian and Dirk Olonscheck for providing constructive feedback on an earlier version of this manuscript that helped shape this study.


## DATA AVAILABILITY STATEMENT

All data used for this study are publicly available. The CMIP6 data can be accessed from the ESGF (`https://esgf-data.dkrz.de/search/cmip6-dkrz/`).

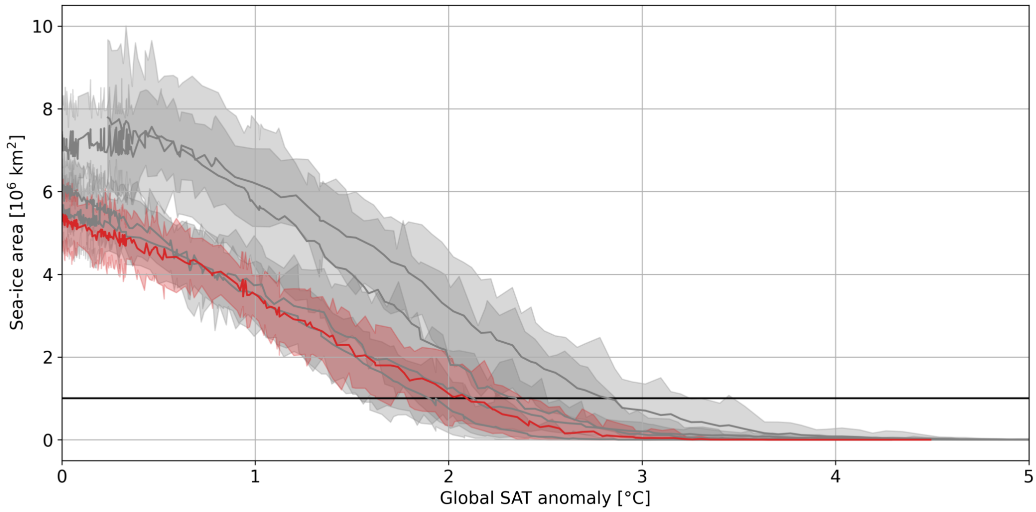


Figure B.7: **Arctic summer sea-ice evolution.** September northern-hemisphere sea-ice area as a function of GSAT anomaly in the different SMILEs. The MPI-ESM-LR model is highlighted in red, the other models are shown in gray. Lines show the ensemble mean and shadings the ensemble spread based on the 2.5th and 97.5th percentiles. Based on the ensemble mean and the threshold of $10^6$ km$^2$ (black line), the September sea ice is lost between 1.9°C and 2.9°C of global warming. In the MPI-ESM-LR model, the September sea ice is lost around 2.1°C global warming.

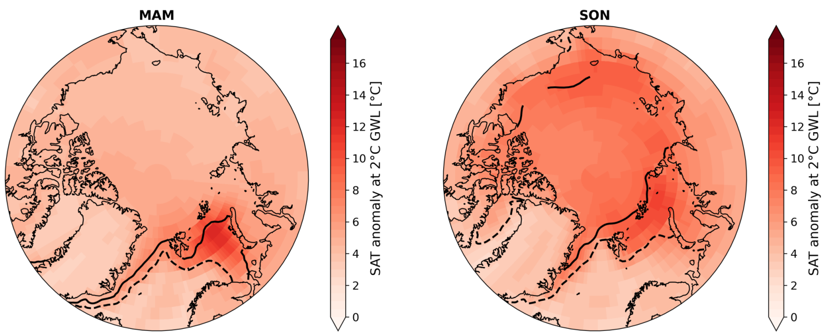


Figure B.8: **Spatial signals of spring and autumn mean warming.** Same as Fig. B.2c-e but for spring (MAM) and autumn (SON).

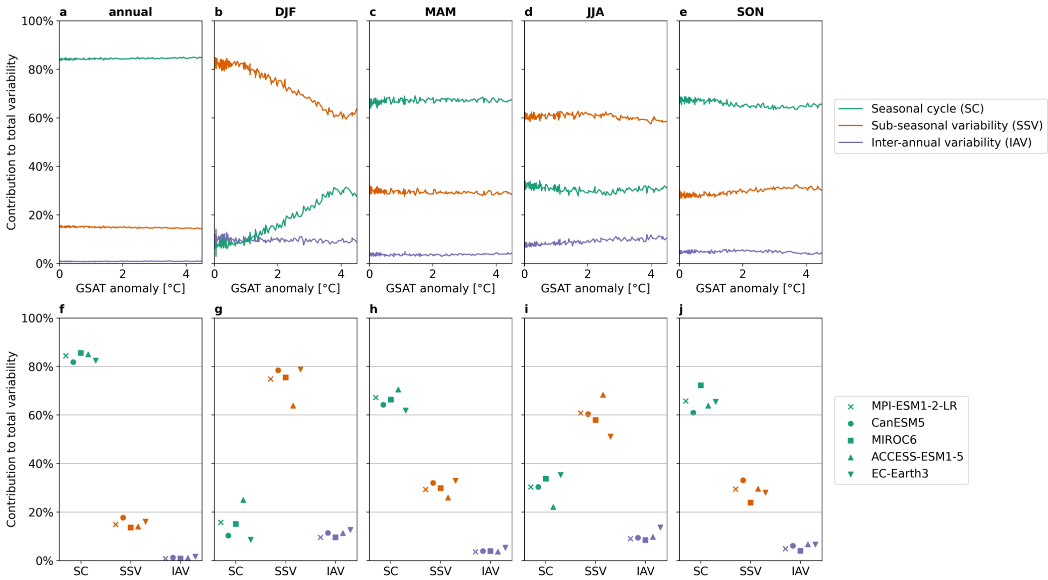


Figure B.9: **Relative contributions of temperature variability components. a-e** Annual and seasonal relative contributions of seasonal cycle-induced variance, sub-seasonal variance, and inter-annual variance to the total variance of grid-cell SAT, averaged over the Arctic domain, as a function of GSAT anomaly in the MPI-ESM-LR model. **f-j** Multi-model comparison of the annual and seasonal contributions of the three variability components averaged over the 0.5 - 4°C global-warming range.

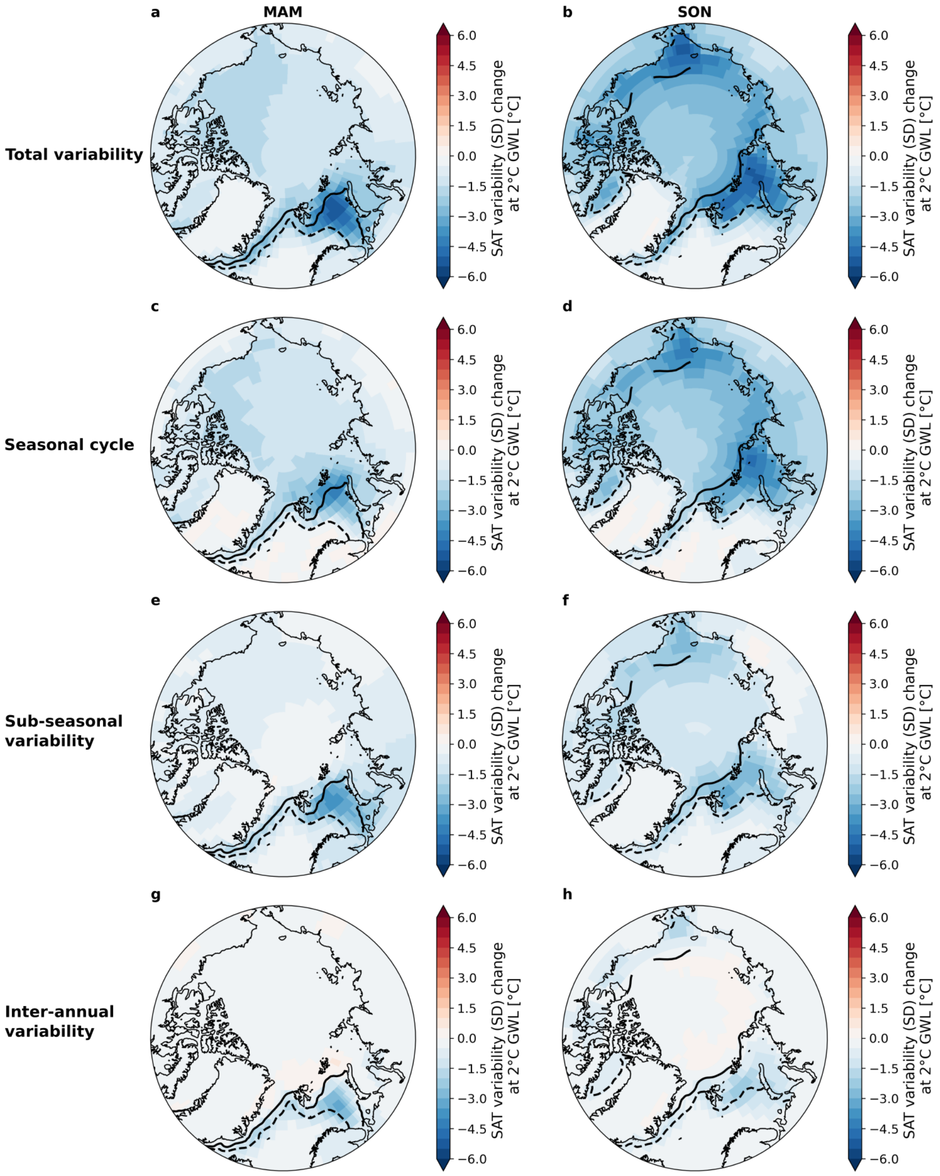


Figure B.10: **Spatial changes in spring and autumn Arctic temperature variability and its components.** Same as Fig. B.4 but for spring (MAM) and autumn (SON).

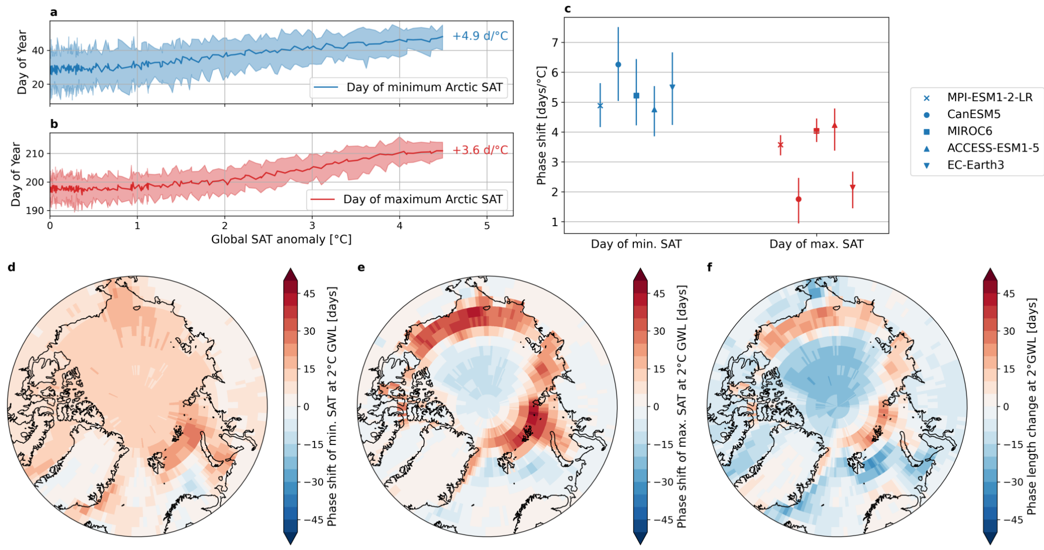


Figure B.11: **Phase shift of the seasonal temperature cycle. a,b** Arctic-mean average day of minimum/maximum daily, grid-cell SAT as a function of GSAT anomaly in the MPI-ESM-LR model. The rates of change based on linear regression within the 0.5 - 4°C global-warming range are indicated. **c** Multi-model comparison of the phase shift of the day of minimum and maximum SAT, based on their rates of change within the 0.5 - 4°C global-warming range. **d-f** Spatial signals of the phase shift in the day of minimum daily SAT (**d**), maximum daily SAT (**e**), and the difference between the days of maximum and minimum SAT (phase length, **f**) at 2°C GWL compared to pre-industrial conditions in the MPI-ESM-LR model.

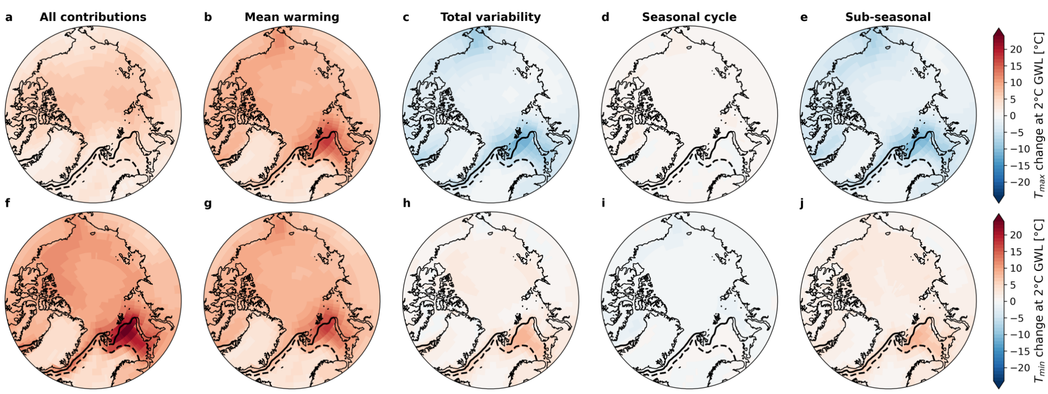


Figure B.12: **Spatial changes in winter extreme temperature intensity and their different contributions.** Same as Fig. B.6 with additional panels showing the contributions from seasonal cycle (**d,i**) and sub-seasonal (**e,j**) variability. The contribution from inter-annual variability is not shown as it is practically zero.

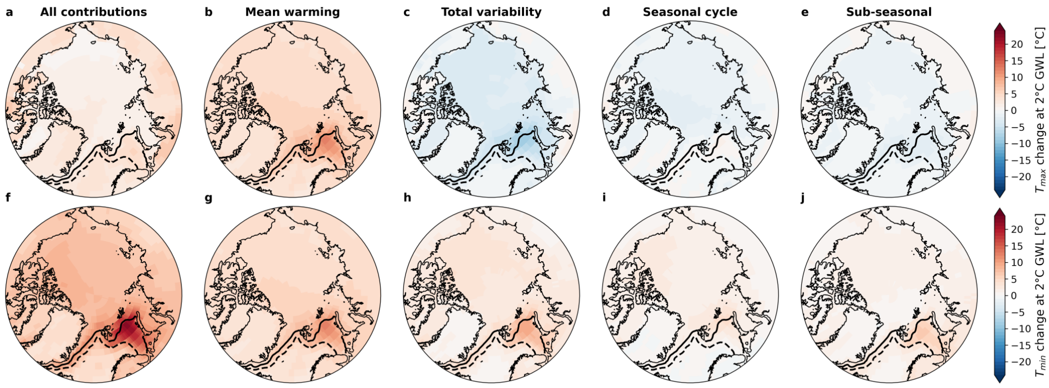


Figure B.13: **Spatial changes in spring extreme temperature intensity and their different contributions.** Same as Fig. B.12 but for spring (MAM).

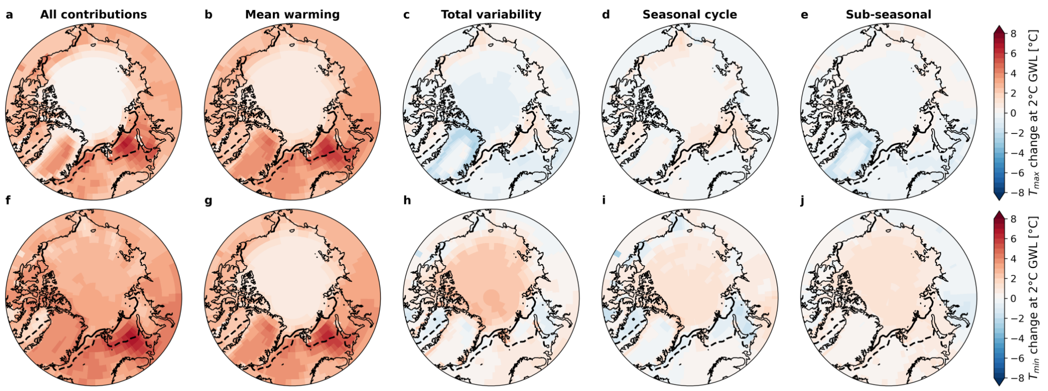


Figure B.14: **Spatial changes in summer extreme temperature intensity and their different contributions.** Same as Fig. B.12 but for summer (JJA).

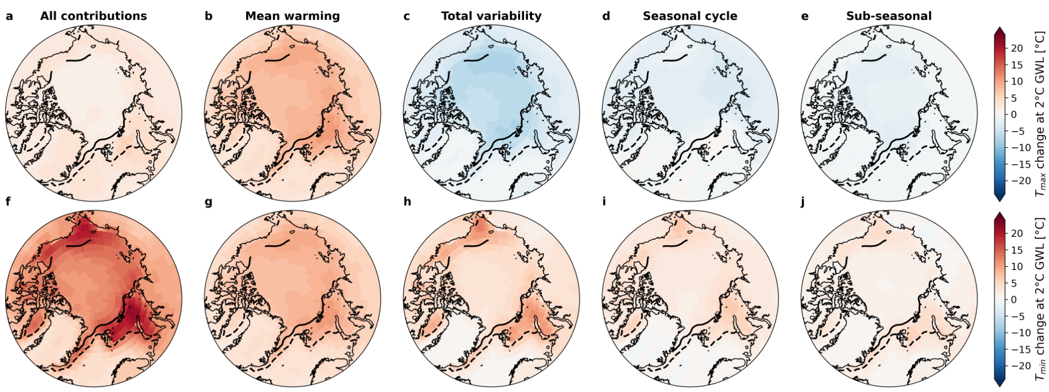


Figure B.15: **Spatial changes in autumn extreme temperature intensity and their different contributions.** Same as Fig. B.12 but for autumn (SON).

# BIBLIOGRAPHY


AMAP (2021). “Summary for Policy-makers.” In: *Arctic Climate Change Update 2021: Key Trends and Impacts*. Tromsø, Norway: Arctic Monitoring and Assessment Programme (AMAP), pp. 1–16.

Armstrong McKay, David I., Arie Staal, Jesse F. Abrams, Ricarda Winkelmann, Boris Sakschewski, Sina Loriani, Ingo Fetzer, Sarah E. Cornell, Johan Rockström, and Timothy M. Lenton (2022). “Exceeding 1.5°C global warming could trigger multiple climate tipping points.” In: *Science* 377.6611, eabn7950. DOI: 10.1126/science.abn7950.

Arrhenius, Svante (1896). “On the influence of carbonic acid in the air upon the temperature of the ground.” In: *The London, Edinburgh, and Dublin Philosophical Magazine and Journal of Science* 41.251, pp. 237–276.

Aschwanden, Andy, Mark A. Fahnestock, Martin Truffer, Douglas J. Brinkerhoff, Regine Hock, Constantine Khroulev, Ruth Mottram, and S. Abbas Khan (2019). “Contribution of the Greenland Ice Sheet to sea level over the next millennium.” In: *Science Advances* 5.6. DOI: 10.1126/sciadv.aav9396.

Bathiany, Sebastian, Vasilis Dakos, Marten Scheffer, and Timothy M. Lenton (2018). “Climate models predict increasing temperature variability in poor countries.” In: *Science Advances* 4.5. DOI: 10.1126/sciadv.aar5809.

Bintanja, R. and E. C. Van Der Linden (2013). “The changing seasonal climate in the Arctic.” In: *Scientific Reports* 3.1, pp. 1–8. DOI: 10.1038/srep01556.

Blackport, Russell, John C. Fyfe, and James A. Screen (2021). “Decreasing subseasonal temperature variability in the northern extratropics attributed to human influence.” In: *Nature Geoscience* 14.10, pp. 719–723. DOI: 10.1038/S41561-021-00826-W.

Blanchard-Wrigglesworth, E., C. M. Bitz, and M. M. Holland (2011a). “Influence of initial conditions and climate forcing on predicting Arctic sea ice.” In: *Geophysical Research Letters* 38.18. DOI: 10.1029/2011GL048807.

Blanchard-Wrigglesworth, E. and M. Bushuk (2019). “Robustness of Arctic sea-ice predictability in GCMs.” In: *Climate Dynamics* 52.9, pp. 5555–5566. DOI: 10.1007/s00382-018-4461-3.

Blanchard-Wrigglesworth, Edward, Kyle C. Armour, Cecilia M. Bitz, and Eric DeWeaver (2011b). “Persistence and Inherent Predictability of Arctic Sea Ice in a GCM Ensemble and Observations.” In: *Journal of Climate* 24.1, pp. 231–250. DOI: 10.1175/2010JCLI3775.1.

Blanchard-Wrigglesworth, E., R. I. Cullather, W. Wang, J. Zhang, and C. M. Bitz (2015). “Model forecast skill and sensitivity to initial conditions in the seasonal Sea Ice Outlook.” In: *Geophysical Research Letters* 42.19, pp. 8042–8048. DOI: 10.1002/2015GL065860.

Bliss, Angela C., Michael Steele, Ge Peng, Walter N. Meier, and Suzanne Dickinson (2019). “Regional variability of Arctic sea ice seasonal change climate indicators from a passive microwave climate data record.” In: *Environmental Research Letters* 14.4, p. 045003. DOI: 10.1088/1748-9326/AAFB84.

Blockley, Edward W. and K. Andrew Peterson (2018). "Improving Met Office seasonal predictions of Arctic sea ice using assimilation of CryoSat-2 thickness." In: *The Cryosphere* 12.11, pp. 3419–3438. DOI: 10.5194/tc-12-3419-2018.

Bonan, D. B., M. Bushuk, and M. Winton (2019). "A Spring Barrier for Regional Predictions of Summer Arctic Sea Ice." In: *Geophysical Research Letters* 46.11, pp. 5937–5947. DOI: 10.1029/2019GL082947.

Bonan, David B., Flavio Lehner, and Marika M. Holland (2021). "Partitioning uncertainty in projections of Arctic sea ice." In: *Environmental Research Letters* 16.4, p. 044002. DOI: 10.1088/1748-9326/ABE0EC.

Böning, Claus W., Erik Behrens, Arne Biastoch, Klaus Getzlaff, and Jonathan L. Bamber (2016). "Emerging impact of Greenland meltwater on deepwater formation in the North Atlantic Ocean." In: *Nature Geoscience* 9.7, pp. 523–527. DOI: 10.1038/NGEO2740.

Borodina, Aleksandra, Erich M. Fischer, and Reto Knutti (2017). "Emergent Constraints in Climate Projections: A Case Study of Changes in High-Latitude Temperature Variability." In: *Journal of Climate* 30.10, pp. 3655–3670. DOI: 10.1175/JCLI-D-16-0662.1.

Box, Jason E. et al. (2022). "Greenland ice sheet climate disequilibrium and committed sea-level rise." In: *Nature Climate Change* 12.9, pp. 808–813. DOI: 10.1038/s41558-022-01441-2.

Brayshaw, David J. (2018). "Weather, climate and the nature of predictability." In: *Weather and Climate Services for the Energy Industry*. Ed. by A. Troccoli. Springer Nature, pp. 85–94. DOI: 10.1007/978-3-319-68418-5_6.

Brode-Roger, Dina (2021). "Starving Polar Bears and Melting Ice: How the Arctic Imaginary Continues to Colonize Our Perception of Climate Change in the Circumpolar Region." In: *International Review of Qualitative Research* 14.3, pp. 497–509. DOI: 10.1177/1940844720968206.

Bunzel, Felix, Dirk Notz, Johanna Baehr, Wolfgang A. Müller, and Kristina Fröhlich (2016). "Seasonal climate forecasts significantly affected by observational uncertainty of Arctic sea ice concentration." In: *Geophysical Research Letters* 43.2, pp. 852–859. DOI: 10.1002/2015GL066928.

Bushuk, Mitchell and Dimitrios Giannakis (2015). "Sea-ice reemergence in a model hierarchy." In: *Geophysical Research Letters* 42.13, pp. 5337–5345. DOI: 10.1002/2015GL063972.

Bushuk, Mitchell, Dimitrios Giannakis, and Andrew J. Majda (2015). "Arctic Sea Ice Reemergence: The Role of Large-Scale Oceanic and Atmospheric Variability." In: *Journal of Climate* 28.14, pp. 5477–5509. DOI: 10.1175/JCLI-D-14-00354.1.

Bushuk, Mitchell, Rym Msadek, Michael Winton, Gabriel A. Vecchi, Rich Gudgel, Anthony Rosati, and Xiaosong Yang (2017). "Skillful regional prediction of Arctic sea ice on seasonal timescales." In: *Geophysical Research Letters* 44.10, pp. 4953–4964. DOI: 10.1002/2017GL073155.

Bushuk, Mitchell, Rym Msadek, Michael Winton, Gabriel Vecchi, Xiaosong Yang, Anthony Rosati, and Rich Gudgel (2019). "Regional Arctic sea–ice prediction: potential versus operational seasonal forecast skill." In: *Climate Dynamics* 52.5, pp. 2721–2743. DOI: 10.1007/s00382-018-4288-y.

Bushuk, Mitchell, Michael Winton, David B. Bonan, Edward Blanchard-Wrigglesworth, and Thomas L. Delworth (2020). "A Mechanism for the Arctic Sea Ice Spring Predictability Barrier." In: *Geophysical Research Letters* 47.13. DOI: 10.1029/2020GL088335.

Bushuk, Mitchell et al. (2022). “Mechanisms of Regional Arctic Sea Ice Predictability in Two Dynamical Seasonal Forecast Systems.” In: *Journal of Climate* 35.13, pp. 4207–4231. DOI: 10.1175/JCLI-D-21-0544.1.

Cai, Ziyi, Qinglong You, Fangying Wu, Hans W. Chen, Deliang Chen, and Judah Cohen (2021). “Arctic Warming Revealed by Multiple CMIP6 Models: Evaluation of Historical Simulations and Quantification of Future Projection Uncertainties.” In: *Journal of Climate* 34.12, pp. 4871–4892. DOI: 10.1175/JCLI-D-20-0791.1.

Cavalieri, Donald J., C. L. Parkinson, P. Gloersen, and H. J. Zwally (1996). “Sea Ice Concentrations from Nimbus-7 SMMR and DMSP SSM/I-SSMIS Passive Microwave Data, Version 1.” In: *NASA National Snow and Ice Data Center Distributed Active Archive Center*. DOI: 10.5067/8GQ8LZQVL0VL.

Chen, D. et al. (2021). “Framing, Context, and Methods.” In: *Climate Change 2021: The Physical Science Basis. Contribution of Working Group I to the Sixth Assessment Report of the Intergovernmental Panel on Climate Change*. Ed. by V. Masson-Delmotte et al. Cambridge, United Kingdom and New York, NY, USA: Cambridge University Press, pp. 147–286. DOI: 10.1017/9781009157896.003.

Chen, Jiao, Aiguo Dai, and Yaocun Zhang (2019). “Projected Changes in Daily Variability and Seasonal Cycle of Near-Surface Air Temperature over the Globe during the Twenty-First Century.” In: *Journal of Climate* 32.24, pp. 8537–8561. DOI: 10.1175/JCLI-D-19-0438.1.

Cheng, Wei, Edward Blanchard-Wrigglesworth, Cecilia M. Bitz, Carol Ladd, and Phyllis J. Stabeno (2016). “Diagnostic sea ice predictability in the pan-Arctic and U.S. Arctic regional seas.” In: *Geophysical Research Letters* 43.22, pp. 11,688–11,696. DOI: 10.1002/2016GL070735.

Chevallier, Matthieu, François Massonnet, Helge Goessling, Virginie Guémas, and Thomas Jung (2018). “The role of sea ice in sub-seasonal predictability.” In: *Sub-seasonal to Seasonal Prediction: The Gap Between Weather and Climate Forecasting*. Elsevier, pp. 201–221. DOI: 10.1016/B978-0-12-811714-9.00010-3.

Chevallier, Matthieu and David Salas-Mélia (2012). “The Role of Sea Ice Thickness Distribution in the Arctic Sea Ice Potential Predictability: A Diagnostic Approach with a Coupled GCM.” In: *Journal of Climate* 25.8, pp. 3025–3038. DOI: 10.1175/JCLI-D-11-00209.1.

Chevallier, Matthieu, David Salas y Mélia, Aurore Voldoire, Michel Déqué, and Gilles Garric (2013). “Seasonal Forecasts of the Pan-Arctic Sea Ice Extent Using a GCM-Based Seasonal Prediction System.” In: *Journal of Climate* 26.16, pp. 6092–6104. DOI: 10.1175/JCLI-D-12-00612.1.

Chung, Eui Seok, Kyung Ja Ha, Axel Timmermann, Malte F. Stuecker, Tamas Bodai, and Sang Ki Lee (2021). “Cold-Season Arctic Amplification Driven by Arctic Ocean-Mediated Seasonal Energy Transfer.” In: *Earth's Future* 9.2, e2020EF001898. DOI: 10.1029/2020EF001898.

Cleveland, William S. (1979). “Robust locally weighted regression and smoothing scatterplots.” In: *Journal of the American Statistical Association* 74.368, pp. 829–836. DOI: 10.1080/01621459.1979.10481038.

Cohen, Judah et al. (2014). “Recent Arctic amplification and extreme mid-latitude weather.” In: *Nature Geoscience* 7.9, pp. 627–637. DOI: 10.1038/ngeo2234.

Cohen, Judah et al. (2020). “Divergent consensuses on Arctic amplification influence on midlatitude severe winter weather.” In: *Nature Climate Change* 10.1, pp. 20–29. DOI: 10.1038/s41558-019-0662-y.

Collow, Thomas W., Wanqiu Wang, and Arun Kumar (2019). “Reduction in Northern Midlatitude 2-m Temperature Variability due to Arctic Sea Ice Loss.” In: *Journal of Climate* 32.16, pp. 5021–5035. DOI: 10.1175/JCLI-D-18-0692.1.

Collow, Thomas W., Wanqiu Wang, Arun Kumar, and Jinlun Zhang (2015). “Improving arctic sea ice prediction using PIOMAS initial sea ice thickness in a coupled ocean-atmosphere model.” In: *Monthly Weather Review* 143.11, pp. 4618–4630. DOI: 10.1175/MWR-D-15-0097.1.

Comiso, Josefino (2017). “Bootstrap Sea Ice Concentrations from Nimbus-7 SMMR and DMSP SSM/I-SSMIS, Version 3.” In: *NASA National Snow and Ice Data Center Distributed Active Archive Center*. DOI: 10.5067/7Q8HCCWS4I0R.

Constable, Andrew J., Sherilee Harper, Jackie Dawson, Kirstin Holsman, Tero Mustonen, Dieter Piepenburg, and Björn Rost (2022). “Cross-Chapter Paper 6: Polar Regions.” In: *Climate Change 2022: Impacts, Adaptation and Vulnerability. Contribution of Working Group II to the Sixth Assessment Report of the Intergovernmental Panel on Climate Change*. Ed. by H.-O. Pörtner et al. Cambridge University Press, Cambridge, UK and New York, NY, USA: Cambridge University Press, pp. 2319–2368. DOI: 10.1017/9781009325844.023.

Crook, Julia A., Piers M. Forster, and Nicola Stuber (2011). “Spatial Patterns of Modeled Climate Feedback and Contributions to Temperature Response and Polar Amplification.” In: *Journal of Climate* 24.14, pp. 3575–3592. DOI: 10.1175/2011JCLI3863.1.

Dai, Aiguo and Jiechun Deng (2021). “Arctic Amplification Weakens the Variability of Daily Temperatures over Northern Middle-High Latitudes.” In: *Journal of Climate* 34.7, pp. 2591–2609. DOI: 10.1175/JCLI-D-20-0514.1.

Dai, Aiguo, Dehai Luo, Mirong Song, and Jiping Liu (2019). “Arctic amplification is caused by sea-ice loss under increasing CO2.” In: *Nature Communications* 10.1, pp. 1–13. DOI: 10.1038/s41467-018-07954-9.

Dai, Haijin (2021). “Roles of Surface Albedo, Surface Temperature and Carbon Dioxide in the Seasonal Variation of Arctic Amplification.” In: *Geophysical Research Letters* 48.4, e2020GL090301. DOI: 10.1029/2020GL090301.

Davy, Richard and Stephen Outten (2020). “The Arctic Surface Climate in CMIP6: Status and Developments since CMIP5.” In: *Journal of Climate* 33.18, pp. 8047–8068. DOI: 10.1175/JCLI-D-19-0990.1.

Day, J. J., E. Hawkins, and S. Tietsche (2014a). “Will Arctic sea ice thickness initialization improve seasonal forecast skill?” In: *Geophysical Research Letters* 41.21, pp. 7566–7575. DOI: 10.1002/2014GL061694.

Day, J. J., S. Tietsche, and E. Hawkins (2014b). “Pan-Arctic and Regional Sea Ice Predictability: Initialization Month Dependence.” In: *Journal of Climate* 27.12, pp. 4371–4390. DOI: 10.1175/JCLI-D-13-00614.1.

Day, Jonathan J. et al. (2016). “The Arctic Predictability and Prediction on Seasonal-to-Interannual TimEscales (APPOSITE) data set version 1.” In: *Geoscientific Model Development* 9.6, pp. 2255–2270. DOI: 10.5194/gmd-9-2255-2016.

Deser, C. et al. (2020). “Insights from Earth system model initial-condition large ensembles and future prospects.” In: *Nature Climate Change* 10.4, pp. 277–286. DOI: 10.1038/s41558-020-0731-2.

Deser, Clara, Adam Phillips, Vincent Bourdette, and Haiyan Teng (2012). “Uncertainty in climate change projections: The role of internal variability.” In: *Climate Dynamics* 38.3, pp. 527–546. DOI: 10.1007/s00382-010-0977-x.

Ding, Qinghua et al. (2017). "Influence of high-latitude atmospheric circulation changes on summertime Arctic sea ice." In: *Nature Climate Change* 7.4, pp. 289–295. DOI: 10.1038/nclimate3241.

Ding, Qinghua et al. (2019). "Fingerprints of internal drivers of Arctic sea ice loss in observations and model simulations." In: *Nature Geoscience* 12.1, pp. 28–33. DOI: 10.1038/s41561-018-0256-8.

Dirkson, Arlan, William J. Merryfield, and Adam Monahan (2017). "Impacts of sea ice thickness initialization on seasonal Arctic Sea ice predictions." In: *Journal of Climate* 30.3, pp. 1001–1017. DOI: 10.1175/JCLI-D-16-0437.1.

Doblas-Reyes, F. J. et al. (2021). "Linking Global to Regional Climate Change." In: *Climate Change 2021: The Physical Science Basis. Contribution of Working Group I to the Sixth Assessment Report of the Intergovernmental Panel on Climate Change*. Ed. by V. Masson-Delmotte et al. Cambridge, United Kingdom and New York, NY, USA: Cambridge University Press, pp. 1363–1512. DOI: 10.1017/9781009157896.012.

Dobricic, Srdjan, Simone Russo, Luca Pozzoli, Julian Wilson, and Elisabetta Vignati (2020). "Increasing occurrence of heat waves in the terrestrial Arctic." In: *Environmental Research Letters* 15.2, p. 024022. DOI: 10.1088/1748-9326/ab6398.

Donat, Markus G. and Lisa V. Alexander (2012). "The shifting probability distribution of global daytime and night-time temperatures." In: *Geophysical Research Letters* 39.14, p. 14707. DOI: 10.1029/2012GL052459.

Donohoe, Aaron, Ed Blanchard-Wrigglesworth, Axel Schweiger, and Philip J. Rasch (2020). "The Effect of Atmospheric Transmissivity on Model and Observational Estimates of the Sea Ice Albedo Feedback." In: *Journal of Climate* 33.13, pp. 5743–5765. DOI: 10.1175/JCLI-D-19-0674.1.

Döscher, Ralf et al. (2022). "The EC-Earth3 Earth system model for the Coupled Model Intercomparison Project 6." In: *Geoscientific Model Development* 15.7, pp. 2973–3020. DOI: 10.5194/GMD-15-2973-2022.

Dwyer, John G., Michela Biasutti, and Adam H. Sobel (2012). "Projected Changes in the Seasonal Cycle of Surface Temperature." In: *Journal of Climate* 25.18, pp. 6359–6374. DOI: 10.1175/JCLI-D-11-00741.1.

EUMETSAT Ocean and Sea Ice Satellite Application Facility (2017). *Global sea ice concentration climate data record 1979-2015 (v2.0, 2017), OSI-450*. DOI: 10.15770/EUM_SAF_OSI_0008.

EUMETSAT Ocean and Sea Ice Satellite Application Facility (2019). *Global sea ice concentration interim climate data record 2016 onwards (v2.0, 2019), OSI-430b*. DOI: 10.15770/EUM_SAF_OSI_NRT_2008.

Einarsson, N., J. Nymand Larsen, A. Nilsson, and O. R. Young (2004). *Arctic human development report*. Tech. rep. Stefansson Arctic Institute.

England, Mark, Alexandra Jahn, and Lorenzo Polvani (2019). "Nonuniform Contribution of Internal Variability to Recent Arctic Sea Ice Loss." In: *Journal of Climate* 32.13, pp. 4039–4053. DOI: 10.1175/JCLI-D-18-0864.1.

Eyring, Veronika, Sandrine Bony, Gerald A. Meehl, Catherine A. Senior, Bjorn Stevens, Ronald J. Stouffer, and Karl E. Taylor (2016). "Overview of the Coupled Model Intercomparison Project Phase 6 (CMIP6) experimental design and organization." In: *Geoscientific Model Development* 9.5, pp. 1937–1958. DOI: 10.5194/gmd-9-1937-2016.

Fetterer, F., K. Knowles, W. N. Meier, M. Savoie, and A. K. Windnagel (2017). *Sea Ice Index, Version 3 [Data Set]*. Boulder, Colorado USA: National Snow and Ice Data Center. DOI: 10.7265/N5K072F8.

Fischer, E. M., U. Beyerle, and R. Knutti (2013). "Robust spatially aggregated projections of climate extremes." In: *Nature Climate Change* 3.12, pp. 1033–1038. DOI: 10.1038/NCLIMATE2051.

Fischer, Erich M. and Christoph Schär (2009). "Future changes in daily summer temperature variability: Driving processes and role for temperature extremes." In: *Climate Dynamics* 33.7, pp. 917–935. DOI: 10.1007/s00382-008-0473-8.

Ford, James D., Graham McDowell, and Tristan Pearce (2015). "The adaptation challenge in the Arctic." In: *Nature Climate Change* 5.12, pp. 1046–1053. DOI: 10.1038/NCLIMATE2723.

Fox-Kemper, B. et al. (2021). "Ocean, Cryosphere and Sea Level Change." In: *Climate Change 2021: The Physical Science Basis. Contribution of Working Group I to the Sixth Assessment Report of the Intergovernmental Panel on Climate Change*. Ed. by V. Masson-Delmotte et al. Cambridge, United Kingdom and New York, NY, USA: Cambridge University Press, pp. 1211–1362. DOI: 10.1017/9781009157896.011.

Frankcombe, Leela M., Matthew H. England, Michael E. Mann, and Byron A. Steinman (2015). "Separating Internal Variability from the Externally Forced Climate Response." In: *Journal of Climate* 28.20, pp. 8184–8202. DOI: 10.1175/JCLI-D-15-0069.1.

Gasparrini, Antonio and Ben Armstrong (2011). "The impact of heat waves on mortality." In: *Epidemiology* 22.1, pp. 68–73. DOI: 10.1097/EDE.0B013E3181FDCD99.

Germe, Agathe, Matthieu Chevallier, David Salas y Mélia, Emilia Sanchez-Gomez, and Christophe Cassou (2014). "Interannual predictability of Arctic sea ice in a global climate model: regional contrasts and temporal evolution." In: *Climate Dynamics* 43.9, pp. 2519–2538. DOI: 10.1007/s00382-014-2071-2.

Giesse, Céline, Dirk Notz, and Johanna Baehr (2021). "On the origin of discrepancies between observed and simulated memory of Arctic sea ice." In: *Geophysical Research Letters* 48.11, e2020GL091784. DOI: 10.1029/2020GL091784.

Giorgetta, Marco A. et al. (2013). "Climate and carbon cycle changes from 1850 to 2100 in MPI-ESM simulations for the Coupled Model Intercomparison Project phase 5." In: *Journal of Advances in Modeling Earth Systems* 5.3, pp. 572–597. DOI: 10.1002/jame.20038.

Goosse, H., O. Arzel, C. M. Bitz, A. De Montety, and M. Vancoppenolle (2009). "Increased variability of the Arctic summer ice extent in a warmer climate." In: *Geophysical Research Letters* 36.23, p. 23702. DOI: 10.1029/2009GL040546.

Goosse, Hugues et al. (2018). "Quantifying climate feedbacks in polar regions." In: *Nature Communications* 9.1, pp. 1–13. DOI: 10.1038/s41467-018-04173-0.

Graham, Robert M., Lana Cohen, Alek A. Petty, Linette N. Boisvert, Annette Rinke, Stephen R. Hudson, Marcel Nicolaus, and Mats A. Granskog (2017). "Increasing frequency and duration of Arctic winter warming events." In: *Geophysical Research Letters* 44.13, pp. 6974–6983. DOI: 10.1002/2017GL073395.

Graversen, Rune G., Peter L. Langen, and Thorsten Mauritsen (2014). "Polar Amplification in CCSM4: Contributions from the Lapse Rate and Surface Albedo Feedbacks." In: *Journal of Climate* 27.12, pp. 4433–4450. DOI: 10.1175/JCLI-D-13-00551.1.

Gross, Mia H., Markus G. Donat, and Lisa V. Alexander (2019). "Changes in daily temperature extremes relative to the mean in Coupled Model Intercomparison Project Phase 5 models and observations." In: *International Journal of Climatology* 39.14, pp. 5273–5291. DOI: 10.1002/JOC.6138.

Gross, Mia H., Markus G. Donat, Lisa V. Alexander, and Steven C. Sherwood (2020). "Amplified warming of seasonal cold extremes relative to the mean in the Northern Hemisphere extratropics." In: *Earth System Dynamics* 11.1, pp. 97–111. DOI: 10.5194/ESD-11-97-2020.
Guemas, Virginie et al. (2016). "A review on Arctic sea-ice predictability and prediction on seasonal to decadal time-scales." In: *Quarterly Journal of the Royal Meteorological Society* 142.695, pp. 546–561. DOI: 10.1002/qj.2401.
Hahn, Lily C., Kyle C. Armour, David S. Battisti, Ian Eisenman, and Cecilia M. Bitz (2022). "Seasonality in Arctic Warming Driven by Sea Ice Effective Heat Capacity." In: *Journal of Climate* 35.5, pp. 1629–1642. DOI: 10.1175/JCLI-D-21-0626.1.
Hasselmann, K. (1976). "Stochastic climate models Part I. Theory." In: *Tellus* 28.6, pp. 473–485. DOI: 10.3402/TELLUSA.V28I6.11316.
Hawkins, Ed and Rowan Sutton (2009). "The Potential to Narrow Uncertainty in Regional Climate Predictions." In: *Bulletin of the American Meteorological Society* 90.8, pp. 1095–1108. DOI: 10.1175/2009BAMS2607.1.
Hedemann, Christopher, Thorsten Mauritsen, Johann Jungclaus, and Jochem Marotzke (2017). "The subtle origins of surface-warming hiatuses." In: *Nature Climate Change* 7.5, pp. 336–339. DOI: 10.1038/nclimate3274.
Hingray, Benoit and Mériem Saïd (2014). "Partitioning Internal Variability and Model Uncertainty Components in a Multimember Multimodel Ensemble of Climate Projections." In: *Journal of Climate* 27.17, pp. 6779–6798. DOI: 10.1175/JCLI-D-13-00629.1.
Holland, M. M. and C. M. Bitz (2003). "Polar amplification of climate change in coupled models." In: *Climate Dynamics* 21.3-4, pp. 221–232. DOI: 10.1007/s00382-003-0332-6.
Holland, Marika M., David A. Bailey, and Steve Vavrus (2011). "Inherent sea ice predictability in the rapidly changing Arctic environment of the Community Climate System Model, version 3." In: *Climate Dynamics* 36.7, pp. 1239–1253. DOI: 10.1007/s00382-010-0792-4.
Holland, Marika M. and Laura Landrum (2021). "The Emergence and Transient Nature of Arctic Amplification in Coupled Climate Models." In: *Frontiers in Earth Science* 9, p. 764. DOI: 10.3389/feart.2021.719024.
Holland, Marika M., Laura Landrum, David Bailey, and Steve Vavrus (2019). "Changing Seasonal Predictability of Arctic Summer Sea Ice Area in a Warming Climate." In: *Journal of Climate* 32.16, pp. 4963–4979. DOI: 10.1175/JCLI-D-19-0034.1.
Holmes, Caroline R., Tim Woollings, Ed Hawkins, and Hylke de Vries (2016). "Robust Future Changes in Temperature Variability under Greenhouse Gas Forcing and the Relationship with Thermal Advection." In: *Journal of Climate* 29.6, pp. 2221–2236. DOI: 10.1175/JCLI-D-14-00735.1.
Huntingford, Chris, Philip D. Jones, Valerie N. Livina, Timothy M. Lenton, and Peter M. Cox (2013). "No increase in global temperature variability despite changing regional patterns." In: *Nature* 500.7462, pp. 327–330. DOI: 10.1038/NATURE12310.
Hurrell, James W., Yochanan Kushnir, Geir Ottersen, and Martin Visbeck (2003). "An Overview of the North Atlantic Oscillation." In: *Geophysical Monograph Series* 134, pp. 1–35. DOI: 10.1029/134GM01.
IPCC (2012). "Summary for Policymakers." In: *Managing the Risks of Extreme Events and Disasters to Advance Climate Change Adaptation*. Ed. by C.B. Field et al. Cam-

bridge, United Kingdom and New York, NY , USA: Cambridge University Press, pp. 1–19.

IPCC (2021a). "Annex IV: Modes of Variability." In: *Climate Change 2021: The Physical Science Basis. Contribution of Working Group I to the Sixth Assessment Report of the Intergovernmental Panel on Climate Change*. Ed. by V. Masson-Delmotte et al. Cambridge, United Kingdom and New York, NY, USA: Cambridge University Press, pp. 2153–2192. DOI: 10.1017/9781009157896.018.

IPCC (2021b). "Annex VII: Glossary." In: *Climate Change 2021: The Physical Science Basis. Contribution of Working Group I to the Sixth Assessment Report of the Intergovernmental Panel on Climate Change*. Ed. by V. Masson-Delmotte et al. Cambridge, United Kingdom and New York, NY, USA: Cambridge University Press, pp. 2215–2256. DOI: 10.1017/9781009157896.022.

IPCC (2021c). *Climate Change 2021: The Physical Science Basis. Contribution of Working Group I to the Sixth Assessment Report of the Intergovernmental Panel on Climate Change*. Ed. by V. Masson-Delmotte et al. Cambridge, United Kingdom and New York, NY , USA: Cambridge University Press. DOI: 10.1017/9781009157896.

IPCC (2021d). "Summary for Policymakers." In: *Climate Change 2021: The Physical Science Basis. Contribution of Working Group I to the Sixth Assessment Report of the Intergovernmental Panel on Climate Change*. Ed. by V. Masson-Delmotte et al. Cambridge, United Kingdom and New York, NY, USA: Cambridge University Press, pp. 3–32. DOI: 10.1017/9781009157896.001.

Isaksen, Ketil et al. (2022). "Exceptional warming over the Barents area." In: *Scientific Reports* 12.1, pp. 1–18. DOI: 10.1038/s41598-022-13568-5.

Jackson, L. C., R. Kahana, T. Graham, M. A. Ringer, T. Woollings, J. V. Mecking, and R. A. Wood (2015). "Global and European climate impacts of a slowdown of the AMOC in a high resolution GCM." In: *Climate Dynamics* 45.11, pp. 3299–3316. DOI: 10.1007/s00382-015-2540-2.

James, Rachel, Richard Washington, Carl-Friedrich Schleussner, Joeri Rogelj, and Declan Conway (2017). "Characterizing half-a-degree difference: a review of methods for identifying regional climate responses to global warming targets." In: *Wiley Interdisciplinary Reviews: Climate Change* 8.2, e457. DOI: 10.1002/WCC.457.

Jeffries, Martin O., James E. Overland, and Donald K. Perovich (2013). "The Arctic shifts to a new normal." In: *Physics Today* 66.10, p. 35. DOI: 10.1063/PT.3.2147.

Johannessen, Ola M., Svetlana I. Kuzmina, Leonid P. Bobylev, and Martin W. Miles (2016). "Surface air temperature variability and trends in the Arctic: New amplification assessment and regionalisation." In: *Tellus, Series A: Dynamic Meteorology and Oceanography* 68.1, p. 28234. DOI: 10.3402/tellusa.v68.28234.

Jung, Thomas et al. (2016). "Advancing Polar Prediction Capabilities on Daily to Seasonal Time Scales." In: *Bulletin of the American Meteorological Society* 97.9, pp. 1631–1647. DOI: 10.1175/BAMS-D-14-00246.1.

Katz, Richard W. and Barbara G. Brown (1992). "Extreme events in a changing climate: Variability is more important than averages." In: *Climatic Change* 21.3, pp. 289–302. DOI: 10.1007/BF00139728.

Kay, J. E. et al. (2015). "The Community Earth System Model (CESM) Large Ensemble Project: A Community Resource for Studying Climate Change in the Presence of Internal Climate Variability." In: *Bulletin of the American Meteorological Society* 96.8, pp. 1333–1349. DOI: 10.1175/BAMS-D-13-00255.1.

Kay, Jennifer E., Marika M. Holland, and Alexandra Jahn (2011). “Inter-annual to multi-decadal Arctic sea ice extent trends in a warming world.” In: *Geophysical Research Letters* 38.15. DOI: 10.1029/2011GL048008.

Kern, Stefan, Thomas Lavergne, Dirk Notz, Leif Toudal Pedersen, and Rasmus Tage Tonboe (2020). “Satellite Passive Microwave Sea-Ice Concentration Data Set Intercomparison for Arctic Summer Conditions.” In: *The Cryosphere* 14.7, pp. 2469–2493. DOI: 10.5194/tc-14-2469-2020.

Kern, Stefan, Thomas Lavergne, Dirk Notz, Leif Toudal Pedersen, Rasmus Tage Tonboe, Roberto Saldo, and Atle MacDonald Sørensen (2019). “Satellite passive microwave sea-ice concentration data set intercomparison: closed ice and ship-based observations.” In: *The Cryosphere* 13.12, pp. 3261–3307. DOI: 10.5194/tc-13-3261-2019.

Kharin, V. V., F. W. Zwiers, X. Zhang, and M. Wehner (2013). “Changes in temperature and precipitation extremes in the CMIP5 ensemble.” In: *Climatic Change* 119.2, pp. 345–357. DOI: 0.1007/s10584-013-0705-8.

King, Andrew D., Todd P. Lane, Benjamin J. Henley, and Josephine R. Brown (2020). “Global and regional impacts differ between transient and equilibrium warmer worlds.” In: *Nature Climate Change* 10.1, pp. 42–47. DOI: 10.1038/s41558-019-0658-7.

Koenigk, Torben and Uwe Mikolajewicz (2009). “Seasonal to interannual climate predictability in mid and high northern latitudes in a global coupled model.” In: *Climate Dynamics* 32.6, pp. 783–798. DOI: 10.1007/s00382-008-0419-1.

Krikken, F. and W. Hazeleger (2015). “Arctic Energy Budget in Relation to Sea Ice Variability on Monthly-to-Annual Time Scales.” In: *Journal of Climate* 28.16, pp. 6335–6350. DOI: 10.1175/JCLI-D-15-0002.1.

Kwok, R. and D. A. Rothrock (2009). “Decline in Arctic sea ice thickness from submarine and ICESat records: 1958–2008.” In: *Geophysical Research Letters* 36.15, p. 15501. DOI: 10.1029/2009GL039035.

Landrum, Laura and Marika M. Holland (2020). “Extremes become routine in an emerging new Arctic.” In: *Nature Climate Change* 10.12, pp. 1108–1115. DOI: 10.1038/s41558-020-0892-z.

Landy, Jack C. et al. (2022). “A year-round satellite sea-ice thickness record from CryoSat-2.” In: *Nature* 609, pp. 517–522. DOI: 10.1038/s41586-022-05058-5.

Lavergne, Thomas et al. (2019). “Version 2 of the EUMETSAT OSI SAF and ESA CCI sea-ice concentration climate data records.” In: *The Cryosphere* 13.1, pp. 49–78. DOI: 10.5194/tc-13-49-2019.

Lehner, Flavio, Clara Deser, Nicola Maher, Jochem Marotzke, Erich M. Fischer, Lukas Brunner, Reto Knutti, and Ed Hawkins (2020). “Partitioning climate projection uncertainty with multiple large ensembles and CMIP5/6.” In: *Earth System Dynamics* 11.2, pp. 491–508. DOI: 10.5194/ESD-11-491-2020.

Lenssen, Nathan J.L., Gavin A. Schmidt, James E. Hansen, Matthew J. Menne, Avraham Persin, Reto Ruedy, and Daniel Zyss (2019). “Improvements in the GISTEMP Uncertainty Model.” In: *Journal of Geophysical Research: Atmospheres* 124.12, pp. 6307–6326. DOI: 10.1029/2018JD029522.

Lenton, Timothy M., Vasilis Dakos, Sebastian Bathiany, and Marten Scheffer (2017). “Observed trends in the magnitude and persistence of monthly temperature variability.” In: *Scientific Reports* 7.1, pp. 1–10. DOI: 10.1038/s41598-017-06382-x.

Lind, Sigrid, Randi B. Ingvaldsen, and Tore Furevik (2018). "Arctic warming hotspot in the northern Barents Sea linked to declining sea-ice import." In: *Nature Climate Change* 8.7, pp. 634–639. DOI: 10.1038/s41558-018-0205-y.

Lorenz, Edward N. (1963). "Deterministic Nonperiodic Flow." In: *Journal of the Atmospheric Sciences* 20.2, pp. 130–141.

Lorenz, Edward N. (1972). "Predictability: does the flap of a butterfly's wings in Brazil set off a tornado in Texas?" In: *139th Meeting*. American Association for the Advancement of Science.

Maher, Nicola, Flavio Lehner, and Jochem Marotzke (2020). "Quantifying the role of internal variability in the temperature we expect to observe in the coming decades." In: *Environmental Research Letters* 15.5, p. 054014. DOI: 10.1088/1748-9326/AB7D02.

Maher, Nicola, Sebastian Milinski, and Ralf Ludwig (2021). "Large ensemble climate model simulations: Introduction, overview, and future prospects for utilising multiple types of large ensemble." In: *Earth System Dynamics* 12.2, pp. 401–418. DOI: 10.5194/ESD-12-401-2021.

Maher, Nicola et al. (2019). "The Max Planck Institute Grand Ensemble: Enabling the Exploration of Climate System Variability." In: *Journal of Advances in Modeling Earth Systems* 11.7, pp. 2050–2069. DOI: 10.1029/2019MS001639.

Manabe, S. and R. J. Stouffer (1980). "Sensitivity of a global climate model to an increase of CO2 concentration in the atmosphere." In: *Journal of Geophysical Research: Oceans* 85.C10, pp. 5529–5554. DOI: 10.1029/JC085IC10P05529.

Manabe, Syukuro and Richard T. Wetherald (1975). "The Effects of Doubling the CO2 Concentration on the climate of a General Circulation Model." In: *Journal of the Atmospheric Sciences* 32.1, pp. 3–15. DOI: 10.1175/1520-0469(1975)032<0003:TEODTC>2.0.CO;2.

Mankin, Justin S., Flavio Lehner, Sloan Coats, and Karen A. McKinnon (2020). "The Value of Initial Condition Large Ensembles to Robust Adaptation Decision-Making." In: *Earth's Future* 8.10, e2012EF001610. DOI: 10.1029/2020EF001610.

Mann, Michael E. and Jeffrey Park (1996). "Greenhouse warming and changes in the seasonal cycle of temperature: Model versus observations." In: *Geophysical Research Letters* 23.10, pp. 1111–1114. DOI: 10.1029/96GL01066.

Marotzke, Jochem and Piers M. Forster (2015). "Forcing, feedback and internal variability in global temperature trends." In: *Nature* 517.7536, pp. 565–570. DOI: 10.1038/nature14117.

Matthes, Heidrun, Annette Rinke, and Klaus Dethloff (2015). "Recent changes in Arctic temperature extremes: warm and cold spells during winter and summer." In: *Environmental Research Letters* 10.11, p. 114020. DOI: 10.1088/1748-9326/10/11/114020.

Meehl, Gerald A. et al. (2021). "Initialized Earth System prediction from subseasonal to decadal timescales." In: *Nature Reviews Earth & Environment* 2.5, pp. 340–357. DOI: 10.1038/s43017-021-00155-x.

Meincke, Jens and Mojib Latif (1995). "Die Rolle des Ozeans im Klimasystem." In: *Geographische Rundschau* 47, pp. 90–96.

Milinski, Sebastian, Nicola Maher, and Dirk Olonscheck (2020). "How large does a large ensemble need to be?" In: *Earth System Dynamics* 11.4, pp. 885–901. DOI: 10.5194/ESD-11-885-2020.

Miner, Kimberley R., Merritt R. Turetsky, Edward Malina, Annett Bartsch, Johanna Tamminen, A. David McGuire, Andreas Fix, Colm Sweeney, Clayton D. Elder,

and Charles E. Miller (2022). "Permafrost carbon emissions in a changing Arctic." In: *Nature Reviews Earth & Environment* 3.1, pp. 55–67. DOI: 10.1038/s43017-021-00230-3.
Moore, G. W. K. (2016). "The December 2015 North Pole Warming Event and the Increasing Occurrence of Such Events." In: *Scientific Reports* 6.1, pp. 1–11. DOI: 10.1038/srep39084.
Moravec, Vojtěch, Yannis Markonis, Oldrich Rakovec, Miroslav Svoboda, Miroslav Trnka, Rohini Kumar, and Martin Hanel (2021). "Europe under multi-year droughts: how severe was the 2014–2018 drought period?" In: *Environmental Research Letters* 16.3, p. 034062. DOI: 10.1088/1748-9326/ABE828.
Msadek, R., G. A. Vecchi, M. Winton, and R. G. Gudgel (2014). "Importance of initial conditions in seasonal predictions of Arctic sea ice extent." In: *Geophysical Research Letters* 41.14, pp. 5208–5215. DOI: 10.1002/2014GL060799.
Nielsen, David Marcolino, Patrick Pieper, Armineh Barkhordarian, Paul Overduin, Tatiana Ilyina, Victor Brovkin, Johanna Baehr, and Mikhail Dobrynin (2022). "Increase in Arctic coastal erosion and its sensitivity to warming in the twenty-first century." In: *Nature Climate Change* 12, pp. 263–270. DOI: 10.1038/s41558-022-01281-0.
Notz, Dirk (2009). "The future of ice sheets and sea ice: Between reversible retreat and unstoppable loss." In: *Proceedings of the National Academy of Sciences of the United States of America* 106.49, pp. 20590–20595. DOI: 10.1073/pnas.0902356106.
Notz, Dirk (2015). "How well must climate models agree with observations?" In: *Philosophical Transactions of the Royal Society A: Mathematical, Physical and Engineering Sciences* 373.2052. DOI: 10.1098/RSTA.2014.0164.
Notz, Dirk (2017). "Arctic sea ice seasonal-to-decadal variability and long-term change." In: *Past Global Changes Magazine* 25.1, pp. 14–19. DOI: 10.22498/pages.25.1.14.
Notz, Dirk and Jochem Marotzke (2012). "Observations reveal external driver for Arctic sea-ice retreat." In: *Geophysical Research Letters* 39.8. DOI: 10.1029/2012GL051094.
Notz, Dirk and SIMIP Community (2020). "Arctic Sea Ice in CMIP6." In: *Geophysical Research Letters* 47.10, e2019GL086749. DOI: 10.1029/2019GL086749.
Notz, Dirk and Julienne Stroeve (2016). "Observed Arctic sea-ice loss directly follows anthropogenic CO2 emission." In: *Science* 354.6313, pp. 747–750. DOI: 10.1126/science.aag2345.
Obu, Jaroslav et al. (2019). "Northern Hemisphere permafrost map based on TTOP modelling for 2000–2016 at 1 km$^2$ scale." In: *Earth-Science Reviews* 193, pp. 299–316. DOI: 10.1016/J.EARSCIREV.2019.04.023.
Olonscheck, Dirk (2018). "Understanding internal variability of sea ice and surface air temperature." PhD thesis. Universität Hamburg.
Olonscheck, Dirk, Thorsten Mauritsen, and Dirk Notz (2019). "Arctic sea-ice variability is primarily driven by atmospheric temperature fluctuations." In: *Nature Geoscience* 12.6, pp. 430–434. DOI: 10.1038/s41561-019-0363-1.
Olonscheck, Dirk and Dirk Notz (2017). "Consistently Estimating Internal Climate Variability from Climate Model Simulations." In: *Journal of Climate* 30.23, pp. 9555–9573. DOI: 10.1175/JCLI-D-16-0428.1.
Olonscheck, Dirk, Andrew P. Schurer, Lucie Lücke, and Gabriele C. Hegerl (2021). "Large-scale emergence of regional changes in year-to-year temperature variabil-

ity by the end of the 21st century." In: *Nature Communications* 12.1, pp. 1–10. DOI: 10.1038/s41467-021-27515-x.

Ono, Jun, Masahiro Watanabe, Yoshiki Komuro, Hiroaki Tatebe, and Manabu Abe (2022). "Enhanced Arctic warming amplification revealed in a low-emission scenario." In: *Communications Earth & Environment* 3.1, pp. 1–9. DOI: 10.1038/s43247-022-00354-4.

Ordoñez, Ana C., Cecilia M. Bitz, and Edward Blanchard-Wrigglesworth (2018). "Processes controlling Arctic and Antarctic sea ice predictability in the community earth system model." In: *Journal of Climate* 31.23, pp. 9771–9786. DOI: 10.1175/JCLI-D-18-0348.1.

Overland, James E., Klaus Dethloff, Jennifer A. Francis, Richard J. Hall, Edward Hanna, Seong Joong Kim, James A. Screen, Theodore G. Shepherd, and Timo Vihma (2016). *Nonlinear response of mid-latitude weather to the changing Arctic*. DOI: 10.1038/nclimate3121.

Peterson, K. Andrew, A. Arribas, H. T. Hewitt, A. B. Keen, D. J. Lea, and A. J. McLaren (2015). "Assessing the forecast skill of Arctic sea ice extent in the GloSea4 seasonal prediction system." In: *Climate Dynamics* 44.1-2, pp. 147–162. DOI: 10.1007/s00382-014-2190-9.

Petty, Alek A., Marika M. Holland, David A. Bailey, and Nathan T. Kurtz (2018). "Warm Arctic, Increased Winter Sea Ice Growth?" In: *Geophysical Research Letters* 45.23, pp. 12,922–12,930. DOI: 10.1029/2018GL079223.

Pistone, Kristina, Ian Eisenman, and V. Ramanathan (2014). "Observational determination of albedo decrease caused by vanishing Arctic sea ice." In: *Proceedings of the National Academy of Sciences of the United States of America* 111.9, pp. 3322–3326. DOI: 10.1073/pnas.1318201111.

Pithan, Felix and Thorsten Mauritsen (2014). "Arctic amplification dominated by temperature feedbacks in contemporary climate models." In: *Nature Geoscience* 7.3, pp. 181–184. DOI: 10.1038/ngeo2071.

Polyakov, Igor V. et al. (2017). "Greater role for Atlantic inflows on sea-ice loss in the Eurasian Basin of the Arctic Ocean." In: *Science* 356.6335, pp. 285–291. DOI: 10.1126/SCIENCE.AAI8204.

Post, Eric, Uma S. Bhatt, Cecilia M. Bitz, Jedediah F. Brodie, Tara L. Fulton, Mark Hebblewhite, Jeffrey Kerby, Susan J. Kutz, Ian Stirling, and Donald A. Walker (2013). "Ecological consequences of sea-ice decline." In: *Science* 341.6145, pp. 519–524. DOI: 10.1126/science.1235225.

Previdi, Michael, Tyler P. Janoski, Gabriel Chiodo, Karen L. Smith, and Lorenzo M. Polvani (2020). "Arctic Amplification: A Rapid Response to Radiative Forcing." In: *Geophysical Research Letters* 47.17, e2020GL089933. DOI: 10.1029/2020GL089933.

Previdi, Michael, Karen L. Smith, and Lorenzo M. Polvani (2021). "Arctic amplification of climate change: a review of underlying mechanisms." In: *Environmental Research Letters* 16.9, p. 093003. DOI: 10.1088/1748-9326/AC1C29.

Przybylak, Rajmund (2003). *The Climate of the Arctic*. 1st ed. Dordrecht: Springer Netherlands.

Rahmstorf, Stefan, Jason E. Box, Georg Feulner, Michael E. Mann, Alexander Robinson, Scott Rutherford, and Erik J. Schaffernicht (2015). "Exceptional twentieth-century slowdown in Atlantic Ocean overturning circulation." In: *Nature Climate Change* 5.5, pp. 475–480. DOI: 10.1038/NCLIMATE2554.

Rantanen, Mika, Alexey Yu. Karpechko, Antti Lipponen, Kalle Nordling, Otto Hyvärinen, Kimmo Ruosteenoja, Timo Vihma, and Ari Laaksonen (2022). "The

Arctic has warmed nearly four times faster than the globe since 1979." In: *Communications Earth & Environment* 3.1, pp. 1–10. DOI: 10.1038/s43247-022-00498-3.
Schneider, Tapio, Tobias Bischoff, and Hanna Płotka (2015). "Physics of Changes in Synoptic Midlatitude Temperature Variability." In: *Journal of Climate* 28.6, pp. 2312–2331. DOI: 10.1175/JCLI-D-14-00632.1.
Schuur, E. A.G. et al. (2015). "Climate change and the permafrost carbon feedback." In: *Nature* 520.7546, pp. 171–179. DOI: 10.1038/nature14338.
Schwarzwald, Kevin and Nathan Lenssen (2022). "The importance of internal climate variability in climate impact projections." In: *Proceedings of the National Academy of Sciences of the United States of America* 119.42, e2208095119. DOI: 10.1073/pnas.2208095119.
Schweiger, Axel J., Kevin R. Wood, and Jinlun Zhang (2019). "Arctic Sea Ice Volume Variability over 1901–2010: A Model-Based Reconstruction." In: *Journal of Climate* 32.15, pp. 4731–4752. DOI: 10.1175/JCLI-D-19-0008.1.
Screen, James A. (2014). "Arctic amplification decreases temperature variance in northern mid- to high-latitudes." In: *Nature Climate Change* 4.7, pp. 577–582. DOI: 10.1038/NCLIMATE2268.
Screen, James A. and I. Simmonds (2010). "The central role of diminishing sea ice in recent Arctic temperature amplification." In: *Nature* 464.7293, pp. 1334–1337. DOI: 10.1038/nature09051.
Seneviratne, S.I. et al. (2021). "Weather and Climate Extreme Events in a Changing Climate." In: *Climate Change 2021: The Physical Science Basis. Contribution of Working Group I to the Sixth Assessment Report of the Intergovernmental Panel on Climate Change*. Ed. by V. Masson-Delmotte et al. Cambridge, United Kingdom and New York, NY, USA: Cambridge University Press, pp. 1513–1766. DOI: 10.1017/9781009157896.013.
Serreze, Mark C. and Roger G. Barry (2011). "Processes and impacts of Arctic amplification: A research synthesis." In: *Global and Planetary Change* 77.1-2, pp. 85–96. DOI: 10.1016/j.gloplacha.2011.03.004.
Serreze, Mark C. and Roger G. Barry (2014). *The Arctic Climate System*. 2nd ed. New York: Cambridge University Press.
Serreze, Mark C. and Jennifer A. Francis (2006). "The Arctic Amplification Debate." In: *Climatic Change* 76.3, pp. 241–264. DOI: 10.1007/S10584-005-9017-Y.
Serreze, Mark C. and Julienne Stroeve (2015). "Arctic sea ice trends, variability and implications for seasonal ice forecasting." In: *Philosophical Transactions of the Royal Society A: Mathematical, Physical and Engineering Sciences* 373.2045, p. 20140159. DOI: 10.1098/rsta.2014.0159.
Sigmond, M., J. C. Fyfe, G. M. Flato, V. V. Kharin, and W. J. Merryfield (2013). "Seasonal forecast skill of Arctic sea ice area in a dynamical forecast system." In: *Geophysical Research Letters* 40.3, pp. 529–534. DOI: 10.1002/grl.50129.
Sillmann, J., V. V. Kharin, F. W. Zwiers, X. Zhang, and D. Bronaugh (2013). "Climate extremes indices in the CMIP5 multimodel ensemble: Part 2. Future climate projections." In: *Journal of Geophysical Research: Atmospheres* 118.6, pp. 2473–2493. DOI: 10.1002/JGRD.50188.
Smith, Laurence C. and Scott R. Stephenson (2013). "New Trans-Arctic shipping routes navigable by midcentury." In: *Proceedings of the National Academy of Sciences of the United States of America* 110.13, E1191–E1195. DOI: 10.1073/pnas.1214212110.

Stenseth, Nils Chr, Atle Mysterud, Geir Ottersen, James W. Hurrell, Kung Sik Chan, and Mauricio Lima (2002). "Ecological effects of climate fluctuations." In: *Science* 297.5585, pp. 1292–1296. DOI: 10.1126/SCIENCE.1071281.

Stouffer, Ronald J. and R. T. Wetherald (2007). "Changes of Variability in Response to Increasing Greenhouse Gases. Part I: Temperature." In: *Journal of Climate* 20.21, pp. 5455–5467. DOI: 10.1175/2007JCLI1384.1.

Stroeve, Julienne, Marika M. Holland, Walt Meier, Ted Scambos, and Mark Serreze (2007). "Arctic sea ice decline: Faster than forecast." In: *Geophysical Research Letters* 34.9, p. 9501. DOI: 10.1029/2007GL029703.

Stroeve, Julienne and Dirk Notz (2018). "Changing state of Arctic sea ice across all seasons." In: *Environmental Research Letters* 13.10, p. 103001. DOI: 10.1088/1748-9326/AADE56.

Suarez-Gutierrez, Laura, Chao Li, Wolfgang A. Müller, and Jochem Marotzke (2018). "Internal variability in European summer temperatures at 1.5 °c and 2 °c of global warming." In: *Environmental Research Letters* 13.6, p. 064026. DOI: 10.1088/1748-9326/aaba58.

Suarez-Gutierrez, Laura, Wolfgang A. Müller, Chao Li, and Jochem Marotzke (2020). "Hotspots of extreme heat under global warming." In: *Climate Dynamics* 55.3-4, pp. 429–447. DOI: 10.1007/s00382-020-05263-w.

Sui, Cuijuan, Zhanhai Zhang, Lejiang Yu, Yi Li, and Mirong Song (2017). "Investigation of Arctic air temperature extremes at north of 60°N in winter." In: *Acta Oceanologica Sinica* 36.11, pp. 51–60. DOI: 10.1007/S13131-017-1137-5.

Swart, Neil C., John C. Fyfe, Ed Hawkins, Jennifer E. Kay, and Alexandra Jahn (2015). "Influence of internal variability on Arctic sea-ice trends." In: *Nature Climate Change* 5.2, pp. 86–89. DOI: 10.1038/nclimate2483.

Swart, Neil C. et al. (2019). "The Canadian Earth System Model version 5 (CanESM5.0.3)." In: *Geoscientific Model Development* 12.11, pp. 4823–4873. DOI: 10.5194/GMD-12-4823-2019.

Tamarin-Brodsky, Talia, Kevin Hodges, Brian J. Hoskins, and Theodore G. Shepherd (2020). "Changes in Northern Hemisphere temperature variability shaped by regional warming patterns." In: *Nature Geoscience* 13.6, pp. 414–421. DOI: 10.1038/s41561-020-0576-3.

Tatebe, Hiroaki et al. (2019). "Description and basic evaluation of simulated mean state, internal variability, and climate sensitivity in MIROC6." In: *Geoscientific Model Development* 12.7, pp. 2727–2765. DOI: 10.5194/GMD-12-2727-2019.

Thompson, David W.J. and John M. Wallace (1998). "The Arctic oscillation signature in the wintertime geopotential height and temperature fields." In: *Geophysical Research Letters* 25.9, pp. 1297–1300. DOI: 10.1029/98GL00950.

Thomson, David J. (1995). "The Seasons, Global Temperature, and Precession." In: *Science* 268.5207, pp. 59–68. DOI: 10.1126/SCIENCE.268.5207.59.

Thornton, Philip K., Polly J. Ericksen, Mario Herrero, and Andrew J. Challinor (2014). "Climate variability and vulnerability to climate change: a review." In: *Global Change Biology* 20.11, pp. 3313–3328. DOI: 10.1111/GCB.12581.

Tietsche, S., J. J. Day, V. Guemas, W. J. Hurlin, S. P.E. E Keeley, D. Matei, R. Msadek, M. Collins, and E. Hawkins (2014). "Seasonal to interannual Arctic sea ice predictability in current global climate models." In: *Geophysical Research Letters* 41.3, pp. 1035–1043. DOI: 10.1002/2013GL058755.

Tokinaga, Hiroki, Shang Ping Xie, and Hitoshi Mukougawa (2017). "Early 20th-century Arctic warming intensified by Pacific and Atlantic multidecadal vari-

ability." In: *Proceedings of the National Academy of Sciences of the United States of America* 114.24, pp. 6227–6232. DOI: 10.1073/pnas.1615880114.
Vasseur, David A., John P. DeLong, Benjamin Gilbert, Hamish S. Greig, Christopher D.G. Harley, Kevin S. McCann, Van Savage, Tyler D. Tunney, and Mary I. O'Connor (2014). "Increased temperature variation poses a greater risk to species than climate warming." In: *Proceedings of the Royal Society B: Biological Sciences* 281.1779. DOI: 10.1098/RSPB.2013.2612.
Walsh, John E., Thomas J. Ballinger, Eugénie S. Euskirchen, Edward Hanna, Johanna Mård, James E. Overland, Helge Tangen, and Timo Vihma (2020). "Extreme weather and climate events in northern areas: A review." In: *Earth-Science Reviews* 209, p. 103324. DOI: 10.1016/J.EARSCIREV.2020.103324.
Wang, Wanqiu, Mingyue Chen, and Arun Kumar (2013). "Seasonal Prediction of Arctic Sea Ice Extent from a Coupled Dynamical Forecast System." In: *Monthly Weather Review* 141.4, pp. 1375–1394. DOI: 10.1175/MWR-D-12-00057.1.
Wiel, K. van der, N. Wanders, F. M. Selten, and M. F.P. Bierkens (2019). "Added Value of Large Ensemble Simulations for Assessing Extreme River Discharge in a 2 °C Warmer World." In: *Geophysical Research Letters* 46.4, pp. 2093–2102. DOI: 10.1029/2019GL081967.
Yang, Qian, Timothy H. Dixon, Paul G. Myers, Jennifer Bonin, Don Chambers, and M. R. Van Den Broeke (2016). "Recent increases in Arctic freshwater flux affects Labrador Sea convection and Atlantic overturning circulation." In: *Nature Communications* 7.1, pp. 1–8. DOI: 10.1038/ncomms10525.
Ylhäisi, Jussi S. and Jouni Räisänen (2014). "Twenty-first century changes in daily temperature variability in CMIP3 climate models." In: *International Journal of Climatology* 34.5, pp. 1414–1428. DOI: 10.1002/JOC.3773.
Zemp, M. et al. (2019). "Global glacier mass changes and their contributions to sea-level rise from 1961 to 2016." In: *Nature* 568.7752, pp. 382–386. DOI: 10.1038/s41586-019-1071-0.
Zhang, Rong (2015). "Mechanisms for low-frequency variability of summer Arctic sea ice extent." In: *Proceedings of the National Academy of Sciences of the United States of America* 112.15, pp. 4570–4575. DOI: 10.1073/PNAS.1422296112.
Zhang, Rudong, Hailong Wang, Qiang Fu, Angeline G. Pendergrass, Minghuai Wang, Yang Yang, Po Lun Ma, and Philip J. Rasch (2018). "Local Radiative Feedbacks Over the Arctic Based on Observed Short-Term Climate Variations." In: *Geophysical Research Letters* 45.11, pp. 5761–5770. DOI: 10.1029/2018GL077852.
Ziehn, Tilo, Matthew A. Chamberlain, Rachel M. Law, Andrew Lenton, Roger W. Bodman, Martin Dix, Lauren Stevens, Ying Ping Wang, and Jhan Srbinovsky (2020). "The Australian Earth System Model: ACCESS-ESM1.5." In: *Journal of Southern Hemisphere Earth Systems Science* 70.1, pp. 193–214. DOI: 10.1071/ES19035.

## EIDESSTAATLICHE VERSICHERUNG

Hiermit erkläre ich an Eides statt, dass ich die vorliegende Dissertationsschrift selbst verfasst und keine anderen als die angegebenen Quellen und Hilfsmittel benutzt habe.

*DECLARATION ON OATH*

*I hereby declare upon oath that I have written the present dissertation independently and have not used further resources and aids than those stated.*

Hamburg, December 2022

Céline Gieße

# Hinweis / Reference

Die gesamten Veröffentlichungen in der Publikationsreihe des MPI-M
„Berichte zur Erdsystemforschung / Reports on Earth System Science“,
ISSN 1614-1199

sind über die Internetseiten des Max-Planck-Instituts für Meteorologie erhältlich:
**http://www.mpimet.mpg.de/wissenschaft/publikationen.html**

*All the publications in the series of the MPI -M*
*„Berichte zur Erdsystemforschung / Reports on Earth System Science“,*
*ISSN 1614-1199*

*are available on the website of the Max Planck Institute for Meteorology:*
***http://www.mpimet.mpg.de/wissenschaft/publikationen.html***